

BEHAVIOUR OF BRICK MASONRY  
UNDER  
COMPRESSIVE LOADING

A Thesis  
by  
MD. KAWSAR ALI



Submitted to the Dept. of Civil Engineering of Bangladesh  
University of Engineering & Technology, Dhaka in partial  
fulfilment of the requirements for the degree  
of  
MASTER OF SCIENCE IN CIVIL ENGINEERING



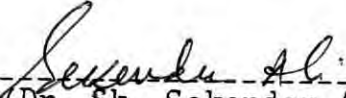
December, 1991

624.183  
1991  
KAW

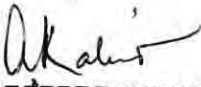
# BEHAVIOUR OF BRICK MASONRY UNDER COMPRESSIVE LOADING

A Thesis  
by  
MD. KAWSAR ALI

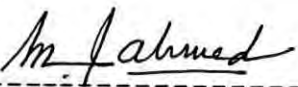
Approved as to style and content by:

  
-----  
(Dr. Sk. Sekender Ali)  
Associate Professor,  
Dept. of Civil Engineering,  
BUET, Dhaka.

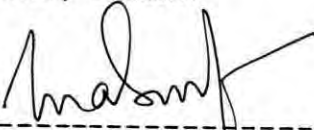
Chairman

  
-----  
(Dr. Ahsanul Kabir)  
Associate Professor  
Dept. of Civil Engineering,  
BUET, Dhaka.


Co-Chairman

  
-----  
(Dr. M. Feroze Ahmed)  
Professor and Head,  
Dept. of Civil Engineering,  
BUET, Dhaka.

Member

  
-----  
(Dr. Md. Abdur Rouf)  
Professor,  
Dept. of Civil Engineering,  
BUET, Dhaka.

Member

  
-----  
(Mr. Kazi Ataul Hoque)  
Ex-Director  
Housing & Building Research  
Institute, Mirpur, Dhaka.

Member

December, 1991

## ACKNOWLEDGEMENTS

I take this opportunity to express my gratitude to my supervisor Dr. Sk. Sekender Ali, Associate Professor of Civil Engineering, BUET for his encouragement and invaluable advice at every stage of this investigation. Sincere gratitude to my co-supervisor Dr. Ahsanul Kabir, Associate Professor of Civil Engineering, BUET for his constructive criticism and comments at various stages of this research program.

Special debt of gratitude to Dr. M. Feroze Ahmed, Professor and Head, Dept. of Civil Engineering, BUET for allowing usage of different facilities in connection with this work.

Gratitude are also due to Dr. M.A. Rouf, Professor and Dr. M. Zoynul Abedin, Associate Professor of Civil Engineering, BUET for their kind help during the study.

Thanks are extended to the technical staff of the Concrete Laboratory and Structural Laboratory. In particular, I would like to express my appreciation to Mr. Md. Barkatullah, Mr. Karim and Mr. Rozario.

Heartiest thanks to Mr. M.A. Malek for typing the thesis with extreme care.

Finally, I acknowledge indebtedness to my elder brother Md. Zakaria and other members of my family whose inspirations and encouragements made this work possible.

## ABSTRACT

This study presents the results of investigations into the compressive behaviour of brick masonry constructed with cement mortar and mud mortar. For cement mortar, a particular cement-sand ratio (1:4) has been used and for mud mortar different percentages of randomly distributed jute fibre and jute mat conforming uniform distribution have been used. Stack bonded prisms of different heights, prisms with vertical joints and wallettes(walls) have been used in the investigation. All the specimens have been tested under vertical compression in the laboratory. The deformation, strength characteristics and failure modes have been analysed and explained in the study. Besides, two dimensional linear elastic finite element method of analysis has been used to investigate the platen effect imposed on the specimens used in the study.

The study reveals that in case of five brick high prism, the effect of platen restraint is substantially minimized. It has been found that the deformation characteristics of masonry can be represented by a parabolic equation of best fit. However, with a minor modification, Saenz's stress-strain relation originally proposed for axially loaded concrete can also be used to represent the deformation characteristics of masonry with good approximation. The study also suggests that the wall(wallette) strength is 0.87 times the strength of five brick high stack bonded prism and 0.75 times the strength of five brick high prism with vertical joint. A theoretical formula has also been proposed from finite element analysis to predict the compressive strength of stack bonded prism. The formula predicts the compressive strength of stack bonded prisms more closely than any other existing formula.

Investigation into the mud mortar reveals that jute fibre prevents the formation of crack in mortar bed joints. A limiting maximum inclusion of 1.9% jute fibre results in a maximum increase of unconfined compressive strength of mud mortar by 35.3%. For resistance to lateral deformation the limiting inclusion lies between 1.5% to 2.0%. Above these limiting values the increase of both strength and resistance to lateral deformation are inhibited. The use of jute fibres in the mud mortar has no appreciable effect on the strength of the masonry.

## CONTENTS

	Page
ACKNOWLEDGEMENTS	ii
ABSTRACTS	iii
LIST OF FIGURES	x
LIST OF TABLES	xiii
NOTATIONS	xv
1. INTRODUCTION	
1.1 GENERAL	1
1.2 USUAL PRACTICE IN BANGLADESH	2
1.3 SCOPE OF UTILIZATION OF MUD MORTAR IN BRICK MASONRY	2
1.4 STATEMENT OF THE PROBLEM	3
1.5 OBJECTIVES OF THE RESEARCH	4
2. LITERATURE REVIEW	
2.1 INTRODUCTION	6
2.2 MATERIAL PROPERTIES	7
2.2.1 Brick Properties	7
a. Compressive Strength	7
b. Tensile Strength	9
c. Biaxial Strength	11
d. Other Brick Properties	15
2.2.2 Mortar Properties	15
2.2.3 Brick Masonry Properties	17
a. Deformation Characteristics of Masonry Under Compression	17
b. Masonry Compressive Strength	18

	Page
2.3 BRICK MASONRY UNDER COMPRESSIVE LOADING	20
2.3.1 Theoretical Investigation	20
2.3.2 Experimental Investigation	23
2.4 MUD MORTAR IN MASONRY AS A BINDING MATERIAL	24
2.5 SUMMARY	25
<b>3. LABORATORY INVESTIGATIONS</b>	
3.1 INTRODUCTION	27
3.2 PROPERTIES OF BRICK	28
3.2.1 Compressive Strength of Brick	29
3.2.2 Tensile Strength of Brick	31
3.2.3 Deformation Characteristics of Brick	33
a. Modulus of Elasticity	33
3.3 PROPERTIES OF CEMENT MORTAR	33
3.3.1 Compressive Strength of Cement Mortar	36
3.3.2 Tensile Strength of Cement Mortar	37
3.3.3 Deformation Characteristics of Cement Mortar	40
a. Modulus of Elasticity	40
3.4 PROPERTIES OF MUD MORTAR	42
3.4.1 Physical Properties of Soil	43
3.4.2 Chemical Properties of Soil	43
3.5 TESTS FOR MUD MORTAR	46
3.5.1 Water Content of Mud Mortar at Workability	46
3.5.2 Shrinkage Limit of Mud Mortar	47
3.5.3 Compressive Strength of Mud Mortar	48

	Page
3.6 FABRICATION OF TEST SPECIMENS	52
3.6.1 Construction of Cement Mortared Masonry	53
3.6.2 Curing of Cement Mortared Masonry	55
3.6.3 Construction of Mud Mortared Masonry	55
3.6.4 Curing of Mud Mortared Masonry	55
3.7 TESTING OF MASONRY SPECIMENS	56
3.7.1 Testing for Deformation Characteristics of Cement Mortared Masonry	56
3.7.2 Testing for Compressive Strength of Cement Mortared Masonry	56
3.7.3 Testing for Compressive Strength of Mud Mortared Masonry	58
4. TEST RESULTS	
4.1 INTRODUCTION	61
4.2 TEST RESULTS OF MASONRY SPECIMENS WITH CEMENT MORTAR	61
4.2.1 Deformation Characteristics	61
4.2.2 Compressive Strength	61
4.2.3 Mode of Failure	63
a. Prisms	63
b. Walette	64
4.3 TEST RESULTS OF MUD MORTAR	68
4.4 TEST RESULTS OF MASONRY SPECIMENS WITH MUD MORTAR	70
4.4.1 Mode of Failure	71



	Page
<b>5. DISCUSSIONS ON TEST RESULTS</b>	
5.1 INTRODUCTION	74
5.2 SELECTION OF SUITABLE PRISM SPECIMEN	74
5.3 BRICK MASONRY WITH CEMENT MORTAR	75
5.3.1 Deformation Characteristics	75
a. Stress-Strain Curve	75
5.3.2 Modulus of Elasticity	80
5.3.3 Compressive Strength	85
a. Compressive Strength of Prism and Walette	85
b. Relation between Prism Strength and Walette Strength	88
5.3.4 Theoretical Formula to Predict the Compressive Strength of Stack Bonded Prism	89
5.3.5 Explanation of the Observed Failure Modes	93
5.4 BRICK MASONRY WITH MUD MORTAR	95
5.4.1 Role of Jute Fibre in Minimizing Cracks	95
5.4.2 Role Of Jute Fibre on the Deformation Characteristics	98
a. Analysis of Lateral Deformation Characteristics	101
5.4.3 Role of Jute Fibre on the Compressive Strength	103
5.4.4 Compressive Strength of Masonry with Mud Mortar	104
<b>6. ELASTIC FINITE ELEMENT ANALYSIS STUDY OF BRICK PRISMS</b>	
6.1 INTRODUCTION	107

	Page
6.2 FINITE ELEMENT METHOD OF ANALYSIS	108
6.3 TWO DIMENSIONAL LINEAR FINITE ELEMENT MODEL	108
6.4 FINITE ELEMENT ANALYSIS OF PRISMS	111
6.5 RESULTS OF THE FINITE ELEMENT ANALYSIS	119
<b>7.CONCLUSIONS AND RECOMMENDATIONS FOR FUTURE STUDY</b>	
7.1 CONCLUSIONS	128
7.2 RECOMMENDATIONS FOR FUTURE STUDY	130
<b>REFERENCES</b>	132
<b>APPENDIX-A EQUATIONS PREDICTING COMPRESSIVE STRENGTH</b>	138
<b>APPENDIX-B BRICK, MORTAR AND BRICK MASONRY PROPERTIES</b>	145

## LIST OF FIGURES

		Page
2.1	Failure Mechanism of Brick Masonry of Compression after Hilsdorf <sup>[18]</sup>	12
2.2	Theoretical Biaxial Tension-Compression Strength Envelope of Brick (Francis et al. <sup>[21]</sup> , Hilsdorf <sup>[18]</sup> , Hamid and Drysdale <sup>[21]</sup> )	14
2.3	Typical Experimental Biaxial Tension-Compression Strength Envelope of Brick (Khoo and Hendry <sup>[19]</sup> , Atkinson et al <sup>[5]</sup> )	14
2.4	Biaxial Failure Surface of Brick or Mortar (Ali and Page <sup>[23]</sup> )	14
3.1	Splitting Test on Brick	32
3.2	Testing Arrangement for Vertical Deformation of Brick	34
3.3	Average Stress-Strain Curve for Brick	34
3.4	Measurement of Vertical Deformation of Brick and Brick Masonry	41
3.5	Average Stress-strain Curve for Cement Mortar	41
3.6	Grain Size Distribution of Soil	44
3.7	Oven Dried Soil Pats with Different Percentages of Jute Fibre for the Determination of Shrinkage Limit	49
3.8	Mortar Cubes with Jute Fibre after Compression Test	50
3.9	Mortar Cylinders with Jute Fibre after Unconfined Compression Test	50
3.10	Different Test Specimens Constructed with Cement Mortar	54
3.11	Testing Arrangement for Vertical Deformation of Brick Masonry	57
3.12	Loading Arrangement for Prism	59
3.13	Loading Arrangement for Walette	59

	Page	
4.1	Typical Failure Pattern of 5SPC Prism	65
4.2	Typical Failure Pattern of 5VPC-A Prism	65
4.3	Typical Splitting of 5VPC-A Prism on the Narrow Face	66
4.4	Typical Failure Pattern of 5VPC-B Prism	66
4.5	Typical Failure Pattern of Walette	67
4.6	Typical Failure Pattern of Stack Bonded Prism with Mud Mortar	72
4.7	Typical Splitting on the Narrow Face of Stack Bonded Prism with Mud Mortar	72
4.8	Typical Failure Pattern of Stack Bonded Prism with 1.0% Fibre in the Mud Mortar Bed	73
4.9	Typical Failure Pattern of Stack Bonded Prism with Jute Mat in the Mud Mortar Bed	73
5.1	Effect of Prism Height on the Compressive Strength	76
5.2	Stress-strain Curve (Best fit) for Brick Masonry	78
5.3	Extrapolation of Average Stress-strain Curve of Brick Masonry	79
5.4	Computed Stress-strain Curve for Brick Masonry	81
5.5	Failure Criterion of Brick Masonry	91
5.6	Avg. Shrinkage Limit Vs. Jute Fibre Content	97
5.7	Typical Mud Mortar Bed without Jute Fibre	97
5.8	Typical Mud Mortar Bed with Randomly Distributed Jute Fibre	99
5.9	Typical Mud Mortar Bed with Jute Mat at the Middle	99
5.10	Average Vertical Stress-strain Curves for Mud Mortar with Different Jute Fibre Content	100
5.11	Cylindrical Mortar Specimen under Vertical Compression	101

	Page
5.12 Average Unconfined Compressive Strength Vs. Jute Fibre Content of Mud Mortar	105
6.1 Typical Four Noded Element	109
6.2 Two Dimensional Finite Element Mesh for 3SPC Prism	113
6.3 Two Dimensional Finite Element Mesh for 4SPC Prism	114
6.4 Two Dimensional Finite Element Mesh for 5SPC Prism	115
6.5 Two Dimensional Finite Element Mesh for 6SPC Prism	116
6.6 Two Dimensional Finite Element Mesh for 5VPC-A Prism	117
6.7 Two Dimensional Finite Element Mesh for 5VPC-B Prism	118
6.8 Transverse Stress ( $\sigma_x$ ) Distributions Down Centre Line for 3SPC prism	120
6.9 Transverse Stress ( $\sigma_x$ ) Distributions Down Centre Line for 4SPC Prism	121
6.10 Transverse Stress ( $\sigma_x$ ) Distributions Down Centre Line of 5SPC Prism	122
6.11 Transvers Stress ( $\sigma_x$ ) Distributions Down Centre Line for 6SPC Prism	123
6.12 Transverse Stress ( $\sigma_x$ ) Distributions Down Centre Line for 5VPC-A Prism	124
6.13 Transverse Stress ( $\sigma_x$ ) Distributions Down Centre Line for 5VPC-B Prism	125

## LIST OF TABLES

		Page
2.1	Aspect Ratio Correction Factors for Compressive Strength Test	20
3.1	Summary of Brick Properties	30
3.2	Properties of Cement and Sand	35
3.3	Summary of Cement Mortar Properties	36
3.4	Compressive Strength of Cement Mortar for Different Test Specimens	38
3.5	Tensile Strength of Cement Mortar for Different Test Specimens	39
3.6	Physical and Chemical Properties of Soil	45
4.1	Avg. Normal Stress-strain Readings for Masonry with Cement Mortar	62
4.2	Summary of Results of Compression Test on Masonry Specimens with Cement Mortar	62
4.3	Avg. Water Content at Workability of Mud Mortar with Different Fibre Contents	68
4.4	Avg. Shrinkage Limit of Mud Mortar with Different Fibre Contents	68
4.5	Results of Compression Test on Mud Mortar Cubes	69
4.6	Summary of Results of Unconfined Compression Test on Mud Mortar (Mean Stress-Strain Readings)	69
4.7	Summary of Results of Compression Test on Masonry Specimens (5 Brick High Stack Bonded Prism) with Mud Mortar	70
5.1	Value of the Parameters for Uniaxial Stress-Strain Curve for Masonry	77
5.2	Properties of Masonry Constituents	84

	Page
5.3 Comparison between Experimental and Calculated Values of Initial Tangent Modulus	85
5.4 Results of Compression Test on 5-high Prism and Walette	86
5.5 Comparison between the Experimental and Calculated Strengths of Stack Bonded Prism using Different Formulae	93

## NOTATION

Note: The following general terminology has been adopted

$E$	Initial Modulus of Elasticity
$E_{bms}$	Secant modulus of elasticity of brick masonry
$f_{vc}$	Compressive strength of prism/wallatte at first visible crack
$f'_m$	Ultimate Compressive strength of prism/wallatte
$t_b$	Thickness of brick
$t_m$	Thickness of mortar joint
$\epsilon$	Strain
$\epsilon_{bmu}$	Strain in brick masonry at ult. compressive strength
$\sigma$	Stress
$\sigma_{av}$	Av. vertical stress
$\nu$	Poisson's ratio

### Subscript

b	Brick
m	Mortar
bm	Brick masonry
n	Normal direction
x	x-direction
y	y-direction
z	z-direction



## CHAPTER 1 INTRODUCTION



### 1.1 GENERAL

Masonry has been used as a load bearing material for centuries. Only, in the last 100 years Civil Engineers have built exclusively steel and concrete structures. Brick and stone masonry were the dominant materials both for buildings and engineering works until the middle of 19th century. In the last 25 years engineers have re-established brickwork as a high performance and economical-structural material.

In recent years there has been a renewed interest in masonry construction for residential, industrial and other buildings. This has been possible due to recognition of the advantages of masonry in terms of durability, economy and appearance. Besides, masonry walls perform simultaneously a number of functions including division of space, structure, weather exclusion, fire protection, thermal and acoustic insulation.

In the early age, masonry were massive, most of them were gravity type in which level of stress were low and factor of safety against compression failure was high. Therefore, the detailed knowledge of compressive behavior of masonry was not essential. However, in the modern age due to the scarcity of low cost construction materials, masonry is made practicable by the use of thin load bearing walls in buildings for economy. Consequently, those walls are often highly stressed under vertical loads than traditional massive construction. The modern usage of masonry therefore requires a much more detailed knowledge of its strength and behaviour under compressive loading.

## 1.2 USUAL PRACTICE IN BANGLADESH

Brick masonry is popular in Bangladesh. Cement mortar is usually used in it as a binding material. Here Engineers and Builders are hardly aware that brick masonry can be engineered rather leaving it as an all-mason-affair. The contemporary practice of brick masonry in this part of the world has emerged little from antiquity. In general, there has been little improvement in the process of brick making itself during the past fifty years. Both design and construction of brick masonry are still done by thumb rules and traditional methods. There has been a serious lack of efforts even in implementing or utilizing the ready-made findings of valuable research that has been conducted overseas.

Besides, its practice being antique, the vast potentialities of the economic application of brick masonry to almost any type of structure has not been explored. Although small bridges, culverts and retaining walls were built with brick masonry even a few decades ago, its present day applications are virtually limited to one to four-storied buildings.

Moreover, in the rural areas, mud mortar is used as a low cost binding material in the low rise load bearing brick masonry limited to one-story high. Traditional methods varying widely over localities, are being followed in the preparation of mud mortars.

## 1.3 SCOPE OF UTILIZATION OF MUD MORTAR IN BRICK MASONRY

Bangladesh is an over populated country. Every year, with the rapid population growth, there is an increased demand for shelter. The problem of housing is more acute in rural areas since eighty percent of the population live there.

One of the strategies of the new housing policy is to promote the use of locally available low cost building materials. Being the cheapest material, the use of mud in brick masonry will be a step forward towards saving costly material like cement. Also, mud has better sound insulation and fire resistance properties.

#### 1.4 STATEMENT OF THE PROBLEM

The principal function of most masonry elements is to carry compressive loads. Therefore, much attention has been paid to know the compressive behaviour of masonry. It emerges from the reviewed literature (see chapter 2) that several attempts have been made abroad in this area. Though brick masonry is popular in Bangladesh, very few attempts have been made to establish the parameters influencing its compressive strength.

In Bangladesh attempts have been made to find the effect of parameters like mortar strength, fineness modulus of sand, curing condition, moisture content of bricks at the time of laying, geometry and construction of prism etc. on the compressive strength of brickwork<sup>1,2</sup>.

The theoretical formula used to know the compressive behaviour of brick masonry varies from country to country and the results deviate widely from actual behaviour. The compressive strength of the prism determined from the available theoretical formulae either underestimate or overestimate the actual strength reflecting inadequacy of knowledge regarding the behaviour of the constituent materials.

In Bangladesh over the last few years, few attempts have been made to improve the strength and durability of soil, termed as soil stabilization using lime, cement, rice husk, straw, jute

fibre, animal dung etc. as stabilizer. But no research work has been carried out home and abroad to use mud mortar as a binding material in brick masonry.

The present investigation is the beginning of an on-going research on compressive behaviour of brick and concrete masonry using different binding materials. There are two phases in this investigation. In the first phase attempts has been made to predict the strength and behavior of load bearing brick masonry in which cement mortar is the binding material. The second phase will be devoted to the aspect of the inclusion of jute fibre in mud mortar with a view to reduce excessive shrinkage after drying, excessive deformation under compressive loading and to act as a crack arrester and thus to improve the quality of low rise load bearing brick masonry.

#### 1.5 OBJECTIVES OF THE RESEARCH

Although brick masonry is a popular building material in Bangladesh, its use has been limited to some extent due to the lack of proper knowledge and nonavailability of primitive technology in this area. In a poor country like Bangladesh, a comprehensive research is therefore required to explore the possibility of using such a popular building material more efficiently and effectively.

It is emerged from literature review that stack bonded prism is a good predictor of the performance of load bearing masonry walls which is widely used in overseas. Prisms and wallettes therefore, have been used in this investigation as the basis of research experiment with the view of the following objectives:

- 1) To propose a theoretical formula for the deformation characteristics of masonry and to modify the existing theoretical formula normally used to predict the compressive strength of a stack bonded prism.
- 2) To investigate the platen effect imposed during experiment on brick prisms of different heights (aspect ratios) by adopting linear elastic finite element method of analysis.
- 3) To develop an empirical relation between prism strength and single wythe running bonded wall (wallette) strength.
- 4) To find whether a prism with vertical joint represents single wythe running bonded wall (wallette) more realistically than a stack bonded prism.
- 5) To explore the possibility of using mud mortar in low rise load bearing masonry.

## CHAPTER 2 LITERATURE REVIEW

### 2.1 INTRODUCTION

The state of compressive stress of brick masonry has attracted sizable researcher in the last twenty years which has resulted in valuable findings. Compressive loading is very common in masonry structures such as load bearing walls, shear walls, diaphragm walls and infill panels. In order to evolve effective and accurate design concepts for such structural elements, a clear understanding of the strength and behavior of masonry under compressive loading is essential.

Brickwork loaded in uniform compression typically fails by the development of tension cracks parallel to the axis of loading i.e as a result of tensile stresses at right angles to the primary compression. This failure mechanism involves the failure of mortar joint (in some form of bond failure) and the failure of the masonry units.

To realistically predict the strength and behavior of masonry under compressive loading an experimental investigation as well as a thorough knowledge of the deformation and strength characteristic of the materials is needed. This chapter reviews previous literature which has been published on various aspects of the problem. Since solid clay brick masonry has been used in this investigation, the material property of clay brickwork are only reviewed. Previous pertinent theoretical and experimental investigations of masonry subjected to inplane loads are then described.

The possibility of using mud mortar along with the inclusion of jute fibre to improve the quality of low rise load bearing masonry wall will be explored in this investigation. Therefore, the available literature related to mud and mud with fibres will be reviewed.

## 2.2 MATERIAL PROPERTIES

Masonry is a two-phase material and its properties therefore depend upon the properties of its constituents, the bricks and the mortar. To understand the behavior of brick masonry, knowledge of the properties of the bricks, the mortar and the brick mortar assemblage is also required. A brief review of the properties relevant to the inplane behavior of masonry is carried out in this section.

### 2.2.1 Brick Properties

#### a) Compressive Strength

Compressive strength of brick is one of the most important properties. In general, the higher the compressive strength of brick, the higher is the compressive strength of brick masonry. Compressive strength tests are easy to perform and give a good indication of the general quality of the brick and the compressive capacity of the resulting masonry. For these reasons, the compressive strength test has been traditionally used for brick quality control and specification. West et al.<sup>[2]</sup>, Beech and West<sup>[3]</sup> found that brickwall strength averages about 0.3 (0.15-0.45) times the brick strength. Hendry<sup>[4]</sup> reported that the compressive strength of brickwork varies, roughly, as the square root of the normal brick crushing strength.

The standard test for determining compressive strength is influenced by several factors, such as loading rate, specimen size, perforation pattern and specimen end conditions. Because of the influence of these effects, the compressive strength obtained from a standard test is not necessarily the true compressive strength of the material. Atkinson et al.<sup>[5]</sup> carried out standard flatwise one-half unit compressive strength test with and without interface friction reduction system and also on 22 mm. diameter brick cores taken normal to the vertical face of the brick. They concluded that the test method most representative of brick strength could not be determined from those test. Page<sup>[6]</sup>; Render and Phipps<sup>[7]</sup> noticed strong influence of unit aspect ratio (height/minimum width) on the compressive strength. Page<sup>[8]</sup> reported that for a typical specimen having aspect ratio approximately 0.7, significant platen restraint occurs causing an apparent increase in strength to almost double the true compressive strength. Despite these deficiencies, the nominal compressive strength obtained from the standard test provides a good form of quality control as well as an index of compressive strength.

The standard test described in ASTM C67<sup>[9]</sup> for determining brick compressive strength require capping on the top and bottom face of the specimen, Australian Code for concrete masonry units (AS 2733-1984)<sup>[10]</sup> as well as some other overseas code require the use of plywood packing. Such test results will be influenced by the stiffness of the material used in specimen-platen interface and the frictional restraint imposed by the solid platen, with an artificial compressive strength resulting. Grim<sup>[11]</sup> informed that insertion of a teflon pad between the specimen and the machine platen will reduce the apparent compressive strength by one third of three-fourths.

Several investigators have attempted to minimize the effects of platen restraint by using variable stiffness platens and/or



capping materials on the specimen. Shrive<sup>[12]</sup> reported that the capping system may reduce, remove or reverse platen restraint which depends on the thickness of the capping, the restraint applied to it and its flexibility in comparison with that of the specimen. Shrive<sup>[13]</sup> also noticed that the capping material should have same mechanical properties as the specimen. Flexible steel brush platens have also been used successfully to eliminate strengthening effect of the platen<sup>[6,14]</sup>. An indication of the magnitude of this strengthening effect has been given recently by Page<sup>[6]</sup> from compression test on calcium silicate bricks. Steel brush and solid platens were used in tests on bricks of varying size and shape. The investigation shows that for a standard size brick (9.5"x4.5"x2.75"), the unconfined compressive strength (with steel brush platen) is almost half the confined compressive strength (with solid steel platens). The effect must therefore be considered when assessing the compressive strength of any material.

#### b) Tensile Strength

Brick tensile strength plays an important role on the inplane behavior of brick masonry, as final failure usually occurs in some form of biaxial tension split often originating in the brick.

Numerous attempts have been made to determine a convenient relationship between the brick tensile strength obtained from a simple test and wall strength. Various tension tests have been investigated, including the modulus of rupture test, splitting test (the Double punch or the Brazilian tests), various forms of shear tests, including indirect tension test. Based on the experimental results, Tasuji et al.<sup>[15]</sup> established a relationship for the uniaxial tensile strength of concrete that may be estimated from the uniaxial compressive strength by

$\sigma_{t0} = 6\sqrt{\sigma_{c0}}$  , where  $\sigma_{t0}$  is the tensile strength (psi) and  $\sigma_{c0}$  is the uniaxial compressive strength (psi).

As direct tensile strength tests are difficult to perform on brittle material several investigators paid attention on indirect test. Many authors have suggested the use of cube and similar prisms as a more practical alternative to the cylinder for measuring indirect tensile strength. Rosenhaupt et al.<sup>[16]</sup> studied the plane strain problem involved when compressive forces are applied along the opposite face of a concrete cube. Using mathematical and photo elastic techniques they showed that the tensile stress was fairly uniform along the middle plane and given by

$$\text{Tensile strength} = 0.648P/dl \quad (2.1)$$

Where, P = applied load, d = equivalent diameter and l = length

Thomas and O'Leary<sup>[17]</sup> found indirect tensile strength calculated by using this formula is similar to that for cylinders ( $2P/\pi dl$ ), the difference being almost 1.5%. He concluded that the indirect tensile strength can be measured by splitting the unit across the width or the length, across the width splitting producing higher strength. Atkinson et al.<sup>[5]</sup> tested the tensile strength of three types of brick with indirect Brazilian split and direct tension method. The Brazilian split tests were done on 2.5 cm thick disk cut from a 5.4 cm diameter core taken lengthwise through the brick. The direct tensile strength method seemed to be a better measure of the tensile strength and generally had shown less scatter of data than the indirect tensile strength results.

### c) Biaxial Strength

The above discussions are only limited to the uniaxial compressive and tensile strength of brittle material (brick and concrete). However in a brick masonry when loaded in axial compression for example, lateral expansion of the brick and mortar takes place. Since the mortar joints are typically more flexible than the brick, the joint deformation is partially restrained by the surrounding bricks due to the bond and friction at the brick mortar interface. This results in a triaxial compressive stress state in the mortar and uniaxial compression and biaxial tension in the bricks.

Since the tensile strength of the brick is low (much lower than its compressive strength), the tensile stress in the brick initiates failure. This mechanism is shown in Fig. 2.1 for the case of a stack bonded prism loaded in uniaxial compression.

The mechanism of failure for solid masonry has been discussed in detail by Hilsdorf<sup>[18]</sup>, Khoo and Hendry<sup>[19]</sup>; for hollow masonry by Shrive<sup>[20]</sup> and for grouted and ungrouted concrete masonry by Hamid and Drysdale<sup>[21]</sup>.

As has been stated above, brick in a brick masonry remains in a state of uniaxial compression and biaxial tension, a detailed knowledge of masonry unit under this state of stress is necessary. Kupfer et al.<sup>[14]</sup> found that the biaxial tensile strength of concrete is approximately equal to its uniaxial tensile strength. However, Tasuji et al.<sup>[15]</sup> proposed that the strength of concrete under biaxial tension is greater than uniaxial tension.

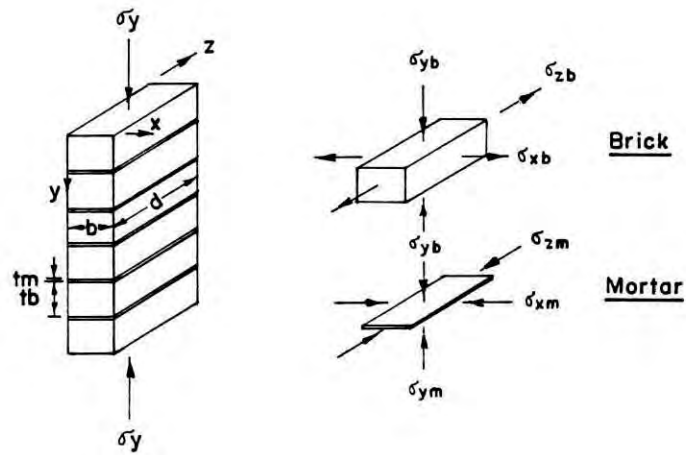


Fig. 2.1 Failure Mechanism of Brick Masonry in Compression after Hilsdorf.<sup>[18]</sup>

Tasuji et al.<sup>[15]</sup> observed that under combined tension and compression, the compressive strength decreases almost linearly as the tensile stress increases. Hilsdorf<sup>[16]</sup>; Francis et al.<sup>[22]</sup>, while formulating brick work prism strength, Hamid and Drysdale<sup>[21]</sup> while formulating prism compressive strength of grouted and ungrouted concrete block masonry assumed the tension-compression strength envelope (brick/concrete block) as straight line as shown in Fig. 2.2.

Khoo and Hendry<sup>[17]</sup> assumed biaxial tension-compression strength envelope of brick as:

$$C / C_0 = 1 - (T / T_0)^n \quad (2.2)$$

where  $T$  = tensile stress,  $C$  = compressive stress,  $T_0$  = direct tensile strength  $C_0$  = compressive strength and  $n = 0.546$

Atkinson et al.<sup>[23]</sup> conducted biaxial tension-compression test on brick and established the failure envelope of the same type as given by eqn. 2.2 but with a value of  $n = 0.58$ . Typical biaxial tension-compression strength envelope is shown in Fig. 2.3.

Recently, Ali and Page<sup>[23]</sup> adopted the failure surface as shown in Fig. 2.4 to predict failure of the concrete brick or the mortar under a state of biaxial tension or tension-compression. For simplicity, a square criterion was used in the tension-tension region and a bi-linear relationship in the tension compression region.

The effect of size, shape and disposition of the perforation on the tensile strength of bricks has been studied by West et al.<sup>[24]</sup> and Anderson<sup>[24]</sup>. Significant reductions in the tensile strength of bricks were reported in the case of bricks with perforation patterns which produced significant stress concentrations.

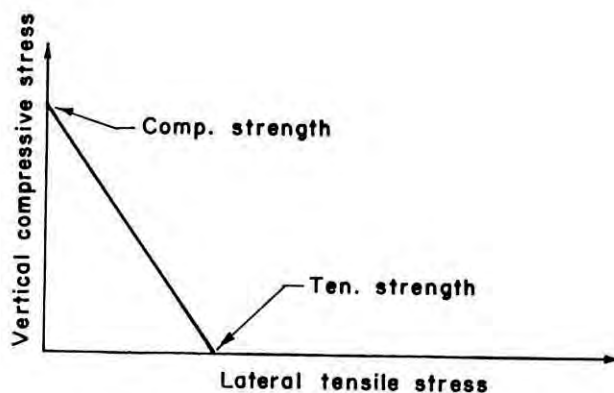
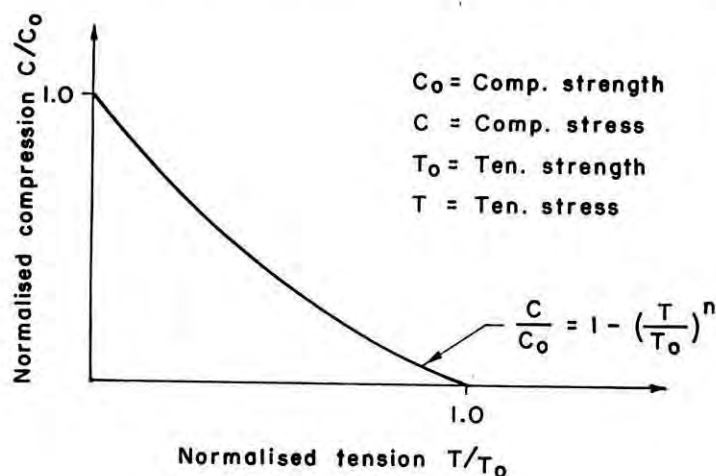


Fig.2.2 Theoretical Biaxial Tension-Compression Strength Envelope of Brick ( Francis et al.,<sup>[22]</sup> Hilsdorf,<sup>[18]</sup> Hamid and Drysdale<sup>[21]</sup> )



2.3 Typical Experimental Biaxial Tension-Compression Strength Envelope of Brick ( Khoo and Hendry,<sup>[19]</sup> Atkinson et al.<sup>[5]</sup> )

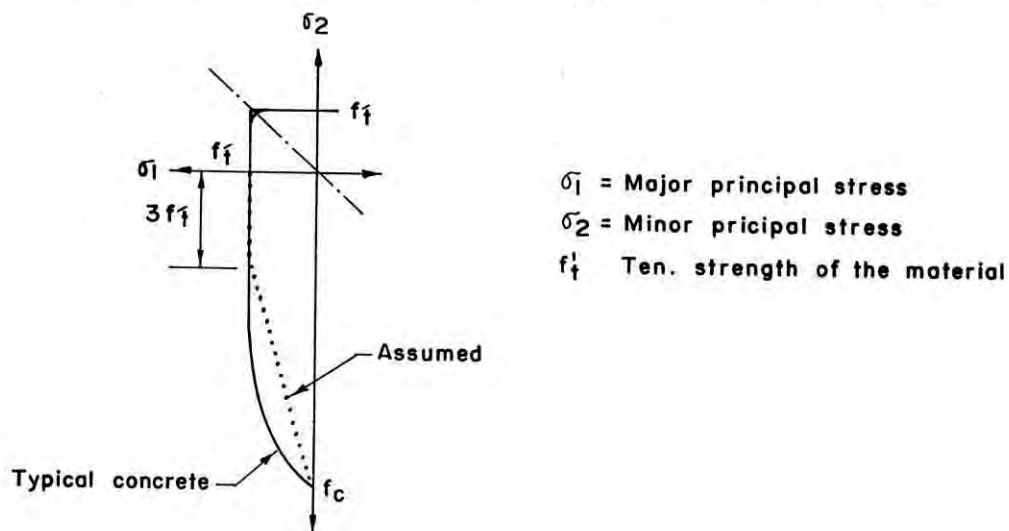


Fig. 2.4 Biaxial Failure Surface of Brick or Mortar ( Ali and Page<sup>[23]</sup> )

Despite the extensive research that has been carried out, no strong relationship between brick tensile strength and brick masonry strength has emerged. As a result, brick compressive strength is still used as a prime indicator of the potential compressive strength of the assemblage.

#### d) Other Brick Properties

There are several other properties such as brick growth, pitting, efflorescence, permeability, dimensional changes, etc. which have a significant influence on the satisfactory performance of masonry structures. However, most of these properties are related to the physical characteristics of the brick and do not influence the masonry strength. One brick property that does significantly influence brick masonry strength is the initial rate of absorption (I.R.A), or brick suction. Brick suction plays an important role in the achievement of bond and as such, significantly influence both the compressive and tensile strength of the masonry.

#### 2.2.2 Mortar Properties

Mortar performs three important functions in brick masonry:

- 1) Provides an even bed for the bricks
- 2) Bonds the bricks together
- 3) Seals the joints against weather

The above functions performed by the mortar depend upon its several properties in plastic state and hardened state. Such properties of plastic mortar include workability, water retentivity, initial flow and flow after suction, most of which are related to water content. Properties of hardened mortar that

help to determine the performance of finished masonry including bond strength, compressive strength, durability and extensibility. Properties of mortar both in plastic and hardened state will be briefly described in the following section.

In its plastic state, the properties required are good workability, good water retentivity and sufficient early stiffening. Mortar workability depends upon the brick and mortar properties, in particular the water retentivity of the mortar and the initial rate of absorption of the brick. These two latter properties will also have a marked effect on the bond strength of the resulting brick masonry. Good water retention is required for several reasons. It is needed to resist brick suction, to prevent bleeding of water from the mortar, to prevent stiffening of the mortar bed before placement of the brick, and to ensure that sufficient water is retained in the mortar to allow proper hydration of the cement.

In its hardened state, the properties required are compressive strength, bond strength and tensile strength. As stated in a previous article, mortar in a masonry remains in triaxial compression, as a result it can carry much higher normal stress than its uniaxial strength. Atkinson et al.<sup>[23]</sup>; McNary and Abrams<sup>[24]</sup> showed that in a masonry, mortar stress curve never cross the mortar failure envelope even with the weakest mortar. So, the compressive strength of mortar is not an important factor for the compressive strength of the masonry. SCPI<sup>[25]</sup> considers compressive strength of mortar much less important than its bond strength as a decisive factor of brick masonry strength. The emphasis is on the achievement of adequate bond between mortar and brick. However, compressive strength of mortar serves as a good indicator of quality control. It may be determined using cube test or prism test. Grim<sup>[11]</sup> has expressed the compressive strength of mortar as a function of shape, curing, age, air content and initial flow rate of mortar.



### 2.2.3 Brick Masonry Properties

The satisfactory performance of brick masonry depends upon the three strength characteristics namely compressive strength, tensile strength and shear strength. Since this investigation deals with the load bearing masonry only, the deformation characteristics as well as the compressive strength under compressive loading is of prime importance.

#### a) Deformation Characteristics of Masonry Under Compression

A knowledge of the deformation characteristics of masonry is required for predicting its strength and state of stress theoretically.

Brick masonry typically exhibits nonlinear stress-strain relations. Most of the nonlinear deformation occurs in the mortar joints with the brick often exhibiting linear stress-strain characteristics. Because of the influence of the bed joints and the possible anisotropic properties of the bricks, the deformation characteristics of the masonry will not necessarily be isotropic and can vary markedly with loading direction.

When stress levels are low, it is reasonable to take the initial tangent modulus as the modulus of elasticity of the masonry. The short term Young's modulus of elasticity ( $E_{bm}$ ) of brick masonry is usually related to its ultimate strength. The S.A.A Brick Code (AS1640-1974)<sup>[27]</sup> relates the  $E_{bm}$  value to the minimum ultimate compressive strength of masonry ( $F_m$ ). For high strength masonry,  $E_{bm} = 1000 F_m$ . This relationship is approximate, and will vary with brick and mortar type. Hendry et al.<sup>[28]</sup> reported that the Young's modulus can be assumed as:

$$E_{bm} = 700 F_m' \quad (2.3)$$

where,  $F_m'$  is the crushing strength of masonry. This will apply up to about 75% of the ultimate strength.

Pedreschi and Sinha<sup>[29]</sup> found a nonlinear stress-strain curve for masonry. Sinha and Pedreschi<sup>[30]</sup> suggested a nonlinear relationship between the Young's modulus of elasticity of brick masonry and its compressive strength as follows:

$$E_{bm} = 1180 (F_m')^{0.83} \quad (2.4)$$

Due to the large number of variables involved, these relationships are the best approximates.

#### b) Masonry Compressive Strength

The compressive strength of masonry is an important parameter in the design of load bearing masonry structures. The important factors influencing the strength of brick masonry are the strength and geometry of brick unit, the strength of mortar, the joint thickness, the suction of the units and the water retention of mortar and the brickwork bonding pattern. The influence of parameters such as brick and mortar properties, dimensional variations, slenderness ratio etc. on the strength of brick masonry have been extensively reviewed by several investigators. The effect of joint thickness on the compressive strength of brick masonry has been reported by Hendry<sup>[4]</sup>, Francis et al.<sup>[22]</sup>, Shrive<sup>[13]</sup>, Grim<sup>[11]</sup> and some others. All of them reported a decrease in masonry strength with increase in joint thickness and suggested the use of thin mortar joint preferably 3/8 inch (10 mm). As reported by Hendry<sup>[4]</sup>, research at Building Research

Laboratories in Australia and at the University of Edinburg and elsewhere establishes the fact that thick bed joints of 16-19 mm reduces the compressive strength by 30% as compared to normal 3/8 inch (10 mm) thick joints. S.A.A Brick Code<sup>[231]</sup> requires that in structural brickwork the joints must not be more than 1/2 inch thick and shall preferably not exceed 3/8 inch in thickness.

For the effective utilization of brick masonry as compression element the accurate estimate of compressive strength is very important. Most of the foreign codes have provision for determining brick masonry strength either from an approximate relationship between brick strength, mortar type and brick masonry strength or from compression test on stack bonded prisms.

The first option is most commonly used in practice but the values obtained will be conservative. Conservative relationships are used to allow for the effects of workmanship, perforation patterns, material variability etc. all of which can influence the masonry strength.

When a more exact estimate of compressive strength is required a prism test is done as this test include the effects just described above. Also, the failure mode of the bricks in the prism is similar to that in the wall. Shrive<sup>[12]</sup>, Anderson<sup>[24]</sup>, James et al.<sup>[32]</sup>, Anderson<sup>[33]</sup>, Jonston and McNeilly<sup>[34]</sup>, James<sup>[35]</sup>, Drysdale and Hamid<sup>[36]</sup> etc. advocated for adoption of prism tests for research experiment.

As described in section 2.2.1(a), the observed compressive strength of a specimen tested in uniaxial compression is significantly influenced by the restraining effect of the platens of the testing machine. The lower the aspect ratio (height/minimum width) the higher the influence of platen restraint. To minimize this influence, Australian Brickwork Code (AS1640-1974)<sup>[27]</sup> and North American Code of practice<sup>[37]</sup>

recommend a 4 brick high stack bonded prism of brickwork. In Britain the corresponding specimen was the six-brick cube but its use is not mentioned in the latest revision of BS5628<sup>[38]</sup>. However Shrive<sup>[12]</sup>, Shrive<sup>[13]</sup> SCPI<sup>[39]</sup> suggested the use of 5 bricks high stack bonded prism.

Page<sup>[6]</sup> established aspect ratio correction factors that can be used as a multiplier for both the brick and brickwork prism to find the unconfined compressive strength (without platen effect) of the specimens from standard test (with platen effect) results. The table of correction factors is given below:

Table 2.1 Aspect Ratio Correction Factors for Compressive Strength Test

Aspect ratio	0	0.4	0.7	1.0	3.0	>5.0
Correction factor ( $k_c$ )	0	0.50	0.6	0.7	0.85	1.00

To relate prism strength to wall strength, important factors such as the aspect ratio of the prisms, size effects, the effects of vertical joints etc. must be considered. This involves the application of an empirical factor obtained through correlating prism tests with wall tests.

## 2.3 BRICK MASONRY UNDER COMPRESSIVE LOADING

### 2.3.1 Theoretical Investigation

Under uniform load brick masonry fails due to vertical splitting. The essential mechanism of failure, which has been accepted is

that the mortar is always weaker than the masonry units and it tends to be squeezed. This movement of the mortar is restrained by the bricks or blocks, which are then subjected to lateral tensile stress.

There are many theories of failure for masonry. The earliest attempt was due to Haller<sup>[40]</sup>. The first rational failure mechanism for masonry in uniaxial compression was proposed by Hilsdorf<sup>[18]</sup> (see Fig.2.1). He suggested that tensile stresses develop in units because of the differential lateral expansion characteristics of the brick and mortar (as described in section 2.2.1(c)). Assuming brick tension-compression failure envelope to be linear (Fig. 2.2), mortar triaxial strength similar to concrete and a co-efficient of nonuniformity between external compression and local compression established the average masonry strength at failure given by eqn. A.1 in Appendix-A. Masonry strengths computed by this equation was compared to the experimental results obtained from compression test on brickwork prisms. Hilsdorf<sup>[18]</sup> found that for higher strength mortars, the computed values were too low. However, the computed values were too high for the low strength mortars. This was thought to be due to an erroneous assumption of the failure criterion for bricks and mortar under triaxial stress states.

Based on elastic analysis of the brick-mortar interaction and assuming tension compression envelope of brick as linear, Francis et al.<sup>[22]</sup> devised a formula for predicting strength and behavior of stack bonded prisms. This formula is given in eqn.A.2 of Appendix-A. Discrepancies between theoretical and experimental results appeared due to the criteria set up for the final failure of the prism. It has been found by many investigators that the fracture process of the brick masonry under vertical compressive loading is gradual and therefore the failure load of the prism on the basis of initial fracture of the unit will lead to the conservative results.

Khoo and Hendry's<sup>[19]</sup> theory extended that of Hilsdorf's by defining masonry failure in terms of a limiting maximum lateral tensile strain for the brick. This tensile strain was assumed to be constant having a value of  $225 \times 10^{-6}$ , regardless of tensile strength. The material properties were derived from triaxial test on mortar and biaxial tests on solid bricks. The theoretical model is presented in eqn. A.3 of Appendix-A. The biaxial tension-compression envelope so found is mathematically expressed in eqn. 2.2.

Recently Atkinson et al.<sup>[20]</sup> have proposed a deformation failure theory for stack bonded brick masonry prisms in uniaxial compression. The theory includes force equilibrium and strain compatibility requirements and accounts for observed nonlinear multi-axial material behavior. Using measured material properties of the constituents, predicted prism deformations and failure load were compared to the experimental results obtained from prism tests. The model predicted upto about 60 to 70% of the experimental prism strength. The prediction of lower values again vindicates the lack of proper understanding of fracture process in the brick masonry.

Baba<sup>[41]</sup> introduced the concept "Biaxial stress coefficient" to predict the possible range of prism strength under uniaxial compression. Using this concept and fracture criteria under uniaxial compression and biaxial tension as well as in triaxial compression, he concluded that the prism strength and the possible range of efficiency could be predicted fairly well from the experimental data of the elastic constants of component materials.

All failure theories mentioned above predicted prism strengths which were either too conservative or nonconservative. This is possibly due to the lack of proper knowledge regarding the behaviour of mortar joint in the loaded prism.

### 2.3.2 Experimental Investigation

To predict the compressive behaviour of brick masonry several investigators used brickwork prisms, wallettes and full size walls as the basis of research experiment. A formula for the compressive strength of brick masonry prism, based on an analysis of a large number of test in the united states has been presented by Grim<sup>[11]</sup> and is shown in eqn. A.4 in Appendix-A.

Kirtsching<sup>[42]</sup> revealed that the strength of masonry subjected to compression is governed by the deformation as well as strength characteristics of the constituents. A large number of walls were tested. The walls were constructed from perforated clay bricks, calcium silicate cellular bricks, and light weight concrete solid bricks. From the results a relationship was obtained between the masonry strength and the modulus of elasticity of the brick and the mortar in the vertical direction. Nearly 60% of the calculated masonry strength were found to differ not more that  $\pm 20\%$  from the test results.

For the purpose of design, compressive strength of wall is the prime consideration. As has been stated in section 2.2.3(b), prism gives a reasonable indication of wall strength. But it will not completely reflect all the factors which influence the strength of the wall. The aspect ratio of prism also has an influence.

Anderson<sup>[24]</sup> carried out tests on four brick high stack bonded prisms and story-height walls and suggested that the ratio of wall strength to prism strength is 0.9.

S.A.A Brick Code (AS1640-1964)<sup>[27]</sup> applies a factor 0.75 to prism strength to obtain the wall strength. This was empirically derived from comparisons of the strength of four brick high prisms and walls constructed from the same brickwork.

## 2.4 MUD MORTAR IN MASONRY AS A BINDING MATERIAL

No research has been carried out home and abroad to introduce mud as a binding material along with the inclusion of jute fibre to improve the quality of load bearing masonry. For this reason no literature is available in this context. However, a very few literature which will help to develop the idea of improving masonry strength in which mud is used as binding material is reviewed below.

Because of wide range of soil composition and properties only one type of stabilizer is not suitable for all type of soil.<sup>[43]</sup> Mitchel<sup>[44]</sup> reported that reinforcement in the soil act as a tension carrier. Inclusion of ideally inextensible material, metal and plastic strip, bars, grids etc. which has rupture strain less than the maximum tensile strain in the soil, strengthens soil and inhibits both internal and boundary deformation. On the other hand extensible inclusion, natural and synthetic fibres, roots, fabrics, geotextiles which has rupture strains larger than the maximum tensile strains in the soil, gives some strengthening effect but more importantly greater ductility.

Swami Saran et al.<sup>[45]</sup> suggested that 33% wheat straw increases the strength of sundried mud brick by 37.5%, 30% and 24% for soils having silt plus clay 90%, 62% and 55% respectively. Compression test on 2cm x 6cm x 4cm bricks revealed these results.

Babu T. Jose et al.<sup>[46]</sup> introduced coconut fibre and bamboo strips to prevent the flow of soil from beneath the loaded earth. The result showed that the ultimate bearing capacity could be improved by 4 to 5 times compared to unreinforced soil for otherwise identical condition. They also reported that rough



reinforcing element gives better result due to greater stress transfer.

Rahman et al.<sup>[47]</sup> found that inclusion of 1.5% jute fibre, 1.5% straw and 15% rice husk (by weight) increase the crushing strength of 6" soil block cube by 50%, 14% and 25% respectively. The soil contained 75% of silt plus clay. The test was carried under simple compression.

Recently, a "Draft Indian Standard Guide for preparation and use of Mud Mortar<sup>[48]</sup>" has been published requiring comments on it. It was collected by communicating "Bureau of Indian Standards". According to the guide mud mortar for masonry should have clay size fraction 18 to 22%, silt size fraction 40 to 45% and sand size fraction 30 to 40%. All are by weight. But it is not clear from what consideration the above proportions have been suggested, also, whether this mortar imparts higher strength to the masonry or minimizes volumetric shrinkage.

## 2.5 SUMMARY

A review of literature relevant to this investigation has been presented in this chapter.

The properties of brick, mortar and brick masonry have been reviewed with particular emphasis on the properties which govern deformation and failure of stack bonded prism subjected to uniaxial compression. In addition, the theoretical ideas have been elaborately discussed. Previous studies regarding reinforced earth have been reported.

All theoretical investigations have considered the brick masonry as brittle material. For mortar joints, either the fracture criterion was derived from triaxial test or the fracture

criterion of concrete was used. Due to the presence of artificial constraint from machine platen most of the experimental investigations have not been representative of the actual behavior of brick masonry. Moreover, the possibility of using reinforced earth as binding material for brick masonry has not been explored.

It is apparent from the literature that no theory has yet been developed that allows the directional property of mortar joints in the loaded masonry. If a reliable formula could be developed to predict the failure load of brick masonry subjected to uniaxial compression, a large number of tests could be simulated and the significance of the parameters influencing the brick masonry under uniaxial compression studied. This thesis is an attempt to address this problem by developing formulae to model the deformation as well as the strength characteristics of brick masonry under uniaxial compression. The possibility of using reinforced earth as a binding material for brick masonry will also be studied.

## CHAPTER 3

### LABORATORY INVESTIGATIONS

#### 3.1 INTRODUCTION

Laboratory investigations have been carried out on two types of brick masonry, one with cement mortar, the other with mud mortar. The role of jute fibre in mud mortar also have been investigated. An experimental program was designed to determine the essential properties of the constituent materials which influence the behaviour of masonry under compression. These properties are required to predict the compressive behaviour of masonry and to provide basic input data for the finite element analysis of prisms presented in chapter 6.

Brick masonry, being as an assemblage of bricks set in a mortar matrix, the properties of bricks, the mortar and masonry itself must be determined. These were established from various types of tests performed on representative samples of the brick, the mortar and the brick masonry used in this investigation. Guided by the reviewed literature prisms were considered to be the specimen suitable for research experiment both for cement mortared and mud mortared masonry. However, due to the limitation of handling and test facilities only wallettes with cement mortar were built and tested as the representative of full size wall.

The laboratory investigation was carried out in two phases. The tests of first phase fell into two categories. The first category comprised of the standard tests to determine the deformation and strength characteristics of brick and cement mortar. The second category of the first phase was concerned with the determination of physical and chemical properties of mud mortar along with its

deformation, strength and volumetric shrinkage characteristics with and without jute fibre inclusion. Moisture content at workability of mud mortar has been determined.

The second phase concerned with the fabrication and testing of prisms and wallettes with cement mortar and only prisms with mud mortar.

In the second phase 2,3,4,5 and 6 brick high prisms and wallettes were constructed with cement mortar and tested under compression. The different heights were considered to investigate the effect of platen restraint on the height of the specimen. Most of the prisms were constructed stack bonded except some 5 brick high prisms with vertical joints in alternate layer. Vertical joints were introduced with the idea that the prisms with vertical joints may represent the wall(wallette) more realistically. The wallettes were 3 brick wide and 10 bricks high.

For masonry with mud mortar, 5 brick high stack bonded prisms were constructed. The mud mortar contained different percentages of randomly distributed jute fibre. However, in some prisms, instead of jute fibre, jute mats were provided in the middle of mortar bed joint to ensure uniform distribution of fibres. All these prisms were tested under compression to determine the effect of the inclusion of jute fibre on the compressive strength of brick masonry.

### 3.2 PROPERTIES OF BRICK

The same type of solid clay bricks were used for all aspects of the investigation. They were procured from a local manufacturing plant (Conforce Brick). All bricks were from the same batch and stored in the laboratory after procurement till their use in the experimental program. The nominal brick size was 9.5"x4.5"x2.75"

having an average weight of 7.5 lbs. Water absorption of these bricks were determined according to ASTM C67<sup>197</sup>. Determination of the strength and deformation characteristics of brick have been described in the following sections. The properties of brick are summarized in Table 3.1.

### 3.2.1 Compressive Strength of Brick

Brick compressive strength is an important property which has been traditionally used for brick quality control as well as a parameter to define strength characteristics. As discussed in chapter 2, the standard compression test involves loading the specimen between the solid steel platen of the testing machine. For typical brick dimension this results in significant artificial strengthening due to aspect ratio effects. To obtain true compressive strength, the effect of platen should be accounted for. Due to nonavailability of flexible brush platen, the standard test method ASTM C67<sup>197</sup> have been followed.

Twelve bricks were selected at random from the stack. From each brick half brick bat was cut by the cutting saw. Neat cement paste was used on both faces to fill frog mark and surface flaws. Thin sulfer capping was used on both the surfaces. Accurate level of the capped surfaces was maintained using sprit level. Test was performed between the steel platen of 250 ton capacity compression testing machine of the concrete laboratory. Load was applied at a rate of 15 tons/min. All the specimens failed by crushing. The mean compressive strength is presented in Table 3.1. Complete test results are contained in Appendix-B.

Table 3.1 Summary of Brick Properties

Type of test		$\bar{X}$	S	C. of V. (%)	No. of specimens
Compressive strength (psi)		3120	577.7	18.5	12
Indirect tensile strength (psi)		126	12.7	10.0	12
$E_b$ (psi)		$2.2 \times 10^6$	-	-	6
Water absorption (%)	Air-dry condition	0.49	0.9	18.18	12
	Immersed for 30 min.	14.97	1.39	9.32	12
	Immersed for 1 hr.	15.77	1.55	9.84	12
	Immersed for 24 hrs.	15.99	1.53	9.56	12

Note:  $E_b$  = Initial modulus of elasticity of brick.

$\bar{X}$  = Mean, S = Standard deviation,

C.of V. = Coefficient of variation

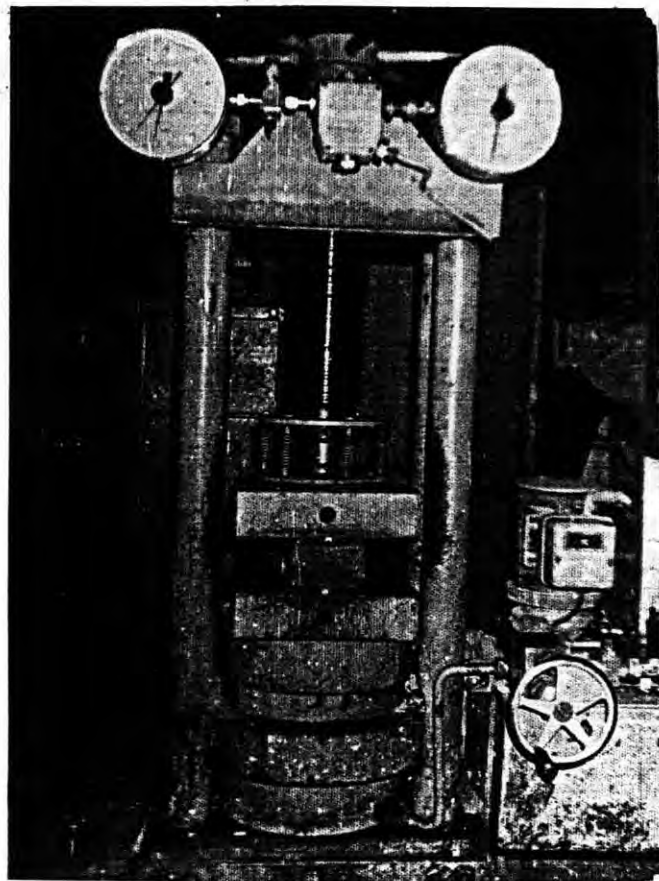
1 psi = 6.896 KPa

### 3.2.2 Tensile Strength of Brick

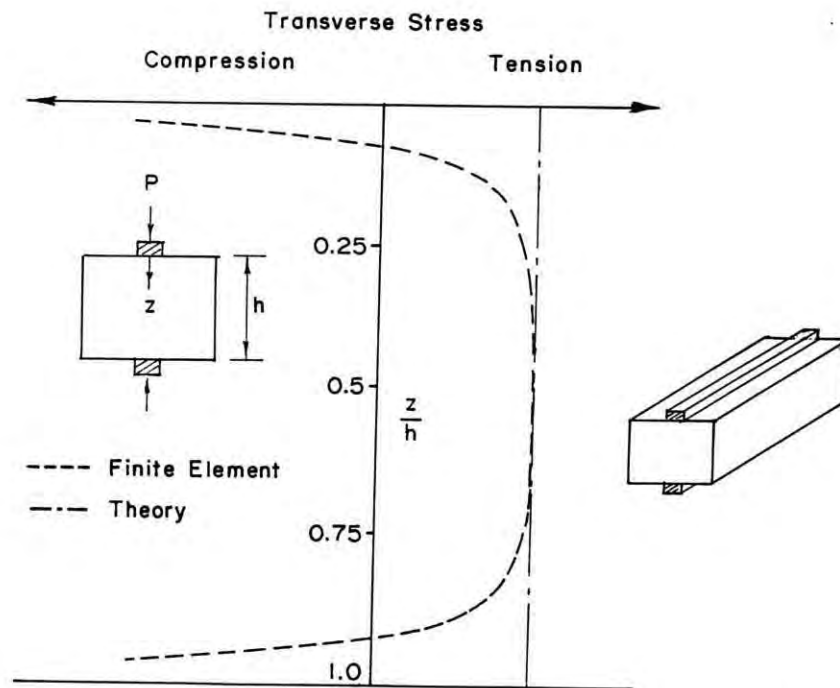
Tensile strength of brick is of great importance in defining the behaviour of brick masonry as final failure often occurs in some form of biaxial tension split originating in the brick. Direct tensile strength test are difficult to perform on brittle materials. Hence indirect tensile strength was determined from a splitting test. A typical testing arrangement of the test is shown in Fig. 3.1(a).

The indirect tensile strength of a homogeneous prism, suggested by Thomas and O'Leary <sup>[17]</sup> as a more convenient alternative to the use of cylinders, can be obtained by the eqn. 2.1 of chapter 2. This equation was verified by Ali <sup>[47]</sup>. The test was modeled using a two-dimensional linear elastic plane stress finite element analysis. A very fine mesh was provided near the loading point. The load was applied through a steel strip whose width was 10% of the width of the specimen. It revealed that the tensile stress is fairly uniform along the middle plane with the maximum value being equal to the value obtained using eqn. 2.1 and is shown in Fig. 3.1(b).

A total of 12 randomly selected dry bricks from the batch were tested. The load was applied through a steel plate 0.45 inch wide and 0.2 inch high. The plate width was therefore 10% of the width of the specimen. The load was applied using 250 ton capacity compression testing machine of concrete laboratory with a loading rate of 2 tons/inch. Failure occurred by vertical splitting directly beneath the loading plate. The mean tensile strength is presented in Table 3.1. Detail experimental results are contained in Appendix-B.



(a) Testing Arrangement



(b) Transverse Stress Distribution Along the Centre Line after S. Ali<sup>[49]</sup>

Fig. 3.1 Splitting Test on Brick



### 3.2.3 Deformation Characteristics of Brick

#### a) Modulus of Elasticity

Brick in a masonry wall usually carries load in a direction normal to the bed plane. The evaluation of deformation characteristics of the brick with the load applied normal to the bed plane is more difficult, since a brick loaded in this manner exhibits significant aspect ratio effects. Moreover, the deformation characteristics of a brick between the machine platen will no doubt differ from that of in-situ deformation characteristics due to the presence of mortar joints in the brickwork. To avoid this problem, deformation characteristics of bricks were measured from the central brick of a 5 brick high stack bonded prism loaded in uniaxial compression (see Fig. 3.2). The prism tests were also used to establish the in-situ properties of the mortar joint as well as brickwork with cement mortar (see sections 3.3.3 and 3.7.1).

In this investigation 6 prisms were used. The prisms were constructed and cured in the same manner as the masonry specimens with cement mortar. Detail construction and test procedure are given in section 3.6.1 and 3.7.1 respectively. Deformations were measured on a central 50 mm gauge length on opposite faces of the central brick using Demec gauge. The readings were averaged to avoid bending effect. A plot of the average stress-strain curve is shown in Fig. 3.3. The mean initial tangent modulus obtained from the test is given <sup>in</sup> Table 3.1. Detail results are presented in Appendix-B.

### 3.3 PROPERTIES OF CEMENT MORTAR

The cement mortar used throughout the investigation was 1:4 (cement:sand). The variation of bulk density in materials were

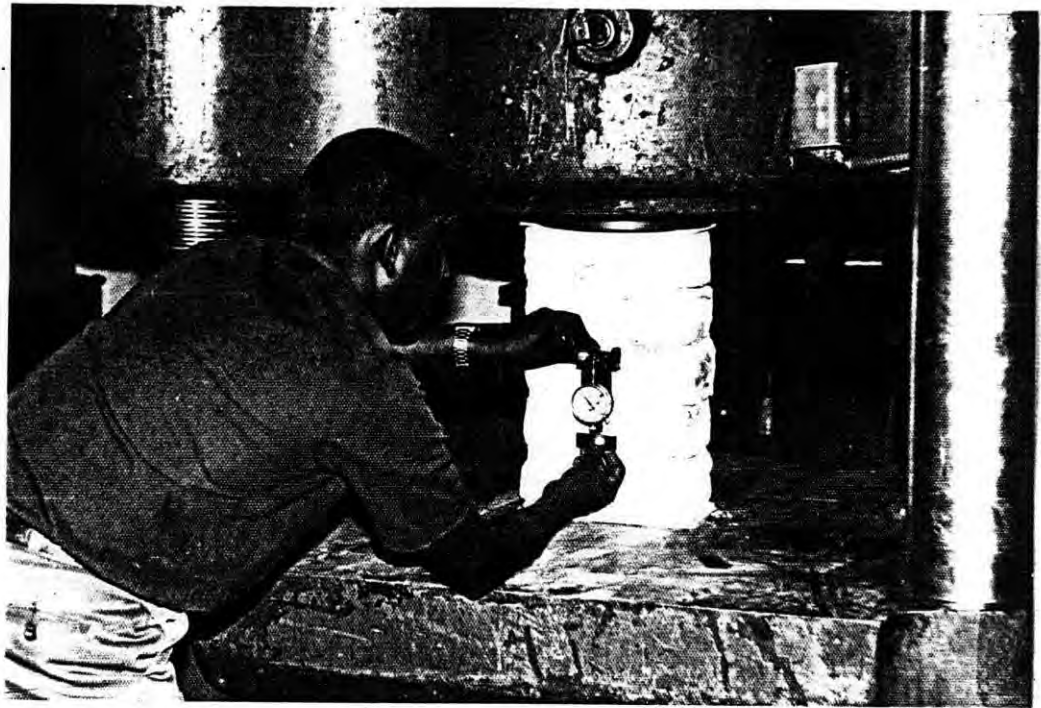


Fig. 3.2 Testing Arrangement for Vertical Deformation of Brick.

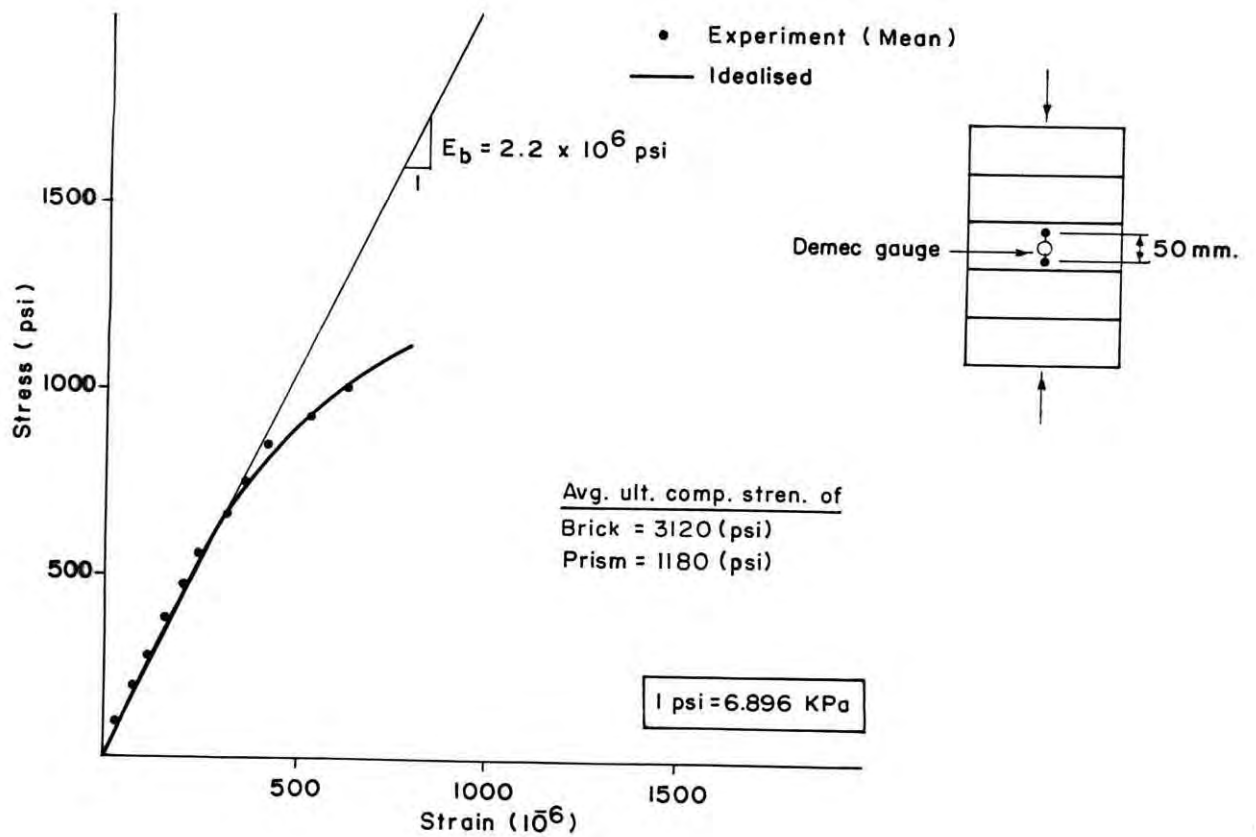


Fig. 3.3 Average Stress-Strain Curve for Brick.

eliminated by weighing measured volumes of fresh materials and thereafter batching by weight. All mix components were stored in the laboratory for the duration of the testing program.

The cement used in this investigation was "Chatak Brand" and the sand was "Sylhet" sand. Properties of the cement and the sand as determined according to ASTM standards are given in Table 3.2.

Table 3.2 Properties of Cement and Sand

Cement	Unit weight	91.0 lbs/cu-ft
	Normal consistency	23.0%
	Initial setting time	2.0 hrs. 5.0 mins.
Sand	Unit weight	94.0 lbs/cu-ft
	Fineness modulus	2.76

Note: 1 lbs/cu-ft = 15.985 Kg/cu-m

An estimate of compressive strength, tensile strength and deformation characteristics of cement mortar is required for the determination of compressive strength of brickwork and to aid in elastic finite element analysis of stack bonded prism presented in chapter 6. The properties of cement mortar are summarized in Table 3.3. Determination of strength and deformation characteristics of cement mortar have been described in the following sections.

Table 3.3 Summary of Cement Mortar Properties

Type of test	$\bar{X}$	S	C. of V. (%)	No. of specimen tested
Comp. strength (psi)	1240	32.17	2.59	36
Ten. strength (psi)	135	7.73	5.73	36
$E_m$ (psi)	$1.0 \times 10^6$	-	-	12

Note:

$E_m$  = Initial modulus of elasticity of cement mortar

$\bar{X}$  = Mean, S = Standard deviation and C. of V. = Coefficient of variation

1 psi = 6.896 KPa

### 3.3.1 Compressive Strength of Cement Mortar

Standard test for compressive strength of cement mortar was performed in order to check the quality of test specimens adopted in this investigation. The compressive strength of mortar was determined from uniaxial compression test of 2" mortar cube prepared and tested according to ASTM C109 [33].

Three 2" cubes were prepared from each batch of mortar mix during the fabrication of test specimens. The cubes were then cured for 28 days and tested under compression. Average compressive strength of each batch of mortar mix used for different types of

test specimens is shown in Table 3.4. The table shows that the compressive strength has negligibly small variation for different batches of mortar mix as well as for different types of test specimens. The table also shows that the coefficient of variation of mortar compressive strengths for different types of test specimens is only 2.59% which indicates a good quality control. Therefore, it can be concluded that the compressive strength of mortar is same for all specimens having a value of 1240 psi.

### 3.3.2 Tensile Strength of Cement Mortar

Tensile failure of masonry can occur either as a tensile bond failure at the brick-mortar interface, or as a tensile failure in the constituent materials. However, the second type of failure is more common in stack bonded prism. In this section only the determination of tensile strength of mortar will be described. The tensile strength of mortar was determined using mortar briquette prepared and tested according to ASTM standard C190 [13]. Three briquettes were prepared from each batch of mortar mix during the fabrication of each type of test specimens. The briquettes were tested at the age of 28 days. Tensile strength of mortar of each batch for different types of test specimens is shown in Table 3.5. The table shows that the variation in mortar tensile strength for different batch of mortar mix and different types of test specimens is not significant. The table also shows that the coefficient of variation of tensile strength of mortar for different types of test specimens is only 5.73%. Ali [49] showed that 50% increase in mortar tensile strength results in only 2.5% increase in masonry strength. Therefore, the variation in mortar tensile strength for different batch of mortar mix and different types of test specimens can be neglected. At the same time, all specimens may be considered of being composed of same mortar having tensile strength of 135 psi.

Table 3.4 Compressive strength of Cement Mortar for different test specimens

Test specimen <sup>(1)</sup>	Specimen designation <sup>(2)</sup>	No. of specimen fabricated	Avg. comp. strength of 3 mortar cubes (psi)			Mean comp. strength of batches (psi)
			Batch No.			
			1	2	3	
Prism	2SPC	6	1303	-	-	1303
	3SPC	6	1235	-	-	1235
	4SPC	6	1182	-	-	1182
	5SPC	24	1195	1206	1278	1227
	6SPC	6	1224	-	-	1224
	5VPC-A	12	1240	-	-	1240
	5VPC-B	12	1250	-	-	1250
Walette		6	1280	1300	1200	1260
$\bar{X}$						1240
S						32.17
C. of V. (%)						2.59

Note: (1) and (2), Figure 3.12

$\bar{X}$  = Mean, S = Standard deviation

C. of V. = Coefficient of variation

1 psi = 6.896 KPa

Table 3.5 Tensile strength of Cement Mortar for different test specimens

Test specimen <sup>(1)</sup>	Specimen designation <sup>(2)</sup>	No. of specimen fabricated	Avg. tensile strength of 3 mortar cubes (psi)			Mean tensile strength of batches (psi)
			Batch No.			
			1	2	3	
Prism	2SPC	6	125	-	-	125
	3SPC	6	135	-	-	135
	4SPC	6	144	-	-	144
	5SPC	24	124	132	128	128
	6SPC	6	125	-	-	125
	5VPC-A	12	145	-	-	145
	5VPC-B	12	135	-	-	135
Walette		6	153	130	143	142
$\bar{X}$						135
S						7.73
C. of V. (%)						5.73

Note: (1) and (2), Figure 3.12

$\bar{X}$  = Mean, S = Standard deviation

C. of V. = Coefficient of variation

1 psi = 6.896 KPa

### 3.3.3 Deformation Characteristics of Cement Mortar

#### a) Modulus of Elasticity

To predict the deformation and strength characteristics of masonry and to aid the finite element analysis of brick prisms the modulus of elasticity of mortar joint is essential. By loading a stack bonded prism in uniaxial compression and measuring the deformation in individual bricks as well as the average deformation on a gauge length encompassing several bricks and mortar joints, the net deformation characteristics of the mortar joints can be determined. The readings of brick deformation obtained in section 3.2.3 and the readings of masonry deformation obtained in section 3.6.1 were used. Longitudinal deformation of brick was measured on a central 50 mm gauge length on opposite faces of the central brick of 5 brick high stack bonded prisms while longitudinal deformation of masonry was measured in the same manner on a 200 mm gauge length encompassing 2 mortar joints, one full brick and parts of 2 bricks as shown in Fig. 3.4. Both the tests have been performed under the same condition.

If it is assumed that all the bricks encompassed by the Demec gauge are in a uniform state of vertical stress the difference between the total measured deformation and the deformation of brick can be attributed to the mortar, and the corresponding mortar strain determined.

The mortar strain at any stress level can therefore be expressed as:

$$\epsilon_m = \frac{\epsilon_t L_t - \epsilon_b L_b}{L_m} \quad (3.1)$$



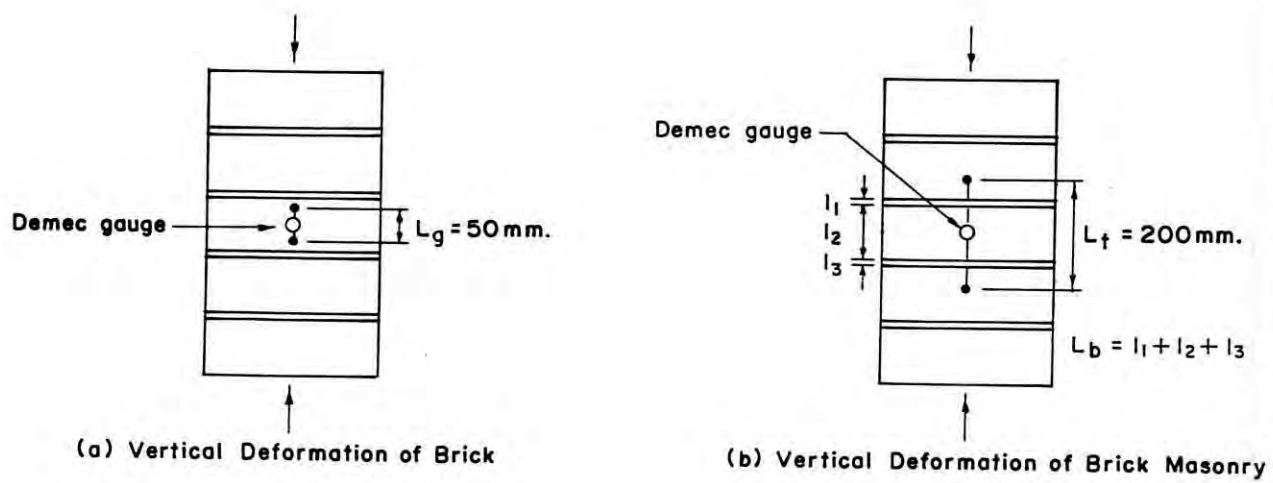


Fig. 3.4 Measurement of Vertical Deformation of Brick and Brick Masonry.

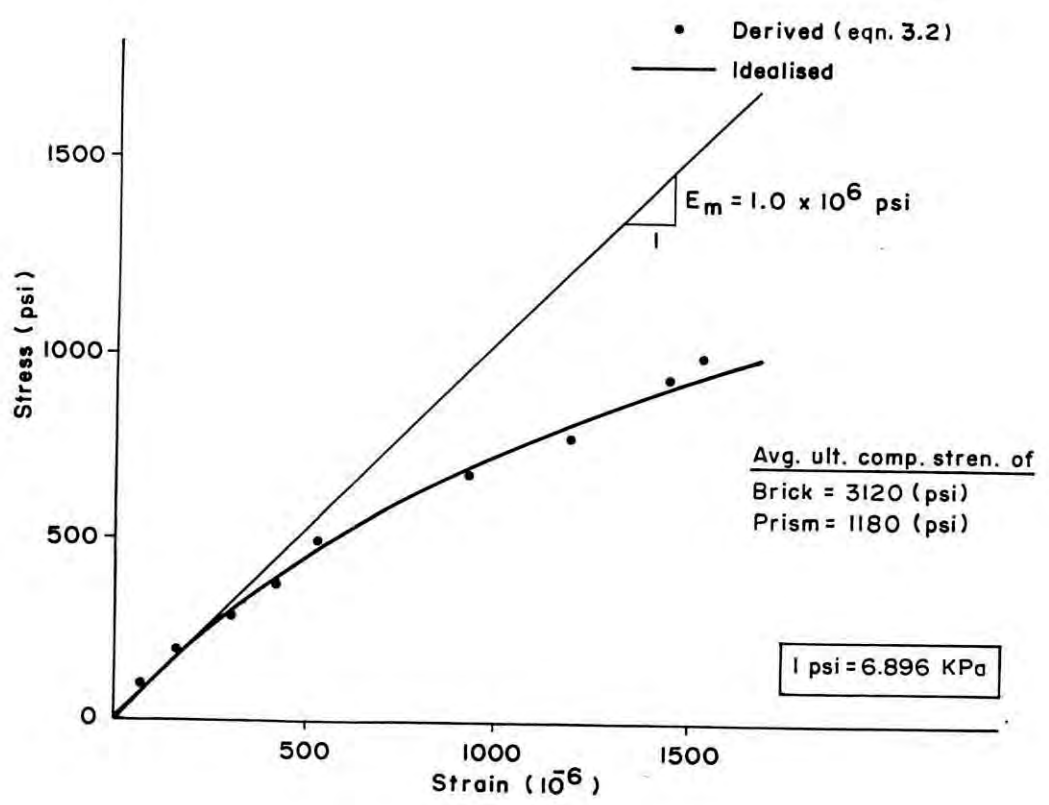


Fig. 3.5 Average Stress-Strain Curve for Cement Mortar.

in which  $\epsilon_t$  = total measured strain;  $\epsilon_b$  = strain in the brick;  $L_m$  = total mortar thickness,  $L_b$  = total thickness of brick included within  $L_t$  and  $L_t$  = total gauge length. Substituting the appropriate values of  $L_m$ ,  $L_b$  &  $L_t$ , the mortar strain is found to be

$$\epsilon_m = 9.045\epsilon_t - 8.045\epsilon_b \quad (3.2)$$

Using equation 3.2, the net stress-strain curve for mortar was derived from the average strain of masonry obtained from a set of 6 prisms and the strain of brick obtained from another set of 6 prisms. A plot of the derived stress-strain curve is shown in Fig. 3.5. The more detailed results have been presented in Appendix-B.

### 3.4 PROPERTIES OF MUD MORTAR

The soil used for preparing mud mortar was collected from Potter's house from Rayer Bazar. After air drying, the soil was stored in the laboratory for the period of testing program. At first, a preliminary investigation was made to determine soil properties. This preliminary investigation includes the determination of physical and chemical properties of the soil. Then tests such as moisture content at workability, shrinkage limit as well as compressive strength of mud mortar before and after the inclusion of fibre were carried out.

### 3.4.1 Physical Properties of Soil

Physical properties of the soil are required for the classification of the soil. The following physical properties of the soil were determined:

- i) Specific gravity
- ii) Grain size distribution
- iii) Atterberg limits (Liquid limit, plastic limit and shrinkage limit)
- iv) Moisture content of stored air dried soil.

For the determination of these properties standard tests were performed in accordance with the procedure specified by the American Society for Testing materials (ASTM). ASTM Standards<sup>300</sup> D854, D422, D423, D427 and D427 were followed for specific gravity, grain size distribution, liquid limit, plastic limit and shrinkage limit respectively. However, moisture content of stored air dried soil was determined by usual method. The test results are presented in Fig. 3.6 and Table 3.6. The soil was then classified according to U.S. Department of Agriculture.

### 3.4.2 Chemical Properties of Soil

The following chemical tests were performed:

- i) pH value.
- ii) Organic content.
- iii) Sulfate content.

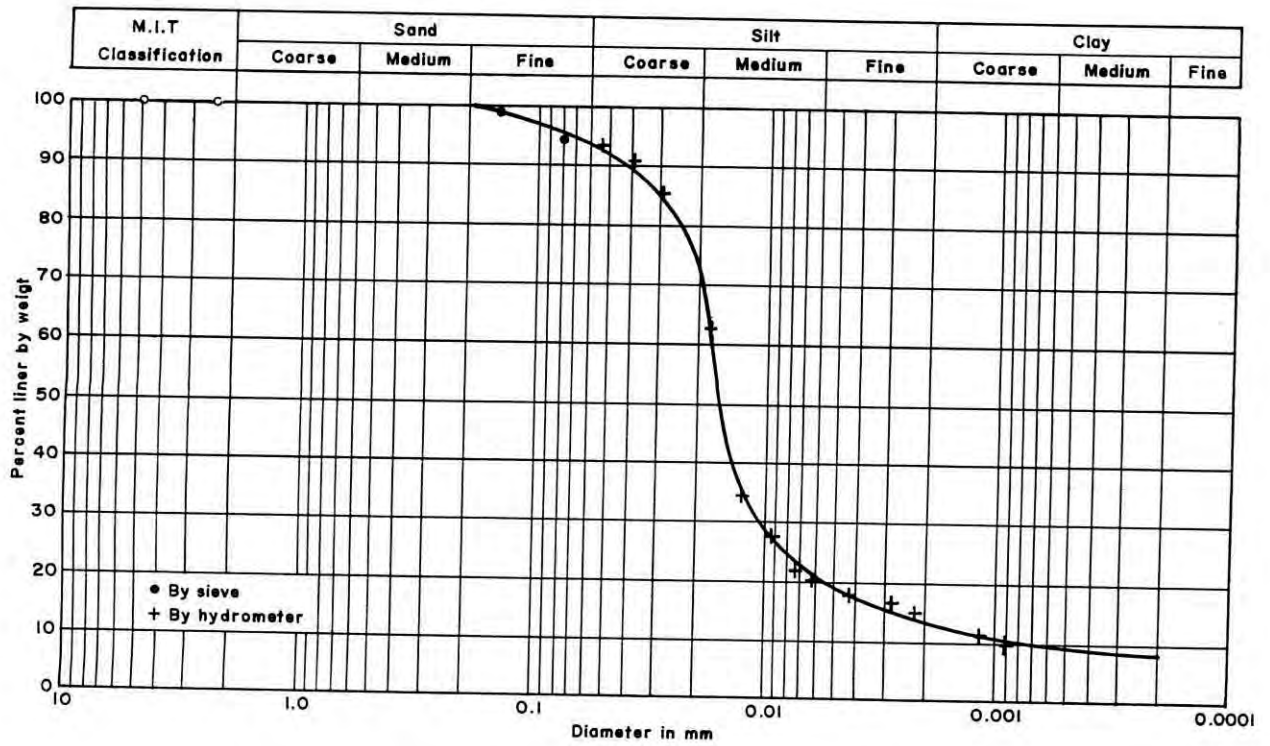


Fig. 3.6 Grain Size Distribution of Soil

Table 3.6 Physical and Chemical Properties of Soil

<u>A. Physical properties:</u>	
i) Grain size distribution	
Fine sand (%)	6
Silt (%)	80
Clay (%)	14
Percent passing # 200 sieve	96
ii) Specific gravity	2.75
iii) Moisture content of stored air dried soil (%)	1.75
iv) Atterberg Indices	
Liquid limit (%)	49
Plastic limit (%)	25.5
Plasticity index (%)	23.5
Shrinkage limit (%)	24.3
v) Group classification of soil (U.S. Dept. Of Agriculture)	silty loam
<u>B. Chemical properties</u>	
i) pH	6.4
ii) Organic matter (%)	3.3
iii) Sulfate content (%)	0.1552

The pH value of the soil was determined by pH indicator papers by inserting a strip of indicator paper into the wet soil for one minute. The wet reverse side of the paper was then compared with the colour scale.

To determine the organic matter two grams of air dry soil after passing through 2 mm sieve was taken into a beaker of 150 ml size. Distilled water was added to the sample to give 1:1 soil-to-water ratio and covered the beaker with a rubber water-glass. Initially 30%  $H_2O_2$  was added in increments of 5 to 10 ml in order to oxidise the organic matter. For complete subsidence of frothing, constant stirring was done with a low heat (65°-70°C) for 10 to 20 minutes using a water bath. When the sample had lost

its dark colour, it was transferred into a centrifuge tube for washing of the solution. After several washing, the sample was placed in a oven and weighed to the nearest 0.001 gm after 24 hrs. The percentage loss of the sample was calculated as organic content of the sample.

The sulfate content was determined according to the British Standard B.S. 1377:1975<sup>[5]</sup>. The experimental results are presented in Table 3.6.

### 3.5 TESTS FOR MUD MORTAR

As mentioned earlier that an effort has been made to investigate the possibility of using mud mortar as binding material for low-rise building in rural areas. Jute fibre and jute mat have been used as reinforcements in this case. The effect of fibre on the volumetric shrinkage and deformation and strength properties of mud mortar have been investigated.

#### 3.5.1 Water Content of Mud Mortar at Workability

To prepare mud mortar of desired consistency and workability certain amount of water is required to be added to the soil. Determination of water content of mud mortar at workability was felt necessary as the difference between the shrinkage limit of the soil and the water content when the soil is in the state of workable mortar determines the degree to which the mortar will undergo volumetric shrinkage after drying. Since, this investigation involves two types of mud mortar (the first without fibre and the second with varying percentages of fibre), a question may arise that water content of mortar without fibre at workability may be different from that of mortar with fibre as the fibre might influence the amount of water required to make

the mortar workable. Moreover, mud mortar with different fibre content may have different water content at workability. However, all these hypothesis are beyond the scope of the experimental interpretation because no National or International Standard has yet been developed which identifies the state of workability of mud mortar and in this investigation it was solely dependent upon the mason's satisfaction. But it may be assumed that for small percentage of fibre, the effect of inclusion on water content at workability will be very negligible.

For the experimental part two types of mud mortar were prepared having desired consistency and workability as per the decision of a mason having more than 15 years experience of constructing brick masonry with cement mortar as well as mud mortar. The first type was fibre free and the second type was with different percentages of jute fibre. For the second type the selected percentages of fibre by air dried weight of soil were 0.5%, 1%, 1.5%, 2%, 2.5% and 3% respectively.

The length of fibre was one inch. These mortars were also used for the test of shrinkage limit and compressive strength presented in sections 3.5.2 and 3.5.3 respectively. Three mortar mixes were prepared for each soil-fibre combination for the determination of water content. The average water content at workability of different mortar mix is presented in Table 4.3 in the next chapter.

### **3.5.2 Shrinkage Limit of Mud Mortar**

Factor controlling the volumetric shrinkage and formation of channels in the mortar bed joint is shrinkage limit defined as the moisture content below which if any loss of moisture takes place, the soil undergoes no volumetric shrinkage. Therefore, if the shrinkage limit of mud mortar is increased to its water

content at workability no volumetric shrinkage should take place and consequently no cracks will form in the mortar joint when it dries. Therefore, it is required to check the shrinkage limit of the soil before and after the inclusion of fibre.

The same mortar mixes used for the determination of water content at workability in the previous section were used in this case. The mortar mixes had inclusions of 0%, 0.5%, 1%, 1.5%, 2%, 2.5% and 3% jute fibre by weight of air dried soil. The mortar mixes were taken in the shrinkage dishes to form pats. Oven dried pats of different mortar mixes are shown in Fig. 3.7. These pats were used to determine shrinkage limit by mercury displacement method according to ASTM Standard D427<sup>[50]</sup>. The test results are presented in Table 4.4 in the next chapter.

### 3.5.3 Compressive Strength Of Mud Mortar

In this investigation jute fibre was included in the mud mortar with the view that the inclusion will impart higher strength to the masonry. The role of inclusion of fibre on the compressive strength of mud mortar becomes necessary because of the fact that with the same bricks the higher the mortar strength, the higher the masonry strength.

To determine the compressive strength of mud mortar with or without jute fibre, two types of tests were performed. The first was on 2" mortar cubes following ASTM Standard C109<sup>[53]</sup> and the second was unconfined compression test on 1.4 inch diameter by 2.8 inch high mortar cylinders following ASTM Standard D2166<sup>[50]</sup>. Since, compressive strength of soil is greatly dependent upon the moisture content of the test specimens, all specimens were air dried for sufficient days so that their moisture contents comes at a constant value at or near the moisture content of the soil at air dried condition. The



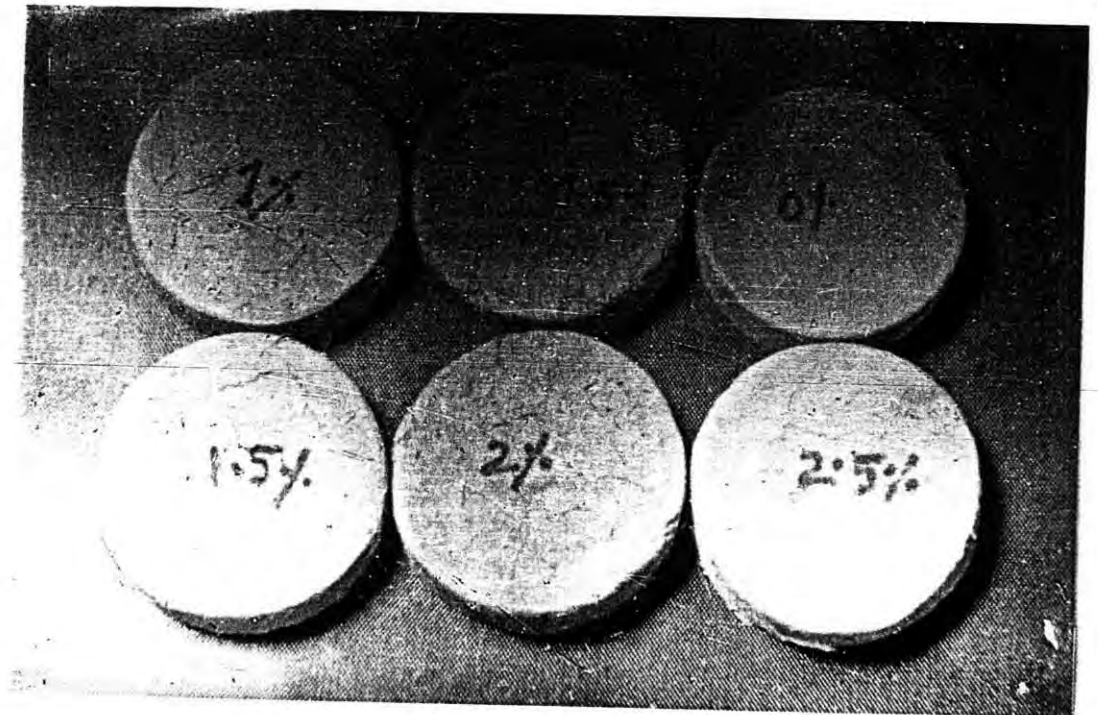


Fig. 3.7 Oven Dried Soil Pats with Different Percentages of Jute Fibre for the Determination of Shrinkage Limit.

specimens with 0%, 0.5%, 1.0%, 1.5%, 2.0%, and 2.5% fibre by air dried weight of the soil have been considered for this investigation.

For the preparation of mortar cubes, 2 lbs of air dried soil was taken for each batch and the required amount of fibre and water were added. Mixing was done properly by hand. The mortar mixes were then taken in the mould and compacted according to ASTM Standard C109<sup>[10]</sup>. For each batch of mortar mix three cubes were prepared. The cubes were kept inside the mould for 10 days and air dried in the laboratory for 35 days. The air dried specimens showed slightly irregular faces. Two faces of the cubes on which load will be applied were gently rubbed on sand paper and leveled using spirit levels before test. These cubes were then tested under compression in the concrete laboratory. Following the test water content of each specimen was determined.

For specimens, adopted for unconfined compression test the same procedure was followed to prepare each batch of mortar mix. The mixes were then taken in the mould and compacted by standard procedure. The compacted samples were then extracted from the mould by an extruder. From compacted samples 1.4 inch diameter by 2.8 inch high cylindrical specimens were prepared by trimming with a piano wire. Three specimens were prepared for each batch of mortar mix. The samples were air dried for 45 days. The top and bottom faces of all specimens were leveled in the same manner as for mortar cubes. These specimens were tested in unconfined compression testing machine in the soil laboratory. Water content of each specimen was determined following the tests.

Mortar cubes without fibre failed by sudden crushing while those with fibre behave as perfectly plastic material with an increase in lateral dimension with the incremental load and no failure load was obtained. Some of the cubes after compression test are shown in Fig. 3.8.



Fig. 3.8 Mortar Cubes with Jute Fibre after Compression Test.

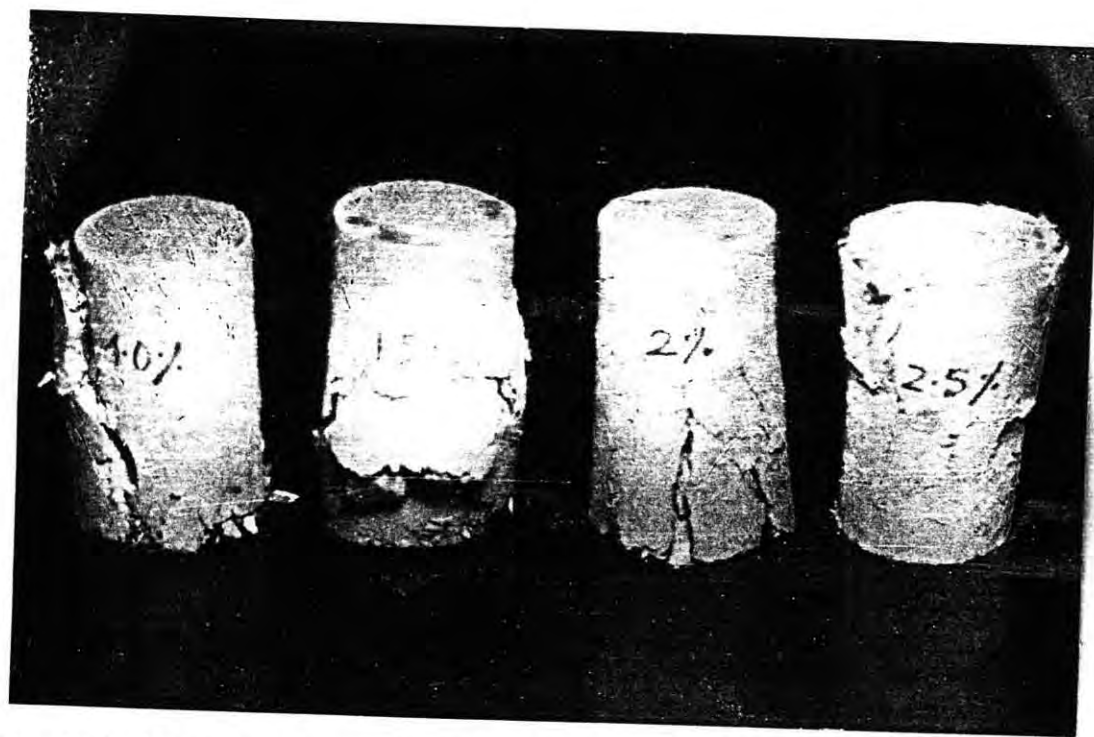


Fig. 3.9 Mortar Cylinders with Jute Fibre after Unconfined Compression Test.

During unconfined compression test, the specimens without fibre failed by sudden crushing. But the specimens with fibre in contrast to cubes, showed an indication of failure marked by incapability of the specimens to carry further load. These specimens after test is shown in Fig. 3.9.

Summary of the test results along with the water content during test are presented in Tables 4.5 and 4.6 in the next chapter. Detailed experimental results are contained in Appendix-B.

### 3.6 FABRICATION OF TEST SPECIMENS

A total of 130 test specimens were constructed of which 78 were with cement mortar and 52 were with mud mortar.

Among the specimens with cement mortar 6 were wallettes and 72 were prisms with different heights (2,3,4,5 and 6 brick high) having bond pattern either stack bonded or with vertical joints in alternate layer. These specimens were tested to investigate the strength and deformation characteristics and failure mode of masonry with cement mortar under compression. The tests are also useful in defining the in-situ deformation properties of bricks and mortar bed joints under compression (section 3.2.3 and 3.3.3). The specimens with mud mortar were 5 brick high stack bonded prisms. Out of 52 prisms with mud mortar 42 prisms were constructed with randomly distributed jute fibre in the mortar joints. The other 10 prisms were constructed with jute mat in the middle of mortar joints with a view of providing uniform distribution of fibre. Thirty prisms with randomly oriented fibre and 6 with jute mat were tested to investigate the effect of inclusion of randomly as well as uniformly distributed fibres with mud mortar on the compressive strength and failure mode of brick masonry. The remaining 12 prisms with different percentage

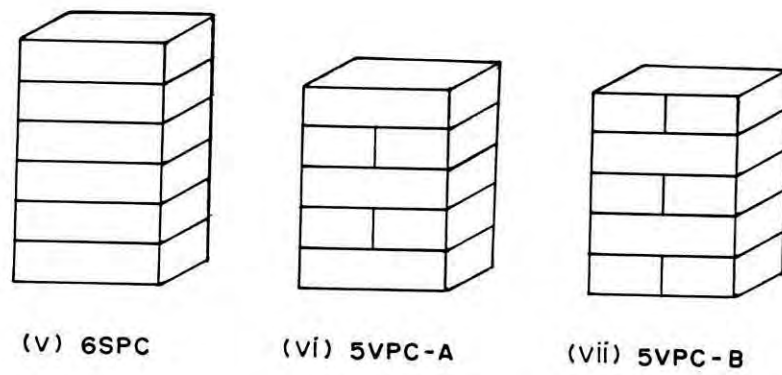
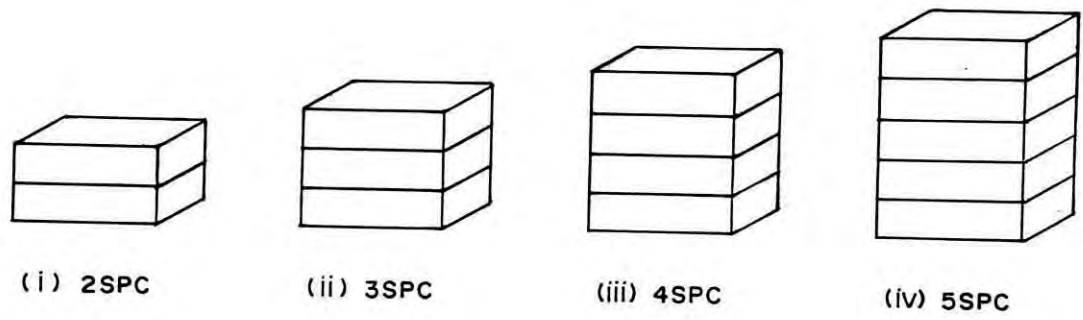
of fibre and 4 prisms with jute mat were used as pilot specimens to determine the role of inclusion of fibre in minimizing random cracks in the mortar bed joint and to detect the extent of curing as described in section 3.6.4.

### 3.6.1 Construction of Cement Mortared Masonry

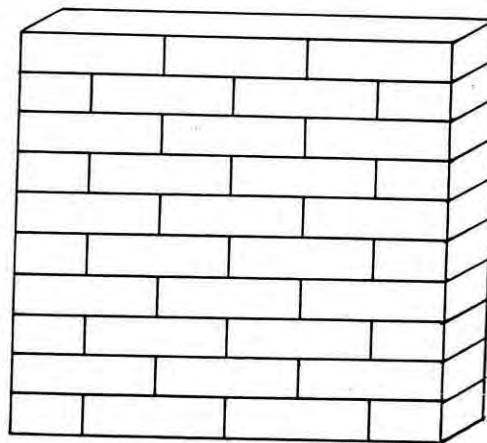
As has been discussed in section 3.6, two categories of test specimens were constructed with cement mortar as binding material. The first category was prisms and the second was wallettes. The prisms were single wythe, 1 brick wide and 2,3,4,5 and 6 brick high stack bonded or with vertical joints as per requirement. The wallettes were also single wythe, 3 brick wide and 10 brick high with an aspect ratio (height/minimum width) of 6.7 built in running bond. Fig. 3.10 depicts the test specimens with their designation. All test specimens were constructed with a joint thickness of  $3/8$  inch (10 mm).

To construct the test specimens, mortar was layed to a thickness of  $3/8$  inch. A polyethylene sheet was used to prevent any adhesion of mortar to the floor. Rods of  $3/8$ " dia were used to facilitate the spreading of mortar. Bricks were laid over this mortar bed as required by the plan of the specimens.

All vertical joints between bricks were filled up with mortar by trowels. Temporary barrier were put at the ends of these vertical joints to prevent mortar from spreading out. Finally a  $3/8$ " (10 mm) thick layer of mortar was placed on the top of all specimens. The mortar topping was smoothened with steel trowels.



(a) Prisms



(b) Wallette

Fig. 3.10 Different Test Specimens Constructed with Cement Mortar

### 3.6.2 Curing of Cement Mortared Masonry

All test specimens with cement mortar were moist cured for 7 days and air cured for 21 days before the tests. Moist curing was done by wrapping the specimens with gunny bags and kept moist by frequent sprinkling of water.

### 3.6.3 Construction of Mud Mortared Masonry

All the specimens with mud mortar were 5 brick high stack bonded prisms (Fig. 3.10(iv)). The construction procedure is similar to the construction with cement mortar (section 3.6.1) with the exception that, in the case of prisms with jute mat, plain mud mortar was first spreaded to a thickness of  $\frac{3}{16}$  inch. After placing a wet jute mat over it, plain mud mortar was again spreaded so that the total mortar bed thickness becomes  $\frac{3}{8}$  (10 mm) inch. Similar to the specimens with cement mortar, a  $\frac{3}{8}$  inch thick layer of cement mortar was placed at the top and bottom of all specimens to avoid surface irregularity.

### 3.6.4 Curing of Mud Mortared Masonry

Control of water content of the mortar bed before testing of specimens is important as the strength and deformation of mud mortar is greatly dependent upon its water content. This was achieved by air curing for 50 days inside the laboratory. Such period of curing was determined by breaking the pilot specimens at different age and determining the water content of the mortar bed. The pilot specimens showed that after 50 days of air curing, the water content of mortar bed comes close to the water content of air dried soil and no further loss of moisture occurs due to aging.

### 3.7 TESTING OF MASONRY SPECIMENS

As mentioned previously, some of the specimens are very useful in determining the in-situ properties of brick and mortar bed joints. The details of preparation of these specimens have been presented earlier. In the following sections the tests for deformation characteristics and compressive strength of masonry are described.

#### 3.7.1 Testing for Deformation Characteristics of Cement Mortared Masonry

To obtain the deformation characteristic of masonry 5 five brick high stack bonded prisms were used. This particular size of prism was considered to be more appropriate for tests from the consideration of platen effect and slenderness ratio. The test procedure is similar to that which has been described in section 3.7.2. The prisms were loaded in uniaxial compression to failure. Longitudinal strain was measured on a central 200 mm gauge length on both faces of the prisms using Demec gauge. These readings were averaged to eliminate bending effects. The gauge length encompassed 2 mortar joints, one full brick and parts of two bricks. The testing arrangement is shown in Fig. 3.11. Test results are summarized in Table 4.1 in the next chapter. Detailed test results are presented in Appendix-B.

#### 3.7.2 Testing for Compressive Strength of Cement Mortared Masonry

For this purpose, compression tests were carried out on prisms designated as 2SPC, 3SPC, 4SPC, 5SPC, 6SPC, 5VPC-A, 5VPC-B, and the wallettes (see Fig. 3.10). Specimens up to 4 brick high



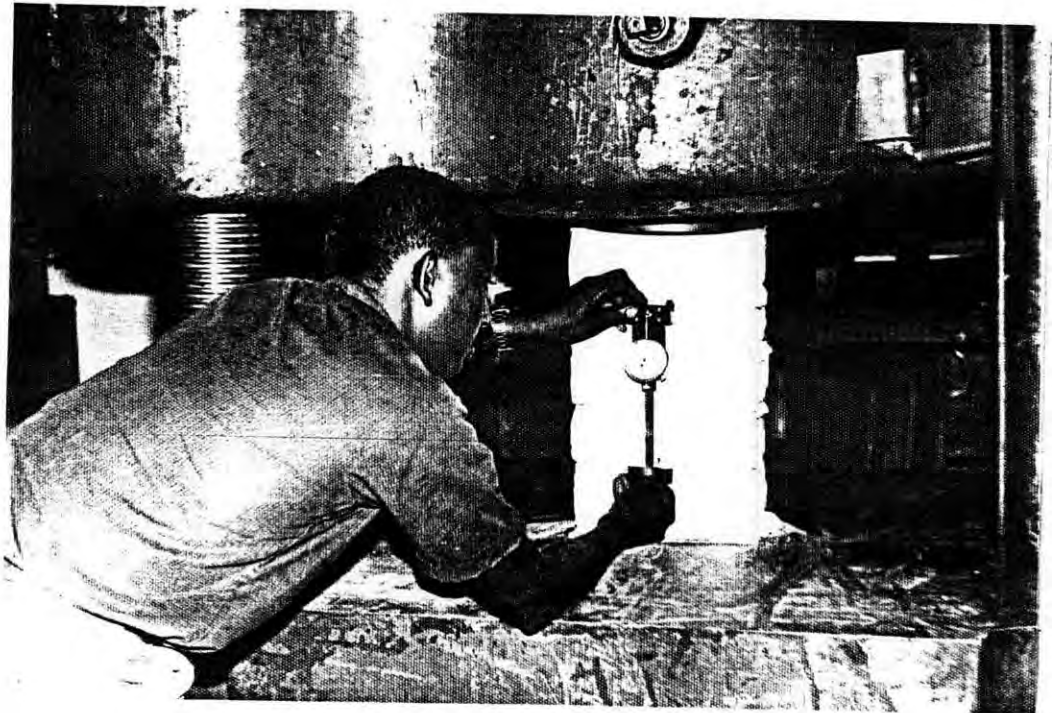


Fig. 3.11 Testing Arrangement for Vertical Deformation of Brick Masonry.

(about 13 inch) were tested in 250 tons capacity Compression Testing Machine. Due to the limitation of the space between the platens of this machine, the taller prisms and wallettes were tested in 4,00,000 lbs capacity Universal Testing Machine.

The prisms were tested directly between the machine platens. However, an I-beam was used to distribute the load over the entire lengths of the wallettes. The ball-seated upper platen of the machine was placed on the I-beam along the vertical axis of the wallettes. One-eighth inch plywood capping was used at the top and bottom of all specimens to absorb local surface irregularities. Typical testing arrangements for prisms and Wallettes are shown in Figs. 3.12 and 3.13.

The specimens were loaded in uniaxial compression to failure. Load was applied in such a convenient rate that the failure of specimens occurred within 1.5 to 2.5 minutes. The load at first visible crack and at ultimate failure were noted. The mode of failure was also observed and noted. Several photographs of the mode of failure were taken. Test results are summarized in Table 4.2 in the next chapter. Detailed experimental results are contained in Appendix-B.

### 3.7.3 Testing for Compressive strength of Mud Mortared Masonry

It has already been mentioned that all masonry specimens with mud mortar were 5 brick high stack bonded prisms. The variables were the amount and distribution of jute fibres in the mortar joints. These specimens were also tested in compression. The test procedure is similar to the one that has been discussed in section 3.7.2. The testing arrangement is same as shown in Fig. 3.12.

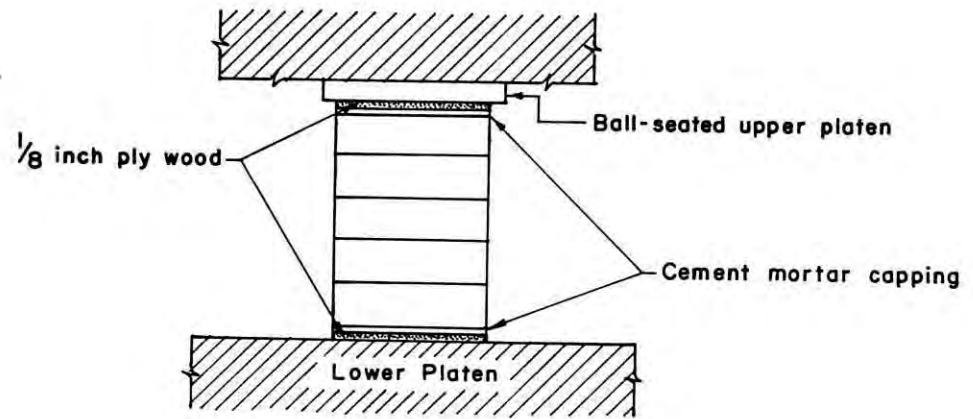


Fig. 3.12 Loading Arrangement for Prism.

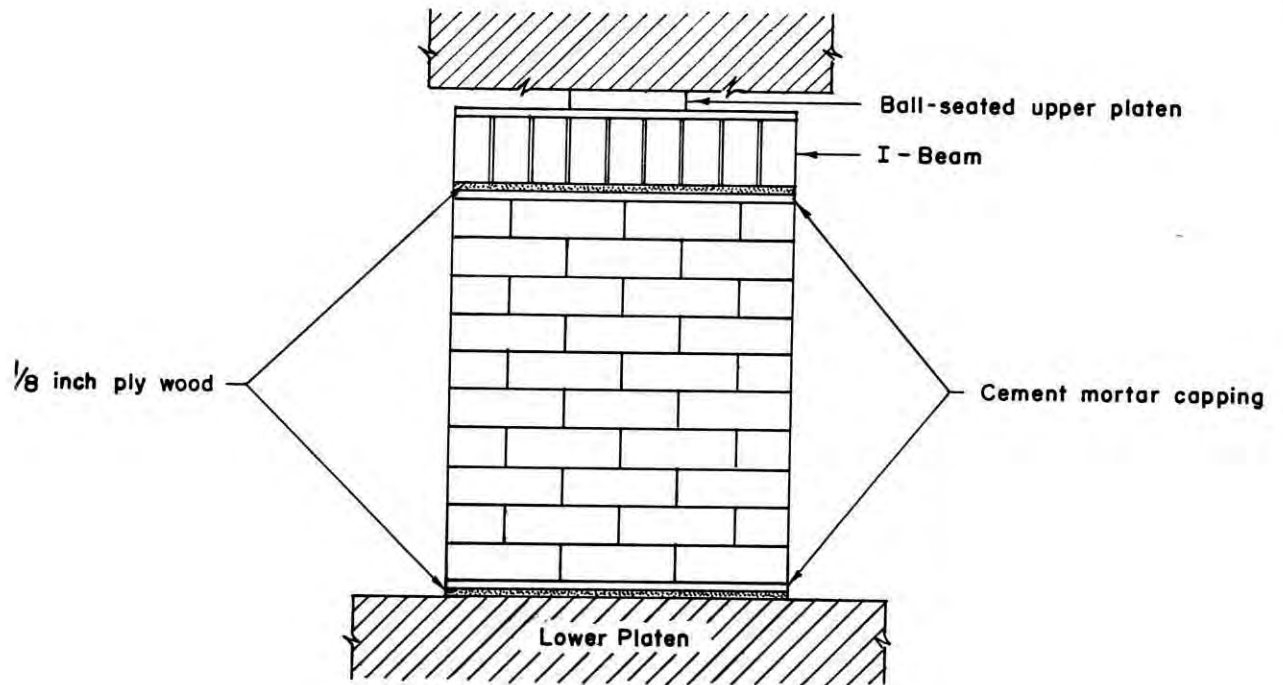


Fig. 3.13 Loading Arrangement for Wallette.

Once again, the specimens were loaded in uniaxial compression to failure. The load at first visible crack and at ultimate failure were noted. The mode of failure was also observed and noted. Several photographs of the mode of failure were taken. Test results are summarized in Table 4.7 in the next chapter. Detailed experimental results are presented in Appendix-B.

## **CHAPTER 4 TEST RESULTS**

### **4.1 INTRODUCTION**

Test results of properties of brick, cement, sand, cement mortar and the soil have already been presented in chapter 3. The following sections will present chronologically the test results of masonry specimens with cement mortar and mud mortar.

### **4.2 TEST RESULTS OF MASONRY SPECIMENS WITH CEMENT MORTAR**

#### **4.2.1 Deformation Characteristics**

Deformation characteristics of masonry was determined from the compression tests on 5 brick high stack bonded prisms (see section 3.7.1). Test results are summarized in Table 4.1. Detailed experimental results are presented in Appendix-B.

#### **4.2.2 Compressive Strength**

Compression tests were carried out on 2SPC, 3SPC, 4SPC, 5SPC, 6SPC, 5VPC-A, 5VPC-B prisms and wallettes (see Fig.3.10). The test procedure of these specimens has been described in section 3.7.2. Strength at first visible crack and ultimate strength for all specimens are summarized in Table 4.2 and presented in Fig. 5.1 in the next chapter. The compressive strength and tensile strength of mortar are also presented in the table. Detailed experimental results are presented in Appendix-B.

Table 4.1 Mean Normal Stress-strain Reading for Masonry with Cement Mortar

Stress (psi)	94	190	285	380	477	568	663	758	853	947	1042	*1180
Strain ( $10^{-6}$ )	40	90	140	190	240	290	370	450	510	620	700	-

Note : \*Ultimate comp. strength  
1 psi = 6.896 KPa

Table 4.2 Summary of the Results of Compression Test on Masonry Specimens with Cement Mortar

Specimen designation	2SPC	3SPC	4SPC	5SPC	6SPC	5VPC-A	5VPC-B	Walette
No. of specimen tested	6	6	6	12	6	12	12	6
$\bar{X}$	*	1603	1093	935	885	937	834	520
$f_{vc}$ (psi) S	-	-	-	160	-	97.7	99.1	-
C. of V. (%)	-	-	-	17.1	-	10.4	11.9	-
$\bar{X}$	2602	1832	1314	1168	1132	1321	1365	1023
$f_m'$ (psi) S	-	-	-	178	-	173	90.5	-
C. of V. (%)	-	-	-	15.2	-	13	10.5	-
X	-	87.5	83.1	80.5	78.3	73	61	50.7
$f_{vc}/f_m'$ (%) S	-	-	-	4.28	-	6.18	5.9	-
C. of V. (%)	-	-	-	5.31	-	8.46	9.6	-
Mortar comp. strength	1303	1235	1182	1227	1224	1240	1250	1260
Mortar ten. strength	125	135	144	128	125	145	135	142

Note: \*Failed to predict,  
 $f_{vc}$  = Strength at first visible crack  
 $f_m'$  = Ultimate strength  
 $\bar{X}$  = Mean  
 S = Standard deviation  
 C. of V. = Coefficient of variation  
 1 psi = 6.896 KPa

### 4.2.3 Mode of Failure

#### a) Prisms

82999  
 Failure of all prisms were initiated by the formation of vertical or inclined cracks in the bricks due to splitting or cracks in the vertical mortar joints. The crack growth was found to be stable initially. As the load increases, it propagated up and down through the mortar bed joints. Meanwhile, other vertical and inclined cracks appeared dividing the prism in a number of regular or irregular shaped columns. These columns were capable of carrying further load. The final failure occurred by the formation of numerous cracks accompanied by unstable crack propagation.

Crushing type of failure occurred in 2SPC prisms. First visible crack and final failure occurred simultaneously. Therefore, it was not possible to predict the first cracking load.

In case of 3SPC and 4SPC prisms first visible crack appeared due to splitting in the brick. For 3SPC prism the first crack appeared in the middle brick whereas for 4SPC the first crack appeared from either of the two middle bricks. Most of the cracks were inclined in nature due to the presence of shear stress near the machine platen. With the increase of load, the cracks propagated up and down through the mortar bed joints in a random manner turning the prisms into a number of almost irregular shaped columns. The final failure was associated with several vertical and inclined cracks on the wider face and splitting of bricks on the narrow face.

The mode of failure for 5SPC and 6SPC prism are similar to those of 3SPC and 4SPC. In case of 5SPC and 6SPC prisms the first crack appeared in the middle bricks. Initially the cracks were vertical in nature. This is due to the absence of shear stresses in the

central bricks which are relatively free from the effect of platen restraint. With the increase of load the cracks propagated through the bed joints and the bricks. Near the machine platen the cracks were inclined in nature due to the presence of shear stress. The final failure was accompanied by the unstable crack growth.

In case of 5VPC-A and 5VPC-B (prisms with vertical joint) first visible crack appeared in a more distinct manner than 5SPC prism. In both cases splitting of brick took place along the vertical joint following the initiation of crack in the joint. With the increase of load, the crack propagated up and down through the mortar bed joints turning the prism into two almost regular shaped columns of half brick width. The final failure occurred by the failure of these two columns in a mode similar to the failure of 5SPC prisms. Typical failure modes of 5SPC, 5VPC-A and 5VPC-B prism are shown in Figs. 4.1, 4.2, 4.3 and 4.4.

#### b) Wallette

All the wallettes failed due to the formation of vertical cracks. The cracks initiated in the vertical joints and propagated up and down towards the nearby vertical joints through the bricks as well as through the mortar bed joints with consequent lateral spreading of the specimens. The irregular shaped columns formed due to the formation of cracks in well defined planes of wallette were capable of sustaining further load, and the final failure occurred at a higher load. At failure load, vertical splitting on the narrow face and spalling of bricks on both sides of the wider face were observed. A typical failure mode of wallette is shown in Fig.4.5.





Fig. 4.1 Typical Failure Pattern of 5SPC Prism.

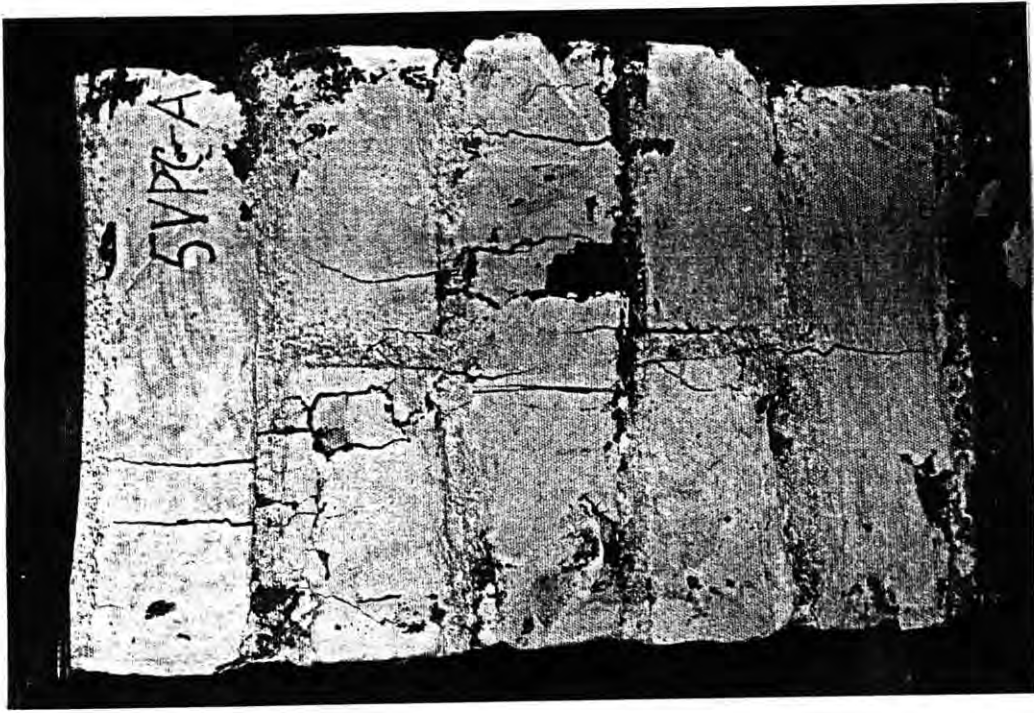


Fig. 4.2 Typical Failure Pattern of 5VPC-A Prism.



Fig. 4.3 Typical Splitting of 5VPC-A Prism on the Narrow Face.



Fig. 4.4 Typical Failure Pattern of 5VPC-B Prism.



Fig. 4.5 Typical Failure Pattern of Walette.

### 4.3 TEST RESULTS OF MUD MORTAR

To find the role of jute fibre in mud mortar, different percentages of fibre were included with it and investigation carried out on its water content at workability, shrinkage limit and compressive strength. The test procedures have already been described in sections 3.5.1, 3.5.2 and 3.5.3 respectively. The following tables present results of those tests. Detailed experimental results are presented in Appendix-B.

Table 4.3 Avg. Water Content at Workability of Mud Mortar with Different Fibre Contents

Fibre content (%)	Water content at workability (%)
0.0	35.5
0.5	38.0
1.0	36.2
1.5	36.7
2.0	39.8
2.5	37.8
3.0	39.2

Note: 1) Fibre content by weight of air dried soil  
2) Workability as per masson's satisfaction

Table 4.4 Avg. Shrinkage Limit of Mud Mortar with Different Fibre Contents

Jute fibre (%)	0.0	0.5	1.0	1.5	2.0	2.5	3.0
Shrinkage limit (%)	24.3	26.2	27.75	28.5	29.51	30.5	32.3

Table 4.5 Results of Compression Test on Mud Mortar Cubes

Jute fibre (%)	0.0	0.5	1.0	1.5	2.0	2.5
Mean comp. str. of three cubes (psi)	402.0	*	*	*	*	*

\*Failed to predict  
1 psi = 6.896 KPa

Table 4.6 Summary of Results of Unconfined Compression Test on Mud Mortar (Mean Stress-Strain Readings)

Strain (10 <sup>-4</sup> )	Stress (psi)					
	Fibre (%)					
	0.0	0.5	1.0	1.5	2.0	2.5
17.85	95.7	109.6	122.0	127.2	115.2	108.1
30.70	147.3	160.6	168.0	172.0	165.2	149.3
53.55	183.0	199.5	210.3	218.0	203.8	175.6
71.40	203.6	234.6	237.7	243.0	226.9	198.2
89.25	-	-	252.8	258.2	246.9	216.8
107.10	-	-	-	267.8	264.1	285.6
124.95	-	-	-	-	272.5	250.2
142.80	-	-	-	-	-	256.1
Mean U.C.S (psi)	210.0	241.0	250.6	272.1	278.9	261.3
Mean W.C (%)	2.33	2.33	2.16	2.13	2.23	2.36

Note: U.C.S= Unconfined compressive strength,  
W.C = Water content during test  
1 psi = 6.896 KPa

#### 4.4 TEST RESULTS OF MASONRY SPECIMENS WITH MUD MORTAR

Compression test was carried out on 5 brick high stack bonded prisms in this case. The mud mortar with different percentages of jute fibre were used as binding material for the prisms. The test procedure has already been described in section 3.7.3. Strength at first visible crack and ultimate strength are summarized in Table 4.7. The corresponding water content of mortar bed at test are also presented in the table. Detailed experimental results are presented in Appendix-B.

Table 4.7 Summary of Results of Compression Test on 5 Brick High Stack Bonded Prism with Mud Mortar

Jute fibre (%)	0.0	0.5	1.0	2.0	2.0 (Jute mat)
No. of specimens tested	12	6	6	6	6
$f_{ve}$	$\bar{X}$ 272	238	235	225	255
	S 49.5	-	-	-	-
	C. of V. (%) 18.16	-	-	-	-
$f'_m$	$\bar{X}$ 909	837	893	748	834
	S 130.5	-	-	-	-
	C. of V. (%) 14.36	-	-	-	-
$f_{ve}/f'_m$ (%)	$\bar{X}$ 30	28.5	26.2	30	30.6
	S 4.51	-	-	-	-
	C. of V. (%) 15	-	-	-	-
W.C (%)	$\bar{X}$ 2.69	2.73	2.59	2.71	2.65
	S 0.10	-	-	-	-
	C. of V. (%) 3.68	-	-	-	-

Note:

$f_{ve}$  = Strength at first visible crack

$f'_m$  = Ultimate strength

W.C = Water content of the mortar bed during test

$\bar{X}$  = Mean

S = Standard deviation

C. of V. = Coefficient of variation

1 psi = 6.896 KPa

#### 4.4.1 Mode of Failure

Failure of all prisms were characterized by the splitting of bricks both on the narrow and wide faces. Spitting of bricks resulted in vertical as well as inclined cracks.

In contrast to 5 brick high stack bonded prisms with cement mortar (5SPC), the first visible crack appeared in any of the three middle bricks rather than only one middle brick of the prisms. As the load is increased the crack widened and propagated up and down. Meanwhile other vertical and inclined cracks appeared and at the same time, reduction in thickness of mortar joints and outward flowing of mortar were also observed. Ultimate failure occurred by the formation of large number of wide cracks as well as the spalling of bricks and mortars. Width of cracks in the prisms with mud mortar were larger than those with cement mortar. It is to be noted that the behaviour of prism containing fibre in the mortar bed were more ductile than those without fibre. In the former case greater number of wider cracks and more spalling of bricks were observed. Typical failure patterns are shown in Figs. 4.6 - 4.9.

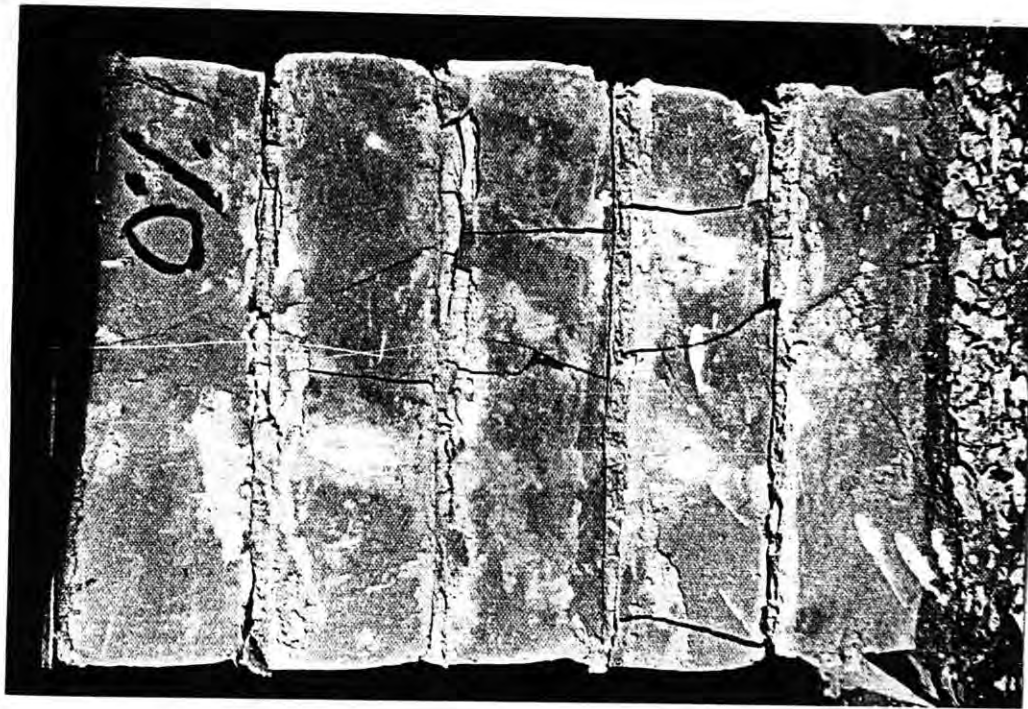


Fig. 4.6 Typical Failure Pattern of Stack Bonded Prism with Mud Mortar.



Fig. 4.7 Typical Splitting on the Narrow Face of Stack Bonded Prism with Mud Mortar.



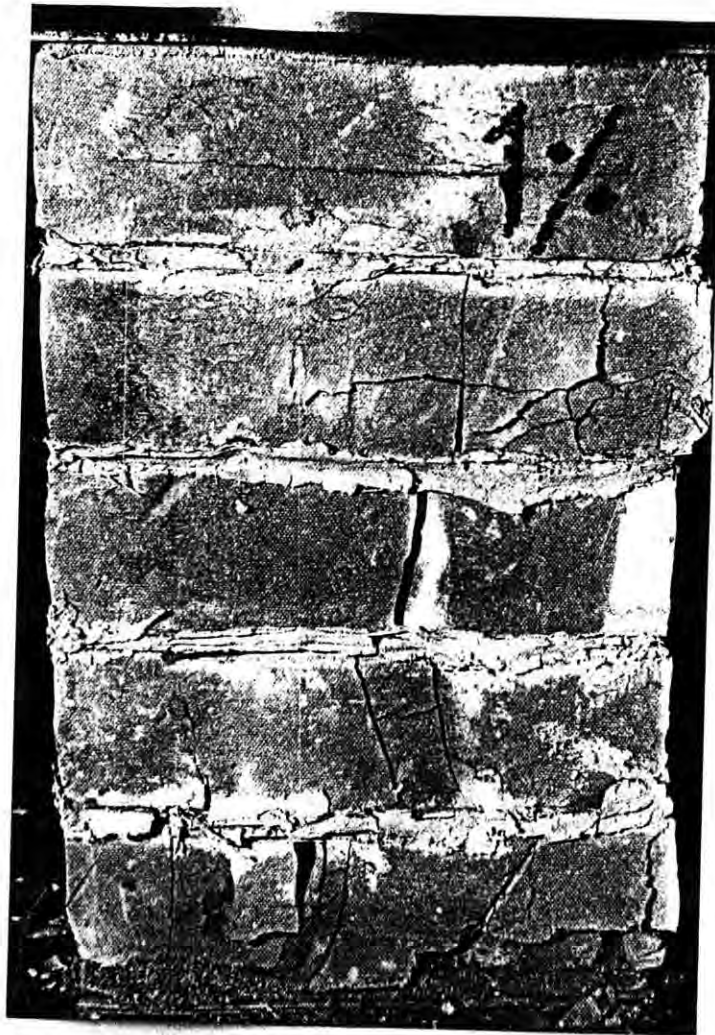


Fig. 4.8 Typical Failure Pattern of Stack Bonded Prism with 1.0% Fibre in the Mud Mortar Bed.



Fig. 4.9 Typical Failure Pattern of Stack Bonded Prism with Jute Mat in the Mud Mortar Bed.

## CHAPTER 5

### DISCUSSIONS ON TEST RESULTS

#### 5.1 INTRODUCTION

Test results of deformation and strength characteristics of masonry with cement mortar and strength characteristics of masonry with mud mortar containing jute fibre reinforcement have been presented in in the previous chapter. The test results will be discussed in the following sections of this chapter. Also, based on elastic analysis a formula to predict the initial tangent modulus of brick masonry will be proposed. Moreover, an existing formula predicting the compressive strength of stack bonded prism will be modified from linear elastic finite element analysis.

#### 5.2 SELECTION OF SUITABLE PRISM SPECIMEN

It has been mentioned earlier that the observed strength of a specimen under compression is significantly influenced by the restraining effect of the machine platen. This restraining effect results in artificial strengthening of the specimen. As a result, the measured strength is always higher than the actual strength of the specimen. Usually, this restraining effect is limited upto certain distance from the platen(see chapter 6 for details). The extent of platen effect depends upon the specimen size and shape and end condition. However, by increasing the height of the specimen it is possible to create a wider zone which is free from the restraining effect. When the specimen is loaded, failure starts in this zone and the measured strength comes closer to the strength without platen restraint. The height of the specimen can be increased by increasing the number of courses in the specimen.

To determine the number of courses in a stack bonded prism which will be suitable for experimental purpose, the test results of stack bonded prisms under compression presented in Table 4.2 have been used. Ultimate strength and strength at first visible crack are plotted against the number of bricks in the prisms. The plot is shown in Fig. 5.1. The figure shows that a dramatic loss of both the strengths takes place as the number of bricks in the prism increases. It also shows that this change in strengths decreases as the number of course increase. The change in strength between 5 brick high stack bonded prism and 6 brick high stack bonded prism is quite small. These results suggest strongly that in a prism with 5 or more bricks high the strength is not appreciably influenced by the platen restraint. It justifies the use of 5 brick high stack bonded prism in determining the strength and deformation characteristics of masonry.

### 5.3 BRICK MASONRY WITH CEMENT MORTAR

#### 5.3.1 Deformation Characteristics

##### a) Stress-Strain Curve

The axial deformation of masonry under compressive loading can be described conveniently by stress-strain diagram. The diagram needs to be represented by a suitable relationship. For this purpose mean normal stress-strain reading of 12 specimens presented in Table 4.1 are used. A statistical analysis of the data presented in the table reveals that the equation of the best fit curve could be represented by

$$\sigma_n = 4.393 \epsilon_n^{0.843} \quad (5.1)$$

where  $\sigma_n$  = normal stress and  $\epsilon_n$  = normal strain.

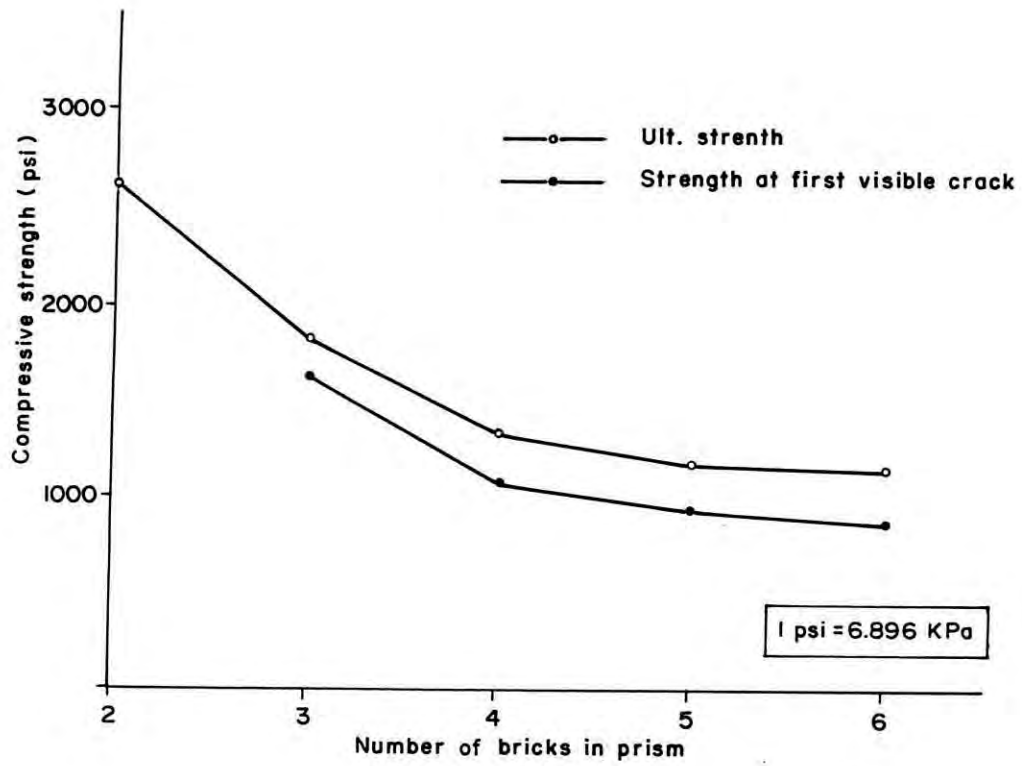


Fig. 5.1 Effect of Prism Height on the Compressive Strength.

The co-efficient of correlation for the best fit curve is found to be 0.997. The curve is shown in Fig. 5.2. This stress-strain curve represents the experimental results quite satisfactorily for lower load but for higher load the relation overestimates the actual stiffness of the prism.

Once again, Saenz's stress-strain relation for concrete can be used with small modifications to characterize the stress-strain curve for the masonry. As reported by Ali<sup>[49]</sup>, Saenz's relation originally developed for axially loaded concrete is given by:

$$\sigma_n = \frac{E_o \epsilon_n}{1 + (E_o/E_{cs} - 2)(\epsilon_n/\epsilon_{cu}) + (\epsilon_n/\epsilon_{cu})^2} \quad (5.2)$$

Where,  $E_o$  is the initial tangent modulus,  $E_{cs}$  is the secant modulus at strain  $\epsilon_{cu}$  and  $\epsilon_{cu}$  is the strain at ultimate compressive strength.

In the present study, the parameters defining the above relation were replaced by the corresponding parameters of masonry. The corresponding values for masonry were determined by extrapolating the experimental stress-strain curve as shown in Fig. 5.3. The values obtained are presented in Table 5.1.

Table 5.1 Value of the Parameters for Uniaxial Stress-Strain Curve for Masonry

Initial tangent modulus ( $E_{om}$ ) (psi)	Secant modulus at ult. strain ( $E_{sm}$ ) (psi)	Ultimate strain ( $\epsilon_{smu}$ )
$1.92 \times 10^6$	$1.3 \times 10^6$	$920 \times 10^{-6}$

Note: 1 psi = 6.896 KPa

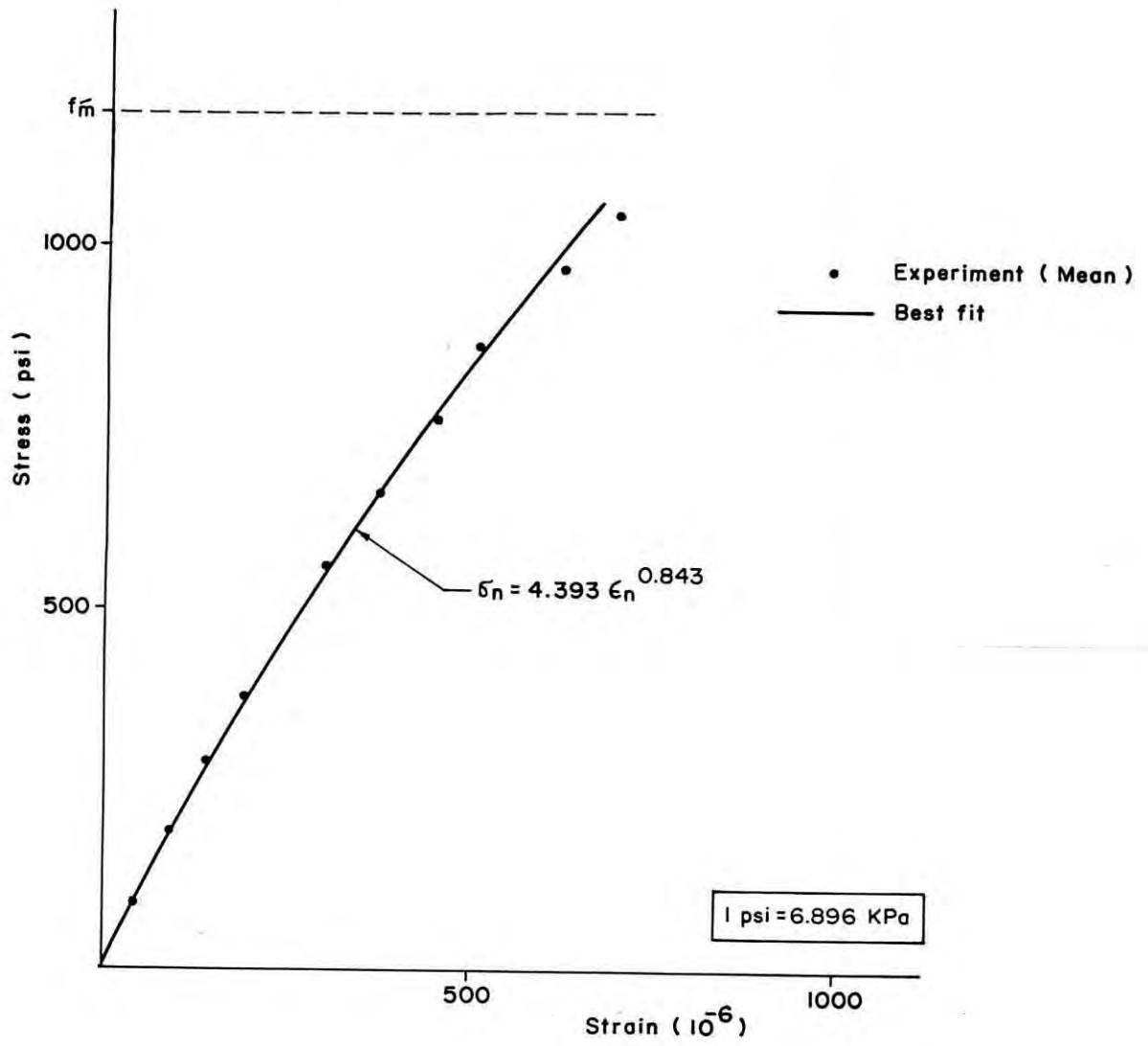


Fig. 5.2 Stress-Strain Curve (Best Fit) for Brick Masonry.

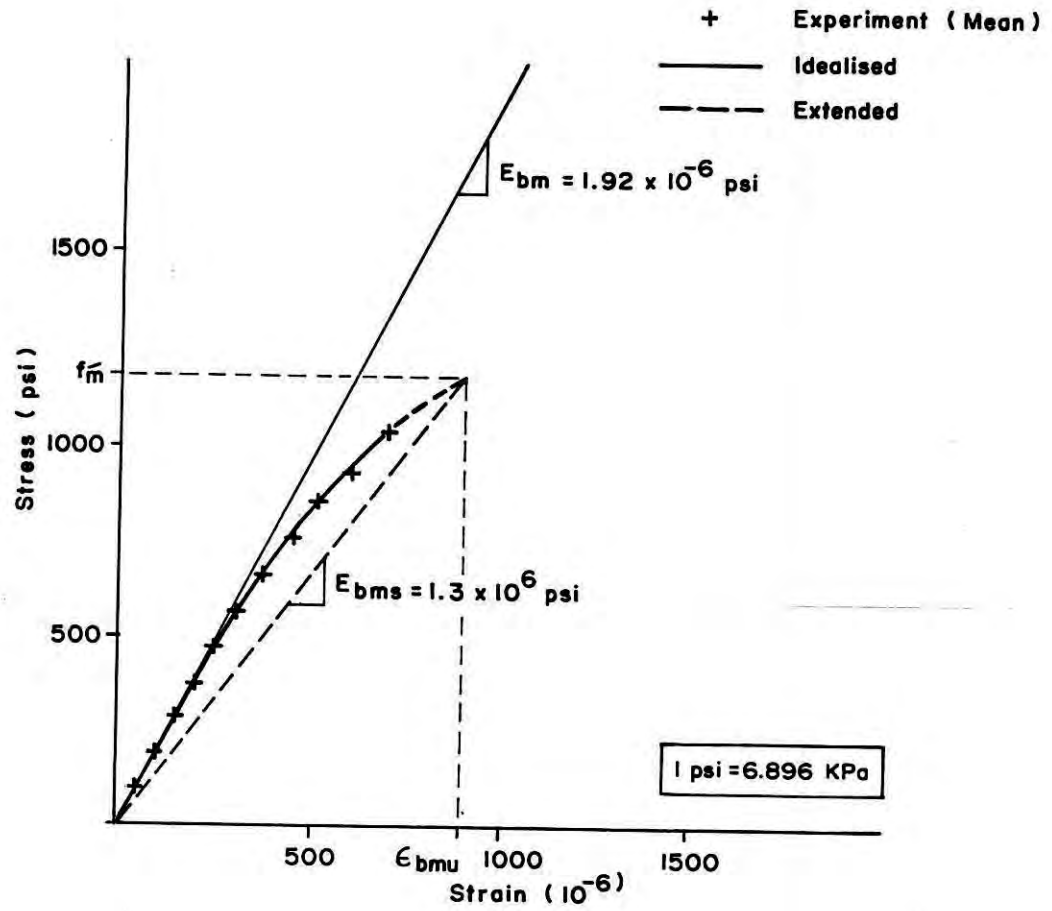


Fig. 5.3 Extrapolation of Average Stress-Strain Curve of Brick Masonry.

Initially, the equation defining the stress-strain curve of masonry may be represented by:

$$\sigma_n = \frac{E_{bm}\epsilon_n}{1 + (E_{bm}/E_{bms} - C)(\epsilon_n/\epsilon_{bmu}) + (\epsilon_n/\epsilon_{bmu})^2} \quad (5.3)$$

Where  $E_{bm}$  is the initial tangent modulus,  $E_{bms}$  is the secant modulus at strain  $\epsilon_{bmu}$ ,  $\epsilon_{bmu}$  is the strain at ultimate compressive strength and  $C$  is a constant for a particular brick-mortar combination.

Substituting the values of  $E_{bm}$ ,  $E_{bms}$  and  $\epsilon_{bmu}$  in eqn. 5.3, different values for  $C$  were assumed and the results obtained were compared with the experimental results. After several trials the value of  $C$  was found to be 1.8. Consequently the equation becomes:

$$\sigma_n = \frac{E_{bm}\epsilon_n}{1 + (E_{bm}/E_{bms} - 1.8)(\epsilon_n/\epsilon_{bmu}) + (\epsilon_n/\epsilon_{bmu})^2} \quad (5.4)$$

Eqn. 5.4 is compared to the experimental results in Fig. 5.4. The agreement is quite satisfactory. Therefore, the stress-strain curve of masonry under compression can be represented by eqn. 5.4. It can be seen from the figure that the equated stress-strain curve represents the experimental results quite well for the full loading range.

### 5.3.2 Modulus of Elasticity

Brick masonry is generally treated as a linearly elastic material, although tests indicate that the stress-strain relation is approximately parabolic. Under service conditions brickwork is



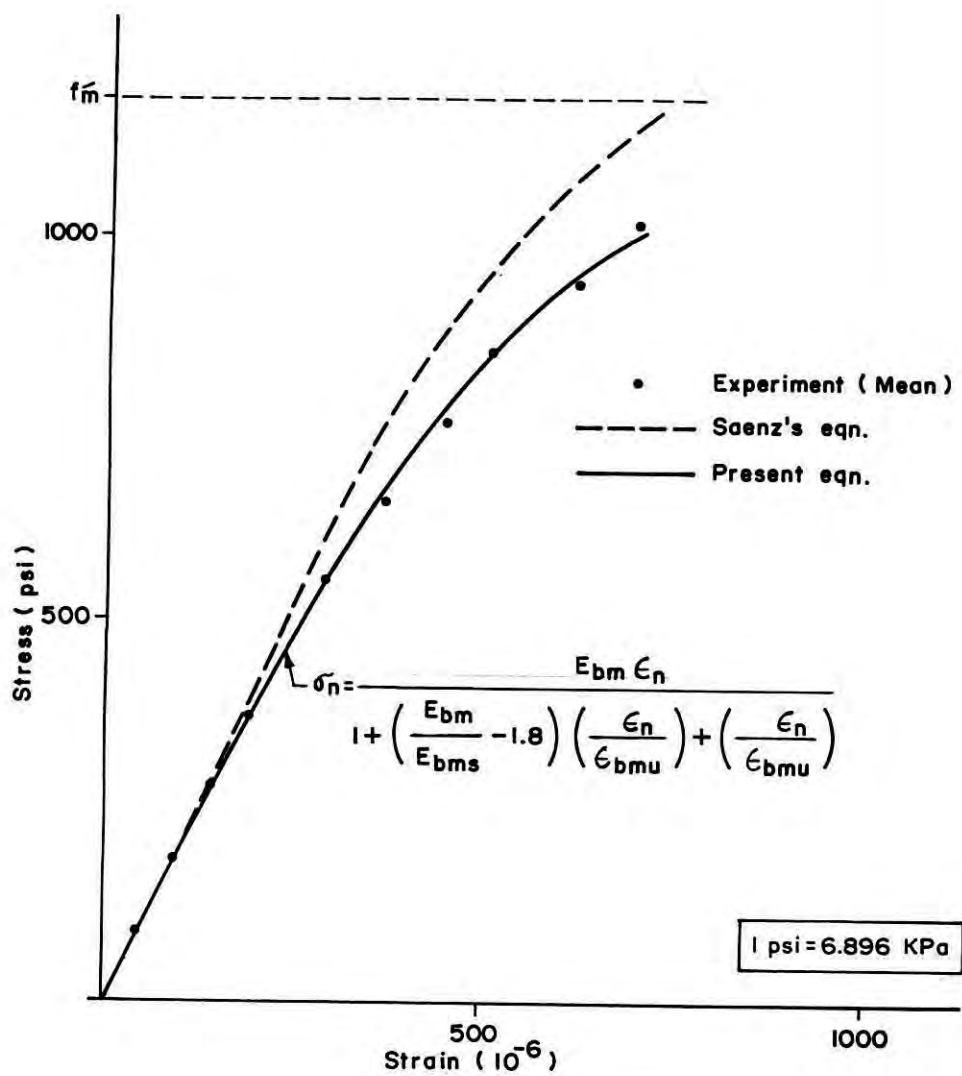


Fig. 5.4 Computed Stress-Strain Curve for Brick Masonry.

stressed only to a fraction of its ultimate load, and therefore the assumption of a linear stress-strain curve is acceptable for the calculation of normal structural deformation. Assuming brick, mortar and the assemblage to be elastic, a formula to predict the initial tangent modulus of brick masonry will be proposed in this thesis. The formula will be applicable for masonry prism subjected to axial compression.

The prism shown in Fig. 2.1 (in chapter 2) is subjected to an axial compressive stress  $\sigma_y$ . Bricks and mortar joints are stressed due this axial compression are also shown in the figure. The lateral strains in the brick in x and z directions are:

$$\epsilon_{xb} = 1/E_b [\sigma_{xb} + \nu_b(\sigma_y - \sigma_{zb})] \quad (5.6)$$

$$\epsilon_{zb} = 1/E_b [\sigma_{zb} + \nu_b(\sigma_y - \sigma_{xb})] \quad (5.7)$$

Similarly in mortar joint the lateral strains are:

$$\epsilon_{xm} = 1/E_m [-\sigma_{xm} + \nu_m(\sigma_y + \sigma_{zm})] \quad (5.8)$$

$$\epsilon_{zm} = 1/E_m [-\sigma_{zm} + \nu_m(\sigma_y + \sigma_{xm})] \quad (5.9)$$

where  $E_b$  and  $E_m$  are the initial tangent moduli of the brick and mortar respectively, and  $\nu_b$  and  $\nu_m$  the corresponding Poisson's ratios. For equilibrium, the total lateral tensile forces in the brick is equal to the total lateral compressive force in the mortar; hence,

$$\sigma_{xm} = \alpha \sigma_{xb} \quad (5.10)$$

$$\sigma_{zm} = \alpha \sigma_{zb} \quad (5.11)$$

Where  $\alpha = t_b/t_m$ ,  $t_b$  = height of brick and  $t_m$  = thickness of mortar bed.

As the lateral strain in the bricks and mortar are the same, equating eqns. 5.6 and 5.8, 5.7 and 5.9, and using eqns. 5.10 and 5.11 gives:

$$\sigma_{xb} = \sigma_{xb} = \frac{\sigma_v(\beta \nu_m - \nu_b)}{1 + \alpha\beta - \nu_b - \alpha\beta\nu_m} \quad (5.12)$$

where  $\beta$  = modular ratio =  $E_b/E_m$ .

The vertical deformation of brick masonry is the sum of the deformation in the brick and deformation in mortar joint. Therefore,

$$\Delta_{bm} = \Delta_b + \Delta_m \quad (5.13)$$

Where  $\Delta_b$ ,  $\Delta_m$  and  $\Delta_{bm}$  are vertical deformation in brick, mortar joint and brick masonry respectively.

From eqn. 5.13, vertical strain in masonry is:

$$\epsilon_{ybm} = \mu\epsilon_{yb} + \Phi\epsilon_{ym} \quad (5.14)$$

$\epsilon_{yb}$ ,  $\epsilon_{ym}$  and  $\epsilon_{ybm}$  are vertical strain in brick, mortar and brick masonry respectively;  $\mu = \alpha/(1 + \alpha)$  and  $\Phi = 1/(1 + \alpha)$ .

Again from Fig. 2.4 vertical strains in brick and mortar are:

$$\epsilon_{yb} = - 1/E_b [ \sigma_v + 2\nu_b\sigma_{xb} ] \quad (5.15)$$

$$\epsilon_{ym} = - 1/E_m [ \sigma_v - 2\alpha\nu_m\sigma_{xb} ] \quad (5.16)$$

Using eqns. 5.15 and 5.16 in eqn. 5.14 and substituting for  $\sigma_{xb}$  from eqn. 5.12,

$$\epsilon_{ybm} = -\sigma_y \left( \frac{\mu}{E_b} + \frac{\Phi}{E_m} \right) - \frac{2\sigma_y(\beta\nu_m - \nu_b)}{(1 - \nu_b) + \alpha\beta(1 - \nu_m)} \left( \frac{\mu\nu_b}{E_b} - \frac{\Phi\nu_m\alpha}{E_m} \right) \quad (5.17)$$

Now, 
$$\epsilon_{ybm} = -1/E_{bm}(\sigma_y) \quad (5.18)$$

Using eqn.5.18 in 5.17,

$$E_{bm} = \frac{E_b}{(\mu + \beta\Phi) + 2 \frac{(\beta\nu_m - \nu_b)(\mu\nu_b - \Phi\alpha\beta\nu_m)}{(1 - \nu_b) + \alpha\beta(1 - \nu_m)}} \quad (5.19)$$

Neglecting the second term in the denominator (since its magnitude is very small), initial tangent modulus of brick masonry can be approximated by:

$$E_{bm} = \frac{E_b}{(\mu + \beta\Phi)} \quad (5.20)$$

The modulus of elasticity obtained from eqns. 5.19 and 5.20 have been compared with the experimental results of the present study and those obtained by Ali<sup>[49]</sup> for concrete brick masonry. Properties of masonry constituents used for comparison are summarized in Table 5.2. The calculated initial tangent moduli from eqns. 5.19 and 5.20 are compared with the experimental results in Table 5.3.

Table 5.2 Properties of Masonry Constituents

	Ali <sup>[49]</sup>	Present study
$E_b$	17000 MPa (2.465 x 10 <sup>4</sup> psi)	2.2 x 10 <sup>4</sup> psi
$E_m$	7400 MPa (1.073 x 10 <sup>4</sup> psi)	1.0 x 10 <sup>4</sup> psi
$\nu_b$	0.16	0.17*
$\nu_m$	0.21	0.20*
$t_b$	75 mm. (2.95 inch)	2.75 inch
$t_m$	10 mm. (0.393 inch)	0.375 inch

\*Assumed  
(1 psi = 6.896 KPa)

Table 5.3 Comparison between Experimental and Calculated Values of Initial Tangent Modulus

	Experimental $E_{tm}$ (psi)	Calculated $E_{tm}$ (psi) from eqns.	
		Eqn. 5.19	Eqn. 5.20
Ali <sup>[49]</sup>	$2.17 \times 10^6$ (1500 MPa)*	$2.14 \times 10^6$	$2.163 \times 10^6$
Present study	$1.92 \times 10^6$	$1.923 \times 10^6$	$1.939 \times 10^6$

\*Experimental results are presented in Appendix - B  
(1 psi = 6.896 KPa)

Table 5.3 shows that the variations between experimental and calculated results using both eqns. 5.19 and 5.20 are very negligible. Therefore, the formulae can be used to predict the initial tangent modulus of masonry with good accuracy.

### 5.3.3 Compressive Strength

It has been stated earlier that the objective of prism and Walette tests was to investigate the deformation and strength property of masonry under vertical loading. Deformation characteristics has already been discussed in Section 5.3.1. In the following section compressive strength of prisms and Walleets tested will be discussed. Then the probable relation between the compressive strength of prism and and walette will be found out. Finally, a formula to predict the compressive strength of stack bonded prism will be proposed.

#### a) Compressive Strength of Prism and Walette

The discussions presented in section 5.2 reveals that the compressive strength of prisms upto 4 brick high is significantly

influenced by the restraining effect of the platen. This artificial strengthening effect of the platen on the compressive strength of the test prisms will be discussed in details in chapter 6 with the help of two dimensional linear finite element analysis. From the discussions in section 5.2 it has emerged that 5 brick high prism is suitable test specimen for the evaluation of the compressive strength. Its suitability lies in the fact that a significant portion of the specimen remains unaffected from the effect of platen restraint. This has been investigated by finite element method and presented in the next chapter.

In the present study 5 brick high prisms tested were 5SPC (stack bonded), 5VPC-A (with vertical joint) and 5VPC-B (with vertical joint). For convenience of comparison, results of compression test on 5 brick high prisms and wallette are taken from Table 4.2 and are further summarized in Table 5.4.

Table 5.4 Results of Compression Test on 5 Brick High Prism and Wallette

Specimen designation	$f_{ve}$ (psi)	$f'_m$ (psi)	$f_{ve}/f'_m$ (%)	Multiplying factor*
5SPC	935	1168	80.5	0.87
5VPC-A	937	1321	73.0	0.77
5VPC-B	834	1365	61.2	0.75
Wallette	520	1023	50.7	1.0

Note:  $f_{ve}$  = Strength at first visible crack,  $f'_m$  = Ult. strength  
 \*Factor =  $f'_m(\text{Wallette})/f'_m(\text{Prism})$ , 1 psi = 6.896 KPa

It has already been mentioned in sections 3.3.1 and 3.3.2 that the variation in the compressive and tensile strengths of the mortar for all specimens with cement mortar are very negligible. The variation in compressive strengths of the test specimens

shown in Table 5.4 is due to the factors involved in the construction procedure and the bond patterns used.

From Table 5.4 it can be seen that in case of 5SPC and 5VPC-A prisms, the first visible crack appears approximately at the same vertical stress. However, in case of 5VPC-B prism first visible crack appears at lower stress level. This can be explained with the help of observed mode of failure of these prisms described in section 4.2.3(a). It was observed that in all 5 brick high prisms first visible crack initiated at the middle brick by tensile splitting. This again reveals that the middle brick of a 5 brick high prism is relatively free from platen effect. At the same time, it may be concluded that the cracking strength of a 5 brick high prism depends upon the tensile strength of the middle brick. Based upon this conclusion, the strength at first visible crack of both 5SPC and 5VPC-A prisms should be the same as both of them contains full brick at the middle. However, in case of 5VPC-B prism this strength will be lower as it contains vertical mortar joint in the middle layer whose tensile strength is lower than that of the brick.

The table also shows that the ultimate compressive strength of 5VPC-A and 5VPC-B prisms is almost same. However, ultimate compressive strength of 5SPC prism is lower than that of 5VPC-A and 5VPC-B prisms. This can again be explained in light of the observed modes of failure. In case of 5SPC prism the appearance of first visible crack or cracks along with their subsequent propagation due to incremental load turned the prism into a number of irregular shaped columns. However, in case of 5VPC-A and 5VPC-B prisms the first visible crack appeared along the vertical joint. With the increase of load the crack propagated up and down turning the prism into two regular shaped column of half brick width. These columns are capable of carrying higher load than those carried by irregular shaped columns formed in case of 5SPC prism. Again the table shows that first visible crack in

5SPC prism appears at higher percentage of ultimate load than those of 5VPC-A and 5VPC-B prisms. This conforms that less reserved strength remains in a stack bonded (5VPC) prism than in prisms with vertical joint (5VPC-A and 5VPC-B) after the appearance of first crack. It is also seen from the table that about 50% strength remains reserved in case of wallette after the appearance of first visible crack.

Once again, Table 5.4 shows that the cracking strength and the ultimate strength of wallette are always lower than the strength of stack bonded prisms. This is due to the presence of large number of vertical joints in wallette and its geometry of construction. The wallette was constructed 3 brick wide and 10 brick high in running bond. Consequently, it has larger zone which is free from platen restraint. Moreover, the vertical joints in this zone acts as places of weakness which are more susceptible to split under tension.

#### b) Relation between Prism Strength and Wallette Strength

It has already been mentioned in chapter 2 that testing of stack bonded prism under uniaxial compression and relating to wall strength by using a reduction factor is widely accepted method throughout the world. In the present investigation stack bonded prisms as well as prisms with vertical joints were tested. On the other hand, wallettes were tested as the representation of full size masonry wall. Prism with vertical joints (5VPC-A and 5VPC-B) were tested with the view that they may represent the behaviour of wallette and thereby masonry strength more realistically than the stack bonded prism. The mode of failure (section 4.2.3(a) and 4.2.3(b))/<sup>and</sup> compressive strength of these specimens have already been discussed.



The failure mode of prisms with vertical joints showed more similarity with the failure mode of wallette. But it can be seen from Table 5.4 that neither stack bonded nor a prism with vertical joint resemble the compressive strength of wallette. However, like present method of practice it is possible to introduce a factor which is to be multiplied with prism strength to get wallette strength. From Table 5.4 the factor seems to be 0.75 for a 5 brick high prism with vertical joint (5VPC-A or 5VPC-B) and 0.87 for 5 brick high stack bonded prism (5SPC). This is in agreement with Page<sup>[4]</sup> and Anderson<sup>[24]</sup>. The former introduce this factor to be 0.75 and latter to be 0.9 for 4 brick high stack bonded prism and masonry wall.

#### 5.3.4 Theoretical Formula to predict the Compressive Strength of Stack Bonded Prism

In early days of research in brick masonry, a number of investigators derived formulae for brickwork strength in compression, based on elastic action of the brick-mortar complex. The earliest attempt would appear to be due to Haller<sup>[40]</sup> published in 1959. Haller's formula however, gives in values of brickwork strength greater than the uniaxial strength of brick, and is thus not valid in a quantitative sense. Formulae based on elastic behaviour of the constituent materials were proposed by Lenczner<sup>[52]</sup> and by Francis et al.<sup>[22]</sup>. An alternative approach to the definition of brickwork strength was proposed by Hilsdorf<sup>[18]</sup> based on an assumed linear relationship between lateral tensile strength and uniaxial compressive strength of bricks. The approach was later modified by Khoo and Hendry<sup>[17]</sup> by adopting nonlinear relationship between lateral tensile strength and uniaxial compressive strength of the bricks. Although the formula proposed by Khoo and Hendry<sup>[17]</sup> is more representative of the behaviour of the prisms than the formula proposed by Hilsdorf

but its use has been restrained due to the complexity of the equation.

All the above theoretical formulae were based on the assumption that the constituent materials of the prism will remain elastic upto fracture. Recently Atkinson et al.<sup>[5]</sup> proposed theories based on the assumption that bricks will remain elastic upto fracture and mortar will be plastic from the beginning. Very recently, Grim<sup>[11]</sup> proposed a formula from the experimental results.

The fracture load predicted by all the formulae mentioned above has been found to be either too conservative or nonconservative. The formula proposed by Francis et al.<sup>[22]</sup>, Hilsdorf<sup>[18]</sup> and Khoo and Hendry<sup>[17]</sup> always overestimates the actual fracture load by a wide margin. Whereas the formulae proposed by Atkinson et al.<sup>[5]</sup> and Grim<sup>[11]</sup> underestimates the actual fracture load. This is possibly due to the lack of proper knowledge of the behaviour of mortar joints in the prisms. It should be pointed out here that all the previous investigators either derived the fracture criterion of mortar joints from triaxial tests or used the fracture criterion of concrete. But the directional properties of mortar joints in the prism are different from the properties of mortar itself. Therefore, in this study an attempt has been made to propose a formula by adopting the fracture criterion of mortar joints in the prism derived from finite element analysis.

Due to simplicity in computation, Hilsdorf's<sup>[18]</sup> formula based on the strength of brick and mortar under multiaxial stress has been modified in this study to make it more representative of the actual strength of the prism. As mentioned earlier Hilsdorf<sup>[18]</sup> assumed that the ultimate failure of the prism is accompanied with the crushing of mortar and this will occur when the line defining the triaxial strength of the mortar, C in Fig. 5.5. intersects the failure line for the brick.

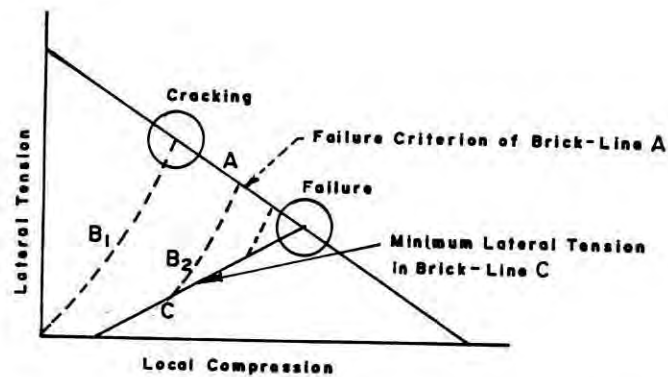


Fig. 5.5 Failure Criterion of Brick Masonry

Hilsdorf<sup>[18]</sup> also assumed that the triaxial strength of mortar could be represented by the equation (obtained originally for concrete):

$$f' = f'_c + K\sigma_c \quad (5.21)$$

where,  $f'$  is the compressive strength of a laterally confined cylinder.

$f'_c$  is the uniaxial compressive strength of a cylinder

$\sigma_c$  is the lateral confinement stress of a cylinder

$K$  is the empirical constant determined from the experiment and for concrete the value of  $K$  is 4.1.

This leads to the minimum lateral confinement of the mortar joint of

$$\sigma_{xj} = 1/K(\sigma_y - f_c') \quad (5.22)$$

in which,

$\sigma_{xj}$  is the lateral compressive stress in the mortar joint

$\sigma_y$  is the local stress in the y direction(see Fig. 2.4)

$f_c'$  is the uniaxial compressive strength of mortar

In this study the value of K has been obtained from linear elastic finite element analysis of the prism . As mentioned earlier that the mortar joints in the prism behave differently from mortar cylinder or mortar cube which are normally used to determine the properties of mortar joints. The use of linear elastic finite element analysis to determine the value of K for mortar joint may be justified since the state of stress in the prism is mainly tension-compression. The finite element analysis has been shown in Fig.6.10(case-I) of chapter 6. The detailed calculation for obtaining the value of K and the strength of prism obtained by adopting the formulae proposed by the previous investigators along with the results of the present study are shown in Appendix-A.

A comparative study of the strength of stack bonded prism for the particular brick-mortar combination using different formulae has been shown in Table 5.5. Table 5.5 shows the strength of the prism eliminating the aspect ratio effect. Aspect ratio effect was eliminated using correction factors(see table 2.1) proposed by Page<sup>[9]</sup> for all the constituent materials.

Table 5.5 Comparison between the Experimental and Calculated Strengths of Stack Bonded Prism using Different Formulae

Experimental strength(psi)	Predicted strength(psi)				
	Formula used				
	Francis et al. [21]	Hilsdorf [18]	Khoo & Hendry [19]	Grim [11]	Modified Hilsdorf*
1027	1392	1145	1282	258	1028

\*Proposed by the author (1 psi = 6.896 KPa)

It can be seen from the table that the strength predicted by the modified Hilsdorf's formula (proposed by the author) is more representative of the actual strength of prism than any other existing formula.

### 5.3.5 Explanation of the Observed Failure Modes

It is well accepted that in masonry the vertical load is transferred through the units to the weaker and less stiff mortar bed joints producing a greater tendency of mortar to expand laterally. This lateral expansion of the mortar is resisted by the unit producing a state of uniaxial compression and bilateral tension in the unit and triaxial compression in the mortar. The failure of prism is mainly governed by the biaxial tension-compression stresses in the unit.

As described in section 4.2.3 failure of all masonry specimen is associated with the tensile splitting of the bricks and the mortar joints. This argues that lateral tension is the dominating stress in the biaxial stress state. Although mortar in the bed joints are initially in a state of triaxial compression, during failure splitting of bed joints is observed. This is due to the

fact that when a brick cracks, the tensile stress previously carried by the uncracked section is redistributed in the adjacent mortar joints. With the increase of load additional tensile stresses which are likely to be carried by the uncracked section of the brick are also redistributed in the adjacent mortar joints. As a result, compressive stresses in the mortar joint in the direction perpendicular to the crack become tensile stresses. When the tensile stress reaches to the tensile strength of mortar, the mortar bed cracks.

2 brick high stack bonded (2SPC) prisms failed almost explosively near the ultimate load. This indicates apparent significant restraining effect of the platens. The influencing zone of both platen (upper and lower) may have overlapped which prevents the lateral expansion of the specimen. Consequently, the prisms failed under a state of triaxial compressive stresses.

In case of 3 and 4 brick high stack bonded (3SPC and 4SPC) prisms splitting of bricks were observed before the final failure. But it is to be noted that the cracks developed in the middle of the specimens were mainly diagonal rather than vertical cracks in case of 5 and 6 brick high stack bonded (5SPC and 6SPC) prisms. This is due to the presence of shear stresses near the ends of the specimens. This again conforms the influence of platen restraint but to a lesser degree than those for 2 brick high stack bonded (2SPC) prisms.

The appearance of first visible crack in the middle portion of 5 and 6 brick high stack bonded (5SPC and 6SPC) prisms and prisms with vertical joints (5VPC-A and 5VPC-B) suggest that this portion (middle brick of 5 brick high prism and two middle bricks of 6 brick high prism) is relatively free from platen restraint. Again, 5SPC, 5VPC-A, 5VPC-B and 6SPC prisms split predominantly up the narrow face. This is in agreement with that observed by Shrive<sup>[12]</sup>. Shrive<sup>[12]</sup> explained this as the tendency of longer

length to be restrained more towards plain strain condition. The plane strain condition leads to higher lateral stresses across the narrow face. According to the above explanation the wallettes are more susceptible to split up the narrow face as it has longer length than the prisms. However, in case of wallettes first visible cracks appeared on the wider face. This is because the tensile bond strength of vertical joint is much lower than the tensile strength of bricks. Consequently, crack initiates at the interface of these joints at lower stress level. Splitting of brick was also observed on the narrow face of the wallette.

#### 5.4 BRICK MASONRY WITH MUD MORTAR

To improve the quality of masonry with mud mortar, the factors requiring much more attention are compressive strength of mortar, minimization of excessive lateral deformation i.e a decrease in Poisson's ratio and minimization of crack in the mortar bed joints that occurs due to excessive volumetric shrinkage when the mortar bed dries. Guided by the reviewed literature, jute fiber was included with mud mortar to serve the aforesaid purposes and some tests were carried out in this connection on mud mortar before and after the inclusion of fibre. Also, masonry prisms were constructed in which mud mortar with and without fibre act as the binding materials. These prisms were tested under compression to determine the effect of inclusion of fibre on the compressive strength of masonry.

##### 5.4.1 Role of Jute Fibre in Minimizing Cracks

According to the definition of shrinkage limit, theoretically, no crack will be formed in the mud mortar (after drying) if the inclusion of fibre increases its shrinkage limit to the water content at workability. Test results of water content at

workability and shrinkage limit of mud mortar are presented in Table 4.3 and Table 4.4 respectively.

From Table 4.3 it can be seen that about 35-40% water is required to have desired consistency and workability for fibre free as well as fibre included mortar.

The average shrinkage limit against Jute fibre content is shown in Fig. 5.6. The figure indicates that the shrinkage limit increases linearly with the increase in fibre content. The increase is however not so significant. The statistical analysis yields the following relationship with a co-efficient of correlation of 0.995 between the variables:

$$S = 24.63 + 2.49f \quad (5.23)$$

Where, S = shrinkage limit (%) and f = fibre content (%)

From eqn. 5.23 it can be seen that in order to increase the shrinkage limit to 35-40% about 4 - 6% jute fibre is required to be included in the mud mortar. But strength and deformation characteristics, which will be discussed in the following sections prohibit the inclusion more than 2% (nearly) for this particular mud. Moreover, inclusion of such quantity will turn the soil cohesionless. As a result the bond at the interface of mortar and the bricks will be severely impaired.

From the above discussion it is clear that the fibre increases the shrinkage limit of mud mortar towards its water content at workability. Therefore, it is expected that jute fibre will prevent the formation of cracks and consequently the formation of channels in the mud mortar joints. To check this, the dried mud mortar bed of some masonry prisms were observed.



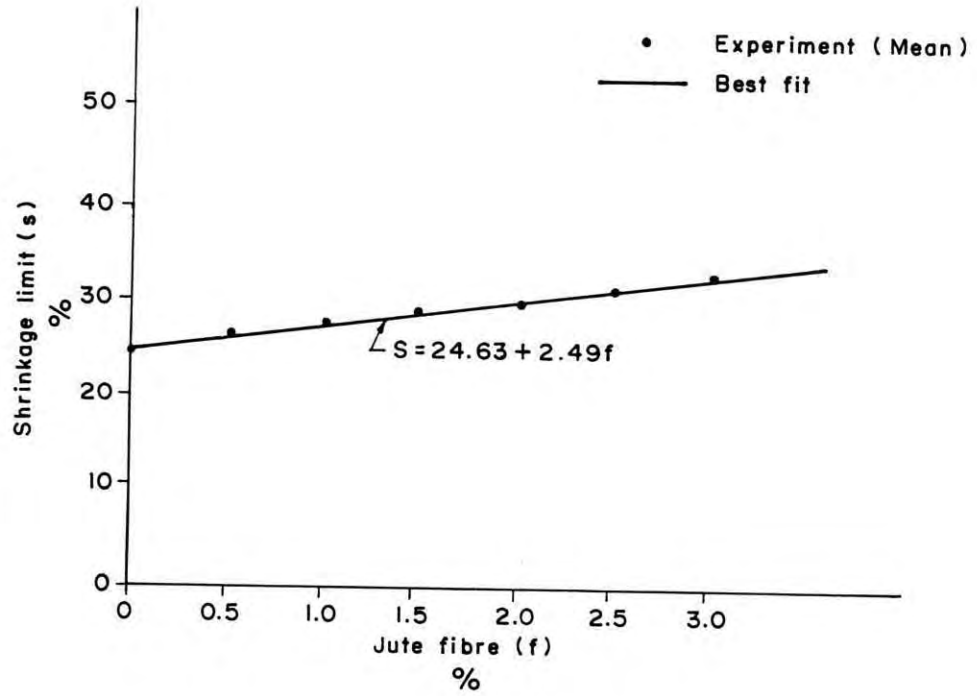


Fig. 5.6 Average Shrinkage Limit Vs. Jute Fibre Content.

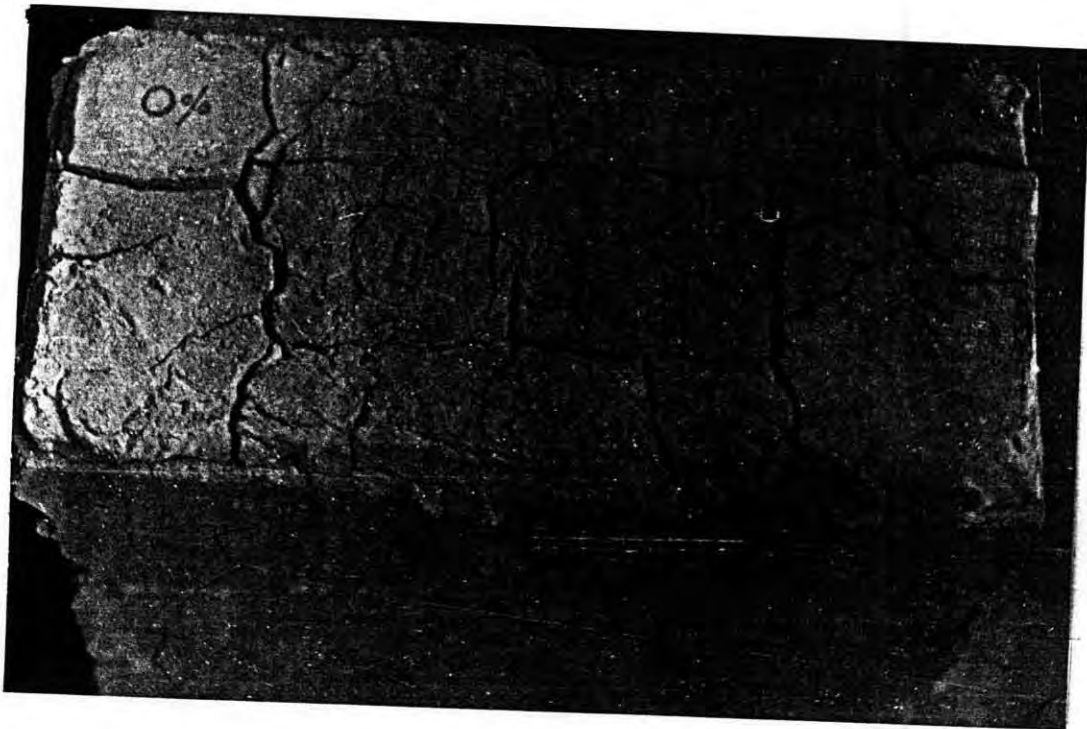


Fig. 5.7 Typical Mud Mortar bed without Jute Fibre.

Mud mortar with randomly distributed jute fibre showed excellent means of crack minimization without any channel in the mortar bed except very small visible local cracks. On the other hand, wide channels were observed in the mortar beds having no fibre as well as having jute mat at the middle. Typical photographs of the mortar beds without fibre, with randomly distributed fibre and with jute mat are shown in Figs. 5.7, 5.8 and 5.9 respectively.

#### 5.4.2 Role of Jute Fibre on the Deformation Characteristics

The strain controlled unconfined compression test results presented in Table 4.6 helps to analyse the role of inclusion of fibre on the deformation characteristics of mud mortar. On the basis of the results, average vertical stress-strain curves for mud mortars with different fibre contents are shown in Fig. 5.10.

The figure shows that mud mortar becomes more ductile as the percentage of jute fibre increases. This is in agreement with that observed by Mitchel<sup>[44]</sup>.

Fig. 5.10 also indicates that at the same vertical stress level, the vertical strain decreases as the percentage of inclusion increases upto 1.5%. Above 1.5% inclusion, this strain reduction property is gradually inhibited. From the nature of the curves it can be concluded that at the same vertical stress level, the vertical strain of mud mortar decreases with the increase of inclusion upto certain limit. For this particular mud mortar the limiting inclusion lies in between 1.5% to 2.0%.

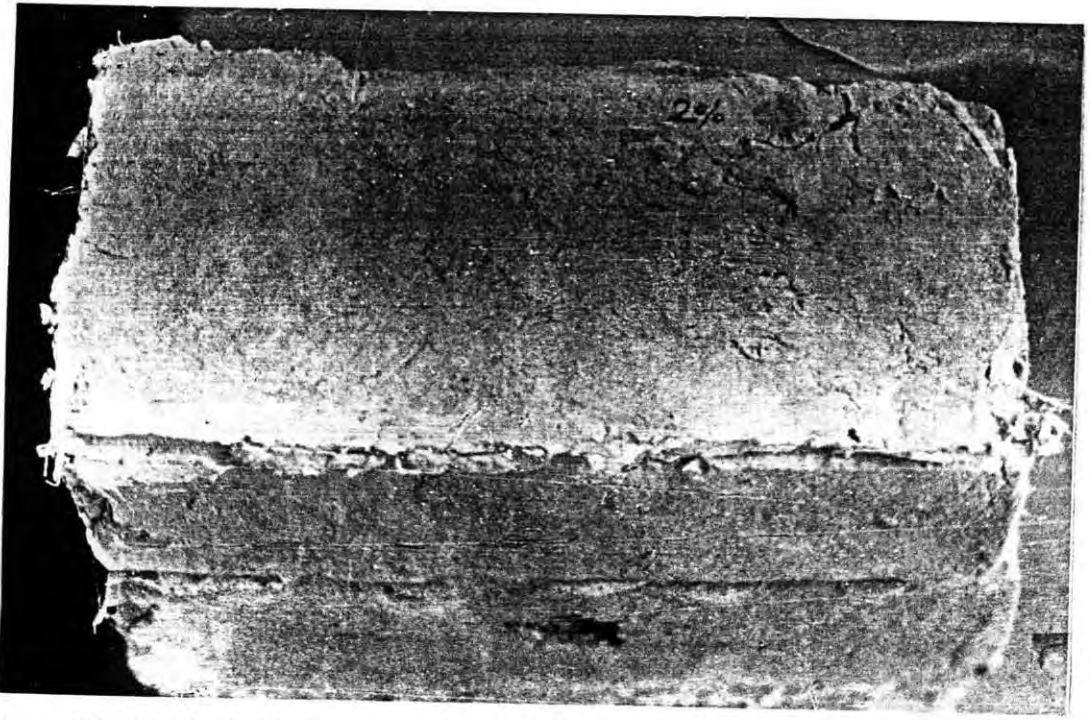


Fig. 5.8 Typical Mud Mortar Bed with Randomly Distributed Jute Fibre.



Fig. 5.9 Typical Mud Mortar Bed with Jute Mat at the Middle.

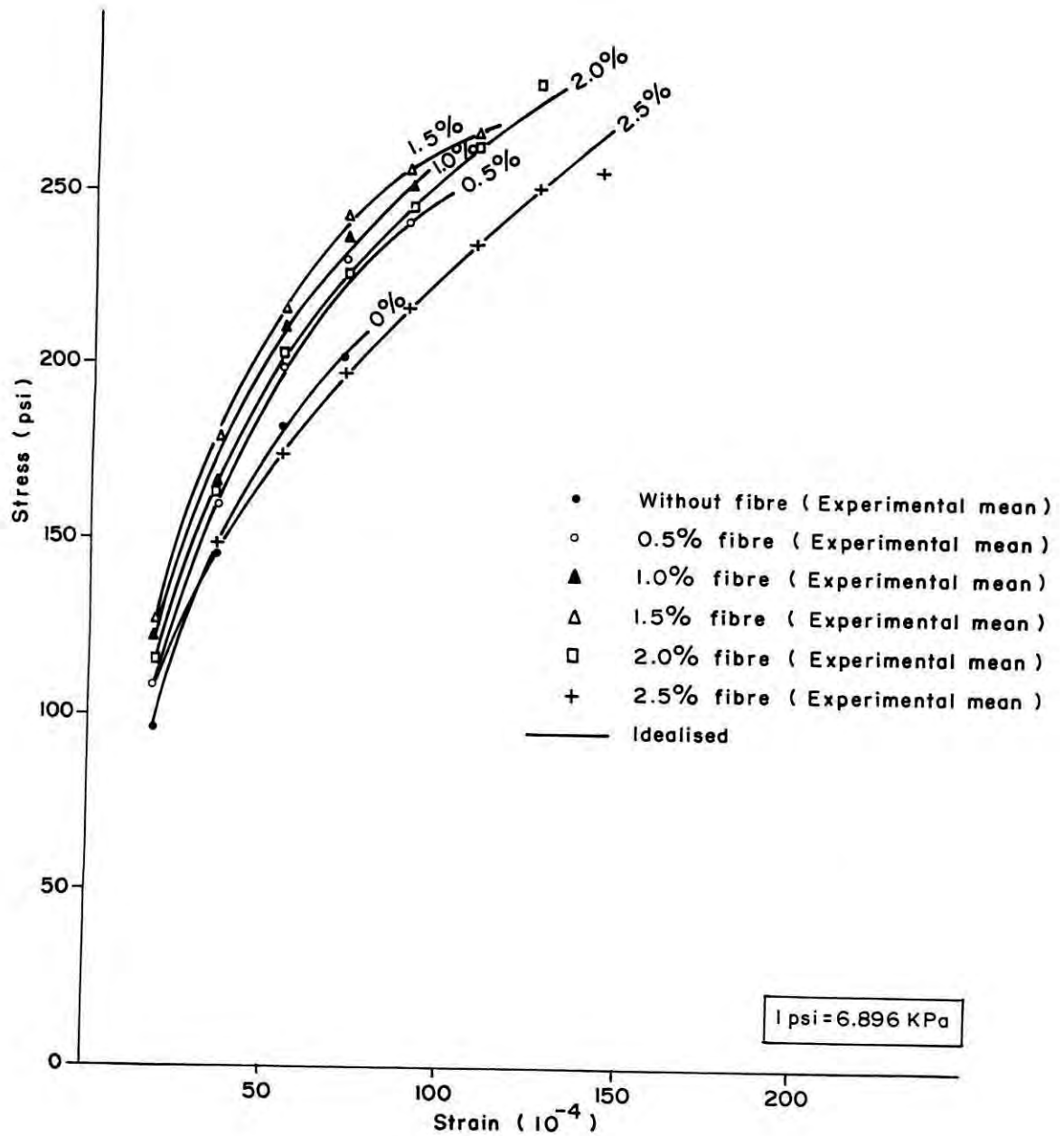


Fig. 5.10 Average Vertical Stress-Strain Curves For Mud Mortar With Different Jute Fibre Content.

### a) Analysis of Lateral Deformation Characteristics

The lateral deformation characteristic can be analysed as follows:

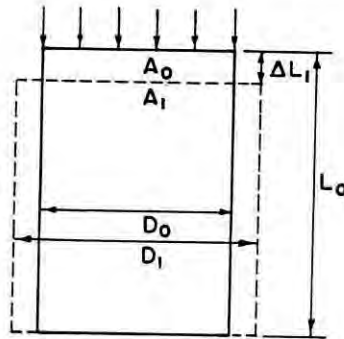


Fig. 5.11 Cylindrical Mortar Specimen under Vertical Compression

Let us consider a cylindrical specimen having length  $L_0$ , diameter  $D_0$  and cross-sectional area  $A_0$ . Let at any vertical stress level  $\sigma_v$  the specimen undergoes a vertical deformation of  $\Delta L_1$ . As a result, its diameter and cross-sectional area becomes  $D_1$  and  $A_1$  respectively.

Considering the volume remaining unchanged due to instantaneous strain relaxation (for mud mortar),

$$A_0 L_0 = A_1 (L_0 - \Delta L_1)$$

Or,

$$A_1 = \frac{A_0}{(1 - \Delta L_1 / L_0)}$$

From which,

$$D_1 = \frac{D_0}{\sqrt{(1 - \Delta L_1/L_0)}}$$

Therefore, lateral deformation =  $D_1 - D_0$

$$= D_0 [1/\sqrt{(1 - \Delta L_1/L_0)} - 1]$$

$$\text{Lateral strain} = \frac{D_1 - D_0}{D_0}$$

$$= [1/\sqrt{(1 - \Delta L_1/L_0)} - 1]$$

$$\text{Poisson's ratio } \nu_1 = [1/\sqrt{(1 - \Delta L_1/L_0)} - 1]/[\Delta L_1/L_0]$$

$$= [1/\sqrt{(1 - \epsilon_1)} - 1]/\epsilon_1 \quad (5.24)$$

Where,  $\Delta L_1/L_0 = \epsilon_1 =$  vertical strain. [The same expression can be obtained if we consider a cubical specimen instead of cylindrical specimen]

If the same specimen of any other strain relaxing material undergoes a vertical strain of  $\epsilon_2$  at the same vertical stress  $\sigma_v$ , then Poisson's ratio of that material,

$$\nu_2 = [1/\sqrt{(1 - \epsilon_2)} - 1]/\epsilon_2 \quad (5.25)$$

If  $\epsilon_1 < \epsilon_2$ , from the above two eqns., for any value of  $\epsilon_1$  and  $\epsilon_2$ ,  $\nu_1 < \nu_2$ . Therefore, at the same vertical stress level, the mud mortar exhibiting smaller vertical strain has smaller Poisson's ratio.

It has been observed earlier, for inclusions in between 1.5 to 2.0%, the vertical strain in fibre included mortar is smaller than that of a mortar without fibre at the same vertical stress level. As such, within this limit of inclusion the Poisson's ratio and consequently lateral deformation of a mortar with fibre is smaller than the mortar without fibre.

#### 5.4.3 Role of Jute Fibre on the Compressive Strength

Two types of compression tests have been carried out on mud mortar. The tests were, compression test on mortar cubes and strain controlled unconfined compression test on mortar cylinders. It is to be noted that jute fibre was used as reinforcement in the mud mortar. Different percentages varying from 0% to 2.5% were used in the present study.

As can be seen from Table 4.5, the mortar cubes without fibre failed by sudden crushing at an average stress of 402 psi. The water content of specimens during test was 2.38%.

The cubes with fibre behaved as perfectly plastic material marked by increase in lateral dimension with the incremental load without any sign of failure. For an instance, some of these cubes were loaded upto 2.8 times the failure load of the cubes without fibre. The cross-sectional area of the cubes increased but not to the extent of 2.8 times the original cross-sectional area. From these observations it can be concluded that inclusion of fibre increases the compressive strength of mud mortar. But the extent of increment can not be determined by simple compression test. Therefore, the strength increment of sundried mud bricks after the inclusion of wheat straw reported by Swami Saran et al.<sup>[45]</sup> and Madhupur soil after the inclusion of jute fibre reported by Rahman et al.<sup>[47]</sup> may not be to the extent they have reported.

Therefore, the failure load of the mud mortar was determined from strain controlled unconfined compression test. The ultimate failure was marked by the incapability of the specimen to carry further load. The summary of the test results have been presented in Table 4.6. Detailed experimental results are contained in

Appendix-B. Table 4.6 shows no appreciable change in water content in the specimens. Therefore, the percentage of fibre can be considered as the only variable.

Fig. 5.12 shows the unconfined compressive strength of mud mortar for different Jute fibre contents. It indicates that unconfined compressive strength of mud mortar increases with the increase in fibre content upto an inclusion of 1.9%. The maximum increase of strength is 35.3%. Above 1.9% inclusion, the unconfined compressive strength decreases with the increase of percentage inclusion.

#### 5.4.4 Compressive Strength of Masonry with Mud Mortar

5-high stack bonded prisms with mud mortar were tested to evaluate the compressive strength of masonry with mud mortar. Jute mat and various percentages of randomly distributed jute fibre were introduced in the mortar bed joints to see the effect of reinforced mud mortar on the compressive strength of masonry. The effect of inclusion of jute fibre on the deformation and strength characteristics of mud mortar have already been discussed in section 5.4.2 and 5.4.3. From the discussions it appears that the inclusion of fibre upto certain percentage improves the properties of mud mortar under vertical load. But the reviewed literature indicates that the improvement in mortar strength due to the inclusion of fibres is very negligible. Moreover, higher ductility (see section 5.4.2) imparted by fibre to the mud mortar may enhance failure. These can be observed from the test results of masonry specimens with mud mortar in Table 4.7. The table shows that the variation in water content of the mortar bed is very negligible. Therefore, the percentage of fibre may be considered as the only variable. The table also shows that the appearance of first visible crack and occurrence of ultimate failure is very early in comparison with 5/high brick



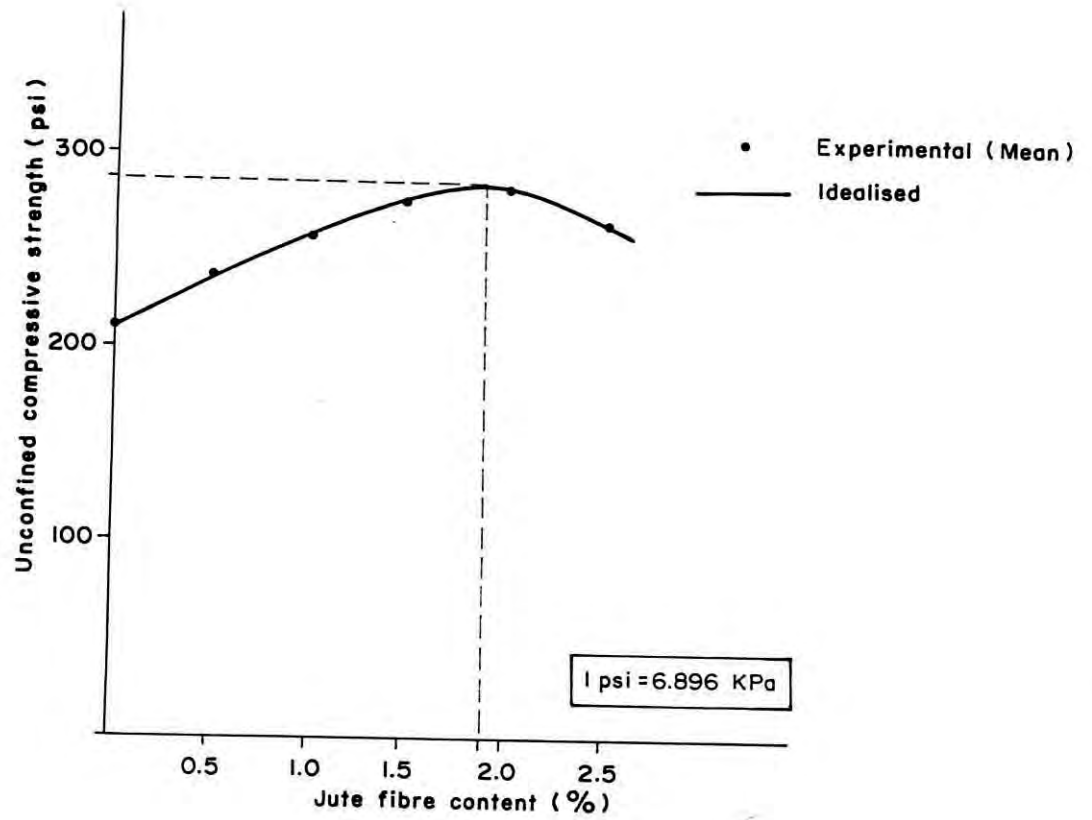


Fig. 5.12 Average Unconfined Compressive Strength Vs. Jute Fibre Content For Mud Mortar.

stack bonded prism made with cement mortar. In case of mortar without fibre, first visible crack appears at 30% of ultimate load. As the percentage of fibre increases this crack appears earlier and at the same time ultimate strength decreases. This decrease in strength is possibly due to the excessive lateral deformation of mud mortar in the bed joint. Based on the test results it may be concluded that neither jute mat nor randomly distributed fibres in the mortar improves the load carrying capacity of masonry.

## CHAPTER 6

# ELASTIC FINITE ELEMENT STUDY OF BRICK PRISMS

### 6.1 INTRODUCTION

Experimental investigation and the observed behavior of the prisms under compression have already been described in the previous chapters. This chapter presents the elastic finite element analysis of different test prisms constructed with cement mortar. The prisms with mud mortar were discarded from this study as the mud mortar does not exhibit elastic properties. Moreover, the interface of brick and mud mortar can not be assumed perfectly bonded.

In this study two-dimensional finite element analyses have been used. The analyses were done by using two-dimensional linear elastic finite element model developed by Ali<sup>[47]</sup>. The model considers the prism to be an assemblage of elastic bricks and joints, each with different material properties determined by experimental investigations presented in Table 3.1 and 3.3. However, due to the limitation of test facilities, Poisson's ratio of the brick and the mortar was not determined. This was assumed to be 0.20 and 0.16 respectively.

For vertical loading, the distribution of transverse stresses in the prism were studied under two different conditions of the loading edge. The first one (Case-I) eliminates the restraining effect of the machine platen and the other (Case-II) considers the effect. The objective of the study is to analyse the observed experimental behavior with an emphasis on the variations in transverse stresses as these critically influence the failure of the prisms.

## 6.2 FINITE ELEMENT METHOD OF ANALYSIS

The present analytical procedure is based on the finite element method. The application of this method has become very common and has been described adequately in many text books. However, it is useful to explain briefly that the method is extremely versatile in being capable of analysing plates or solid bodies which may be not only irregular in shape but in which the physical properties may vary from one part to another.

The finite element method can be thought of as a general method of structural analysis by means of which the solution of a problem in continuum mechanics may be approximated by analysing a structure consisting of an assemblage of properly selected finite elements interconnected at a finite number of joints (nodal points).

For the purpose of structural analysis, a structure can be idealized as a system of nodal points interconnected by discrete elements. The objective of the analysis given the joint loading, the geometry of the structure (location of joints), and the stiffness properties of the structural elements is to find the resulting joint displacements and the internal stresses in the structural elements. The size of the elements is one of the major factors influencing the accuracy of the solution. As a general rule, the size of the elements should be as small as possible. When a large number of elements are required, the technique of mesh-reinforcement is useful.

## 6.3 TWO DIMENSIONAL LINEAR FINITE ELEMENT MODEL

The particular two dimensional model uses four noded isoparametric elements (see Figure 6.1) with two degrees of

freedom per node and linear displacement functions along their edges.

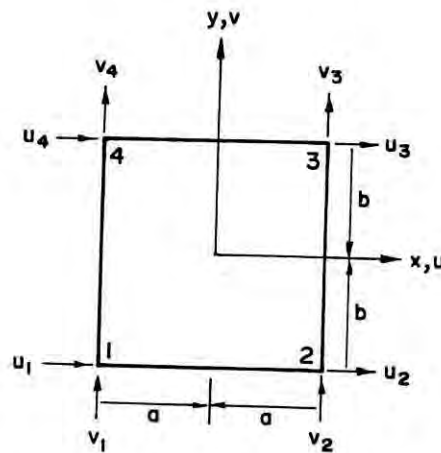


Fig. 6.1 Typical Four Noded Element

A shape function  $N_i$  defines displacements within an element when the  $i$ th nodal displacement has unit value and all other nodal displacements are zero.

The displacement vectors for any point within the element is given by,

$$\begin{bmatrix} u \\ v \end{bmatrix} = \begin{bmatrix} N_1 & 0 & N_2 & 0 & N_3 & 0 & N_4 & 0 \\ 0 & N_1 & 0 & N_2 & 0 & N_3 & 0 & N_4 \end{bmatrix} \begin{bmatrix} u_1 \\ v_1 \\ u_2 \\ v_2 \\ u_3 \\ v_3 \\ u_4 \\ v_4 \end{bmatrix} = [N] [\delta] \quad (6.1)$$

in plain strain problem, the state of strain at any point is defined by three parameters, two direct strains ( $\epsilon_x$  &  $\epsilon_y$ ) and one shear strain ( $\gamma_{xy}$ ),

where,  $\epsilon_x = \delta u / \delta x$ ,  $\epsilon_y = \delta v / \delta x$  and  $\gamma_{xy} = \delta u / \delta y + \delta v / \delta x$

in matrix form,

$$\begin{aligned} \begin{bmatrix} \epsilon_x \\ \epsilon_y \\ \epsilon_{xy} \end{bmatrix} &= \begin{bmatrix} \delta u / \delta x \\ \delta v / \delta y \\ \delta u / \delta y + \delta v / \delta x \end{bmatrix} = \begin{bmatrix} \delta / \delta x & 0 \\ 0 & \delta / \delta y \\ \delta / \delta y & \delta / \delta x \end{bmatrix} \begin{bmatrix} u \\ v \end{bmatrix} \\ &= \begin{bmatrix} \delta / \delta x & 0 \\ 0 & \delta / \delta y \\ \delta / \delta y & \delta / \delta x \end{bmatrix} [N] [\delta] \end{aligned} \quad (6.2a)$$

Hence,

$$[\epsilon] = [B] [\delta] \quad (6.2b)$$

where,

$$[B] = \begin{bmatrix} \delta / \delta x & 0 \\ 0 & \delta / \delta y \\ \delta / \delta y & \delta / \delta x \end{bmatrix} [N]$$

we now consider the strain energy density. The isotropic elastic stress strain relationship in plane stress is:

$$\begin{aligned} \begin{bmatrix} \sigma_x \\ \sigma_y \\ \tau_{xy} \end{bmatrix} &= \frac{E}{1-\nu^2} \begin{bmatrix} 1 & \nu & 0 \\ \nu & 1 & 0 \\ 0 & 0 & (1-\nu)/2 \end{bmatrix} \begin{bmatrix} \epsilon_x \\ \epsilon_y \\ \gamma_{xy} \end{bmatrix} \\ &= [D] \begin{bmatrix} \epsilon_x \\ \epsilon_y \\ \gamma_{xy} \end{bmatrix} \end{aligned} \quad (6.3)$$

here  $[D]$  is called the modulus matrix.

We have, strain energy per unit volume,

$$\begin{aligned} &= \frac{1}{2} [\sigma_x \quad \sigma_y \quad \tau_{xy}] \begin{bmatrix} \epsilon_x \\ \epsilon_y \\ \gamma_{xy} \end{bmatrix} \\ &= \frac{1}{2} [D] \begin{bmatrix} \epsilon_x \\ \epsilon_y \\ \gamma_{xy} \end{bmatrix} \begin{bmatrix} \epsilon_x \\ \epsilon_y \\ \gamma_{xy} \end{bmatrix} \\ &= \frac{1}{2} [\epsilon_x \quad \epsilon_y \quad \gamma_{xy}] [D] \begin{bmatrix} \epsilon_x \\ \epsilon_y \\ \gamma_{xy} \end{bmatrix} \\ &= \frac{1}{2} [\epsilon]' [D] [\epsilon] \end{aligned} \quad (6.4)$$

$$\therefore \text{Strain energy} = \frac{1}{2} \int [\epsilon]' [D] [\epsilon] dV$$

where V = volume.

$$\text{Again, strain energy} = \frac{1}{2} [\delta]' [K] [\delta] \quad (6.5)$$

From eqn. 6.4 & 6.5,

$$[K] = t \int_{-a}^a \int_{-b}^b [B]' [D] [B] dA \quad (6.6)$$

where, A = area, t = thickness.

Now,

$$dV = t dA$$

By integration, each of the element of the stiffness matrix can be determined.

Finally by assembling the element stiffness matrix, structural stiffness matrix of the whole structure is determined. Once the stiffness matrix is determined,

$$\begin{aligned} [\delta] &= [K]^{-1} [F] \\ [\epsilon] &= [B] [\delta] \\ \text{and } [\sigma] &= [D] [\epsilon] \end{aligned}$$

Hence, stresses at different points can be obtained.

#### 6.4 FINITE ELEMENT ANALYSIS OF PRISMS

An approximation adopted for the analysis of brick prisms is that a three-dimensional brick prism can be represented by a two-dimensional plate, i.e. no stresses exist perpendicular to the face of the prism. The particular two dimensional linear elastic finite element computer program used for this analysis is

written in Fortran IV and uses four noded isoparametric elements with two degrees of freedom per node and linear displacement functions along their edges (Fig. 6.1). When run on the IBM 370 computer consisting of upto a maximum number of about 500 elements can be solved. The computer output includes the nodal displacements, the transverse stresses and shear stresses at the nodal points as well as at the centroid of each element. Particular advantage of the model relating to the brickwork problem are that the sizes, Young's modulus and Poisson's ratio can be varied from element to element throughout the brickwork, thus allowing the mortar elements to be clearly distinguished from those of brick. The assumption of linear elastic behaviour until failure was considered reasonable since the specimen is in a state of biaxial tension-compression.

To determine the distribution of stresses, the average elastic properties given in Table 3.1 & 3.5 were assigned to the brick and mortar elements. Three rows of elements were provided through the brick units and two rows of elements were through the mortar joints to obtain the variations of transverse stresses. For each type of specimen two conditions of compressive loading were analysed. One eliminating the restraining effect of the platen and the other considering the platen restraint. Compressive loads were applied in the form of prescribed displacements of the loading edges. To simulate the restraint free condition of the platen, the nodes at the loading edges were kept free for horizontal movement. However, for the rigid steel platen at the edges, the nodes were restrained to simulate the friction developed between the loading plates and the specimen. Two-dimensional finite element meshes used for the specimens adopted for different boundary and loading conditions are shown in Figs. 6.2-6.7.



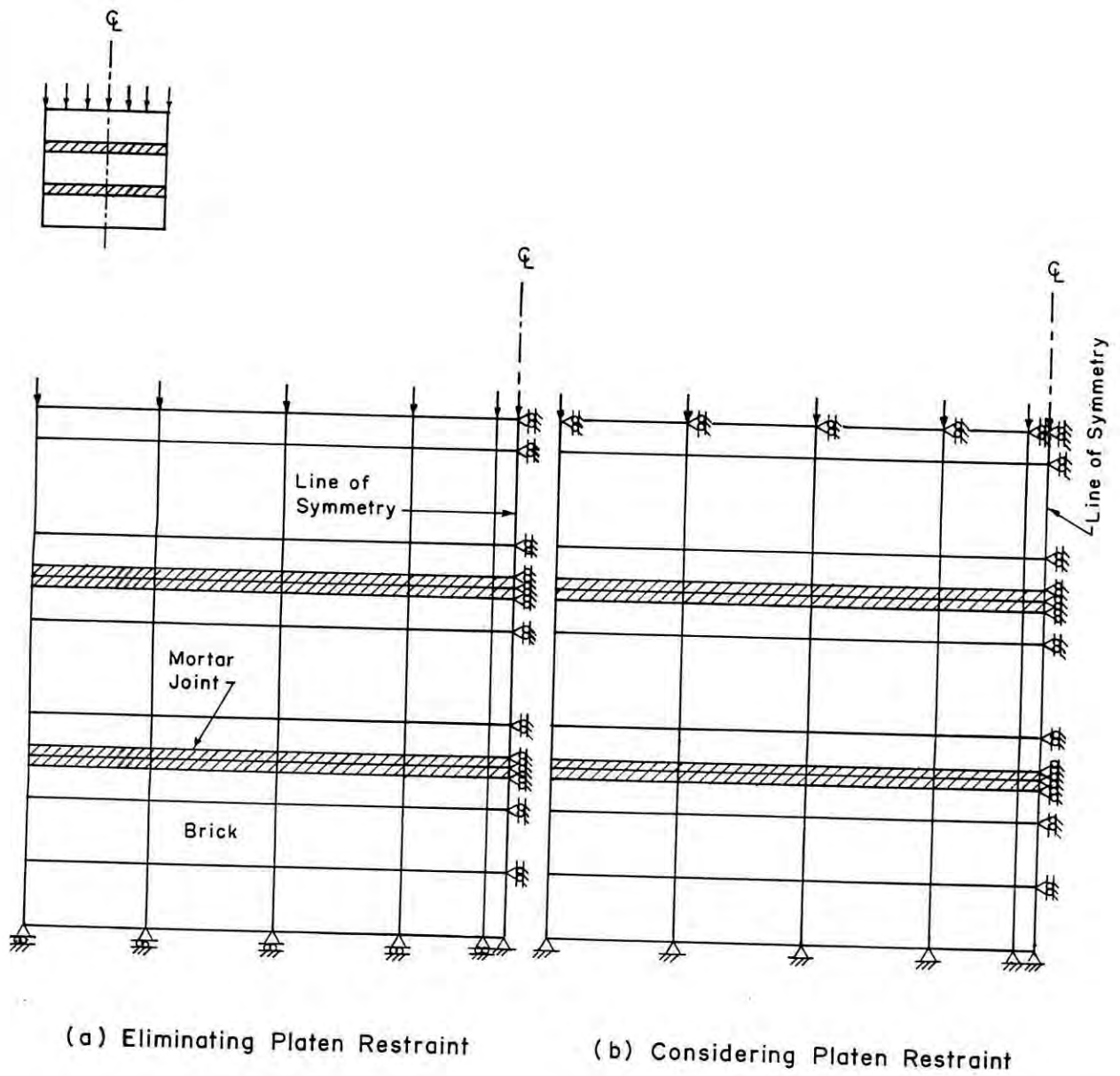
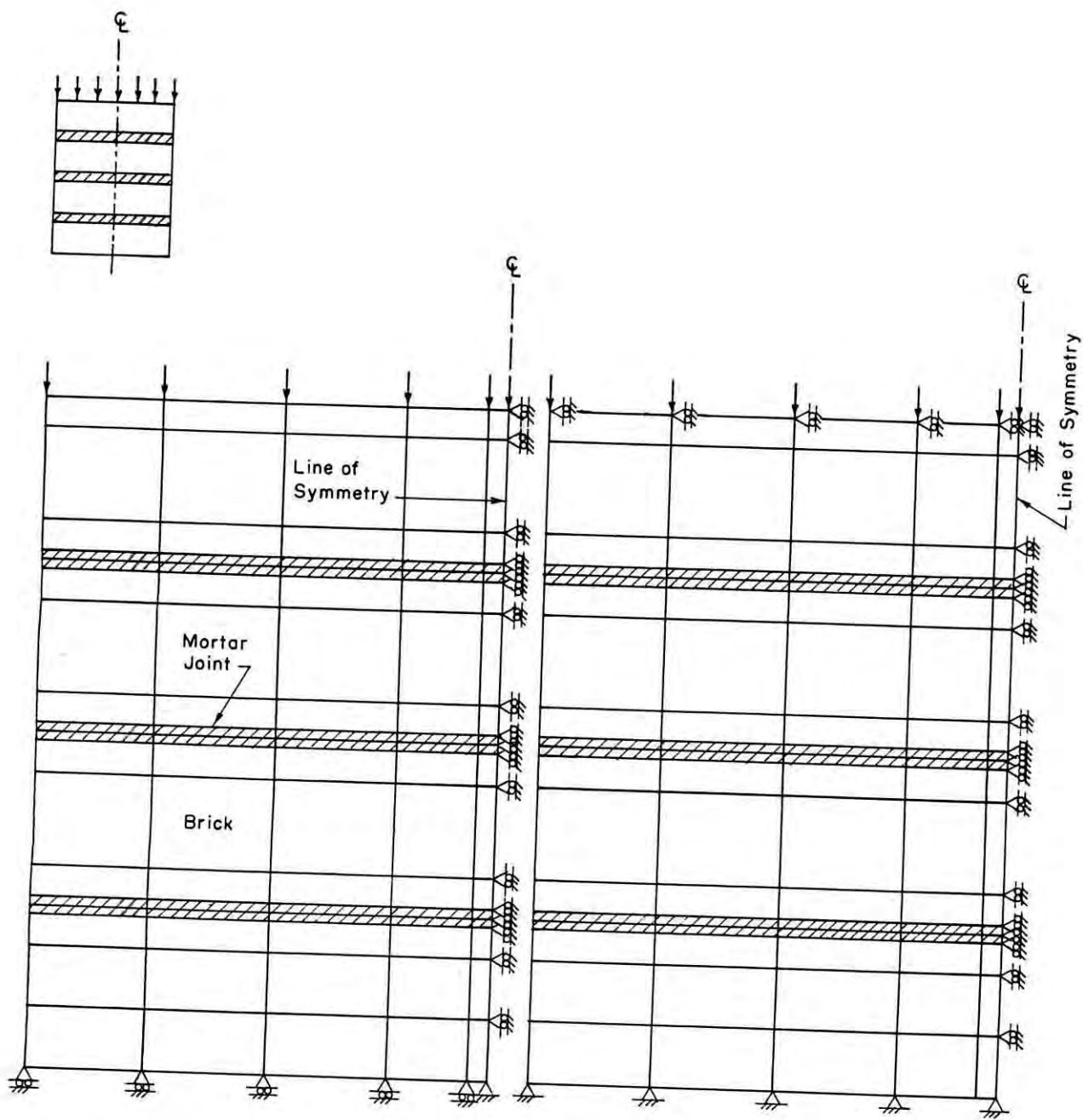


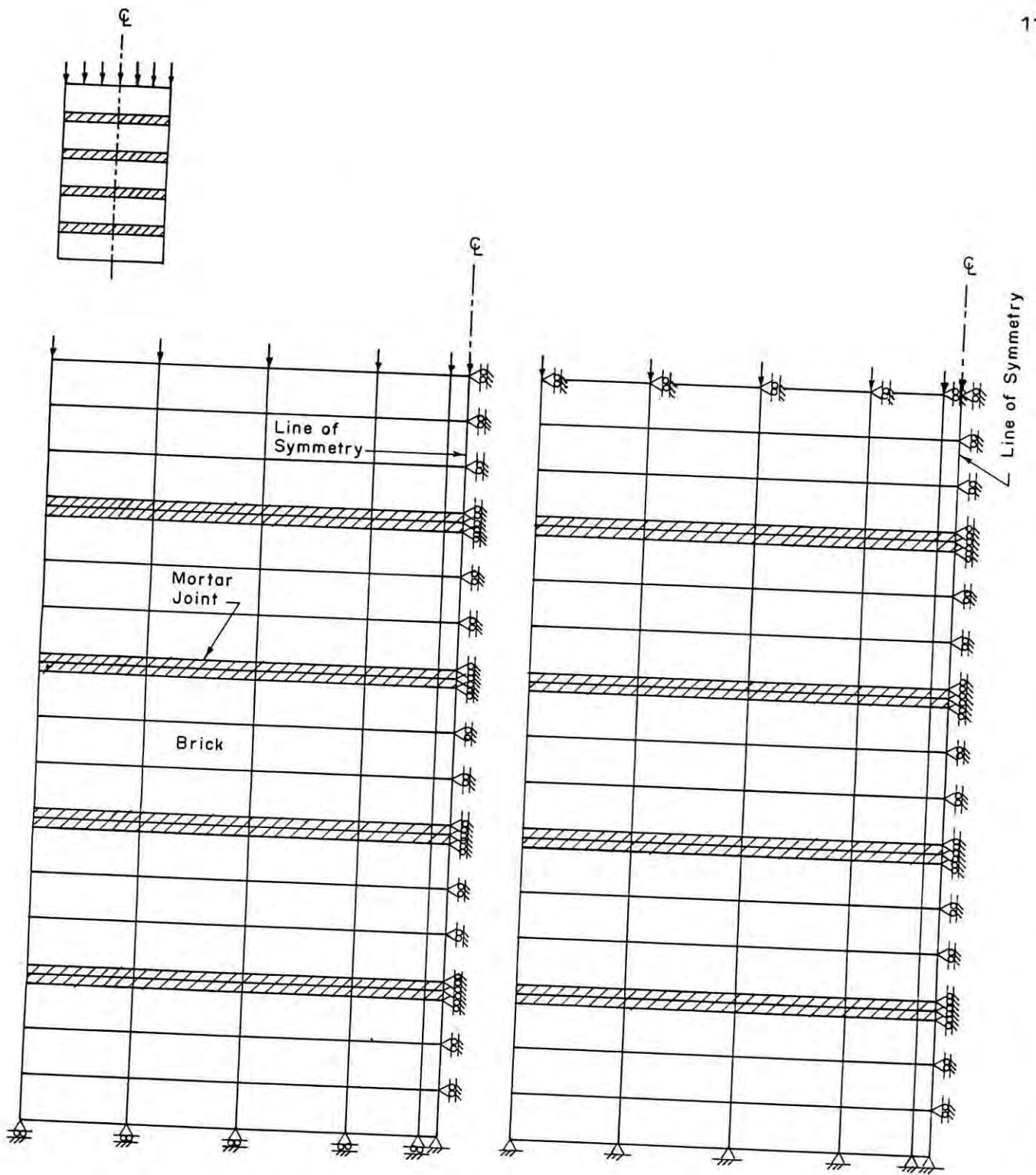
Fig. 6.2 Two Dimensional Finite Element Mesh for 3 SPC Prism.



(a) Eliminating Platen Restraint

(b) Considering Platen Restraint

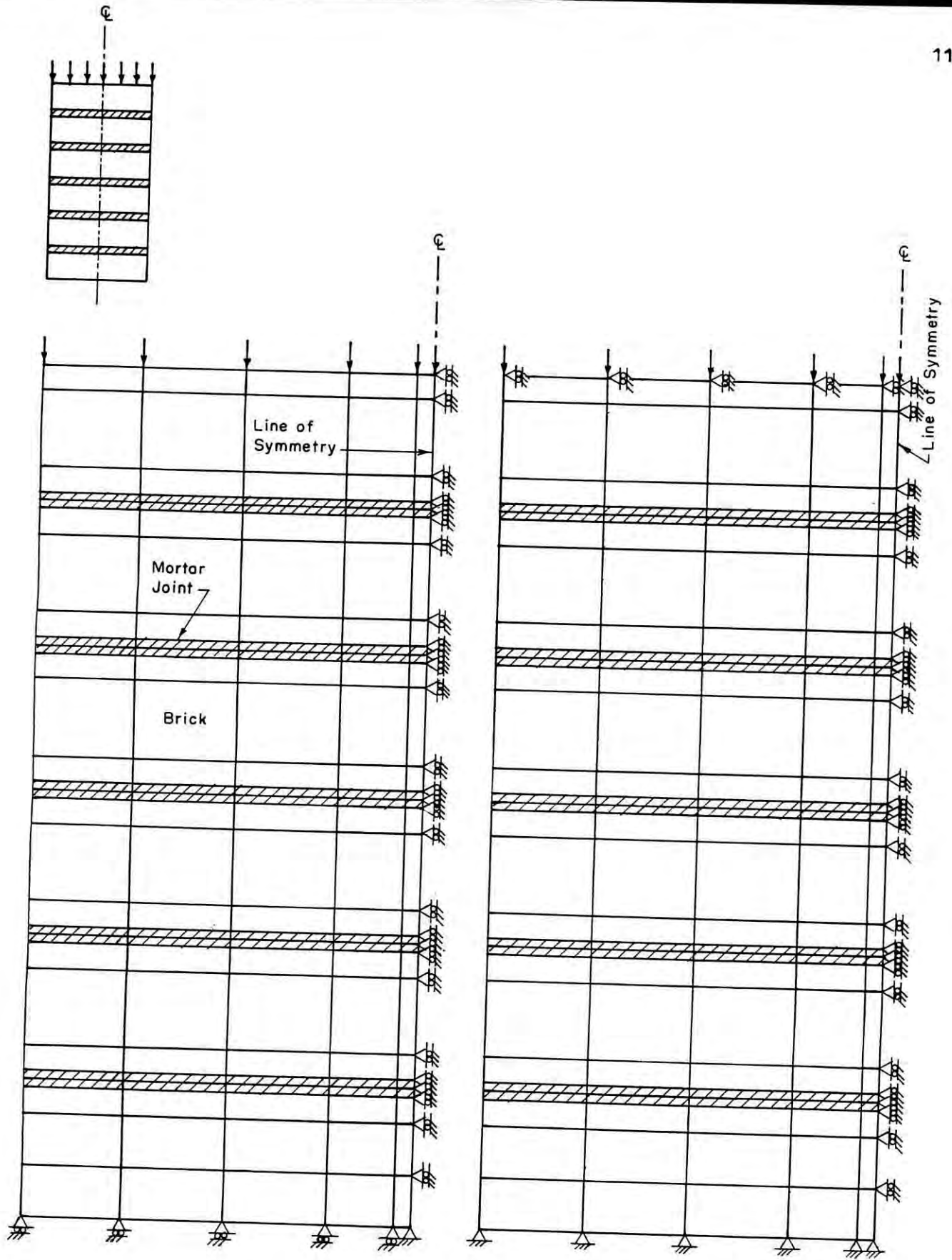
Fig. 6.3 Two Dimensional Finite Element Mesh for 4 SPC Prism.



(a) Eliminating Platen Restraint

(b) Considering Platen Restraint

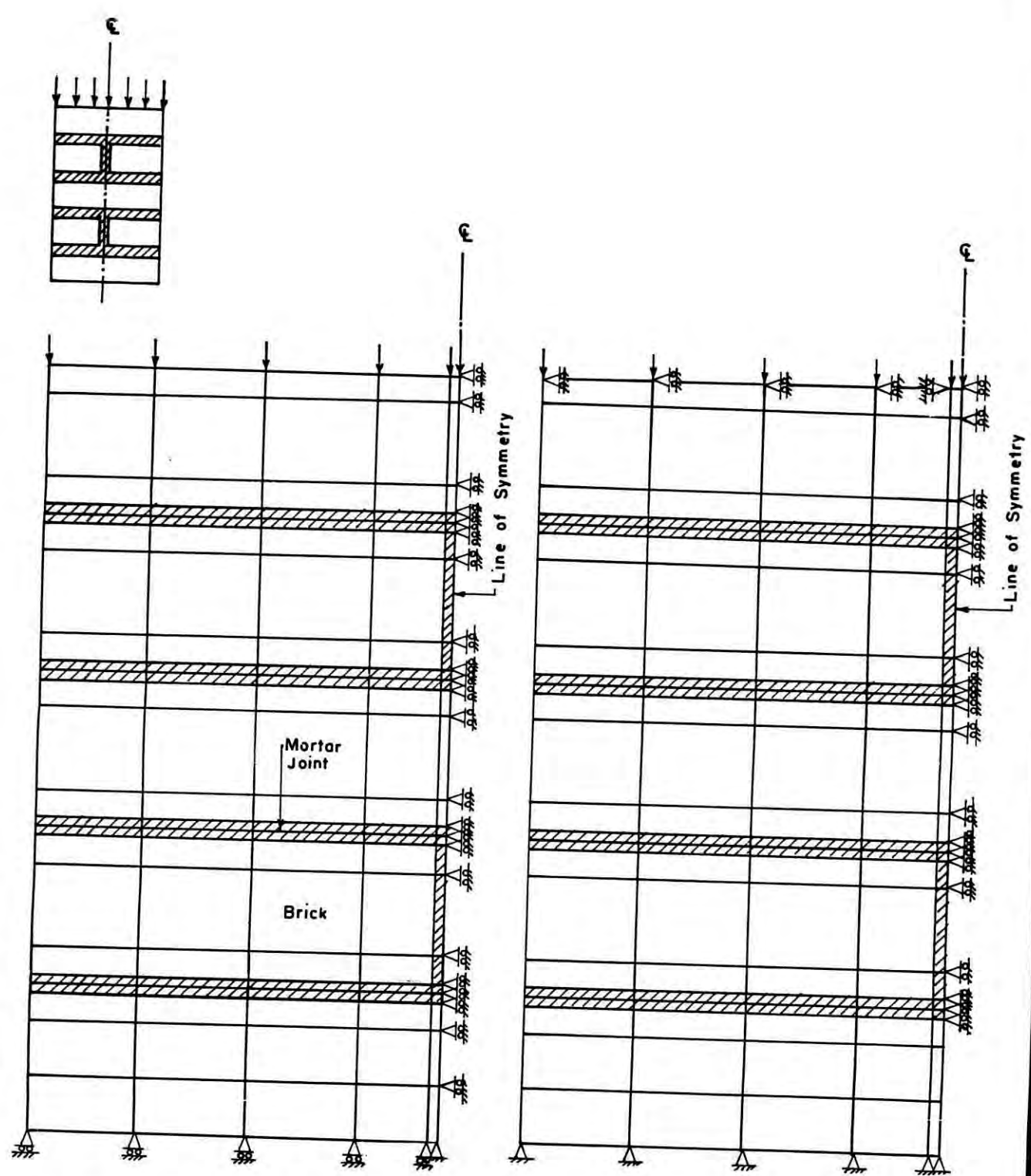
Fig. 6.4 Two Dimensional Finite Element Mesh for 5SPC Prism.



(a) Eliminating Platen Restraint

(b) Considering Platen Restraint

Fig. 6.5 Two Dimensional Finite Element Mesh for 6SPC Prism.



(a) Eliminating Platen Restraint

(b) Considering Platen Restraint

Fig. 6.6 Two Dimensional Finite Element Mesh for 5VPC-A Prism.

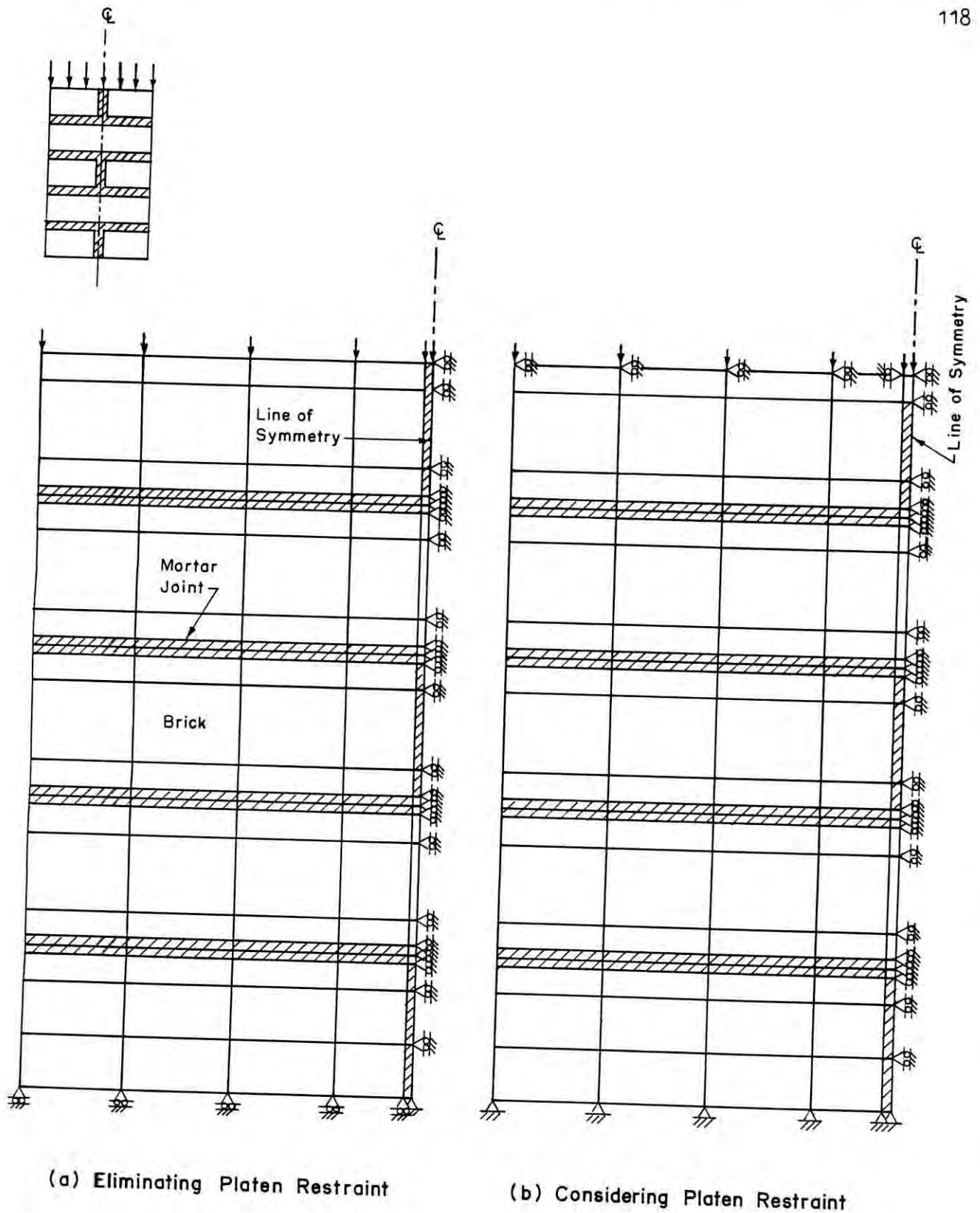


Fig. 6.7 Two Dimensional Finite Element Mesh for 5VPC-B Prism.

## 6.5 RESULTS OF THE FINITE ELEMENT ANALYSIS

Two-dimensional linear elastic finite element analyses have been carried out for 3SPC, 4SPC, 6SPC, 5VPC-A, 5VPC-B prisms. In all the analyses, the load was applied in the form of prescribed displacement at the nodes, simulating the rigid loading platen. Under same vertical load, the distributions of transverse stresses down the centre line of prisms with different height for both Case-I and Case-II are shown in Figs. 6.8-6.13. The central vertical planes have been selected for the presentation. This is because the transverse stresses are possibly the maximum (critical) at this plane of symmetry. Also this plane passes through the centre of the vertical joints of 5VPC-A and 5VPC-B prisms. Therefore, the variation in distribution of transverse stresses due to the provisions of vertical joints in the prism could be studied.

From Figs. 6.8-6.13 it can be seen that for an ideal case of restraint free condition of the loading edge, all mortar joints are in compression and the bricks are in tension in the transverse direction. It implies that in a vertically loaded prism, the mortar bed joints experience triaxial compression and the bricks experiences uniaxial compression and bilateral tension. This transverse tensile stresses critically influence the fracture process of prisms and wallettes as has been observed frequently during experiment.

The figures show that the distribution of transverse stresses for all the specimens with platen effect eliminated (case-I) are very similar. The bricks near the platen in these cases are subjected to tension. As a result the ultimate strength in these cases will be lower than the strength of the specimens with platen effect not eliminated (case-II). It should be mentioned that for this

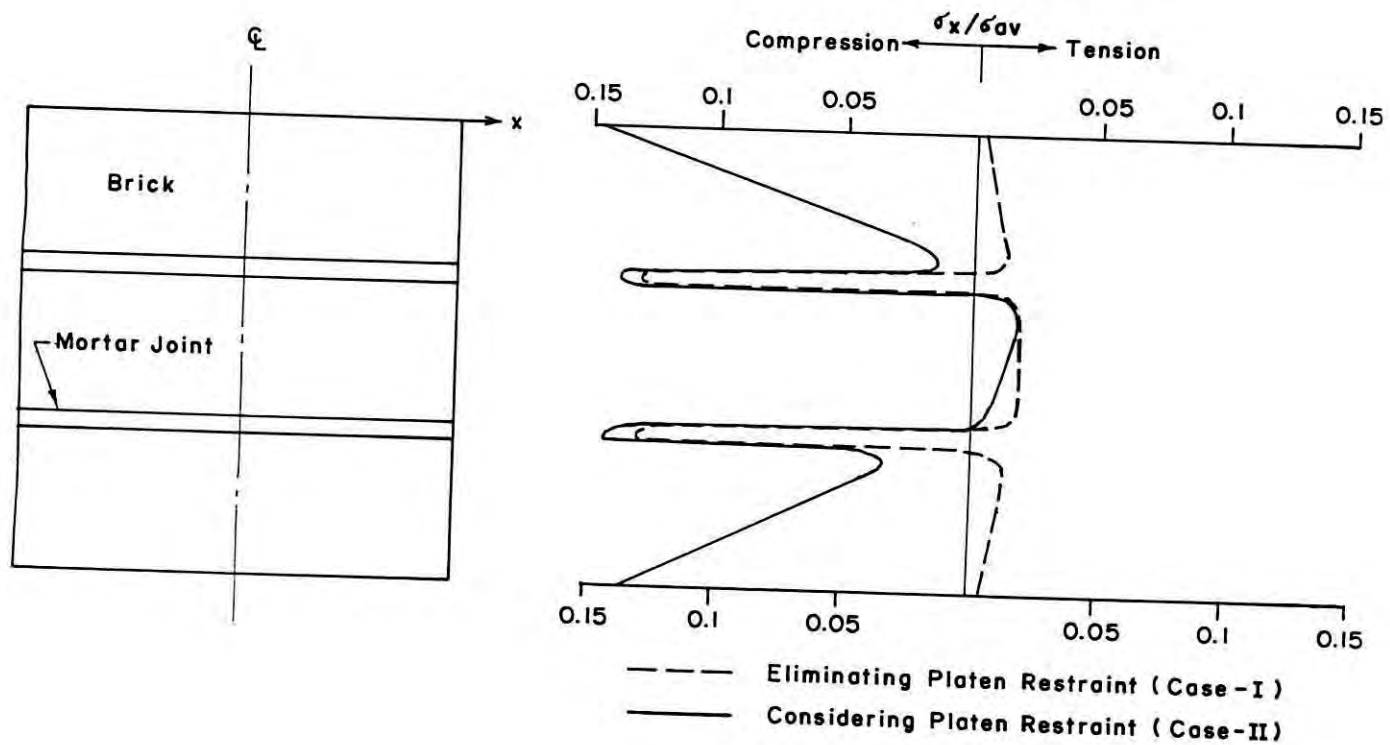


Fig. 6.8 Transverse Stress ( $\sigma_x$ ) Distributions Down Centre Line for 3SPC Prism.



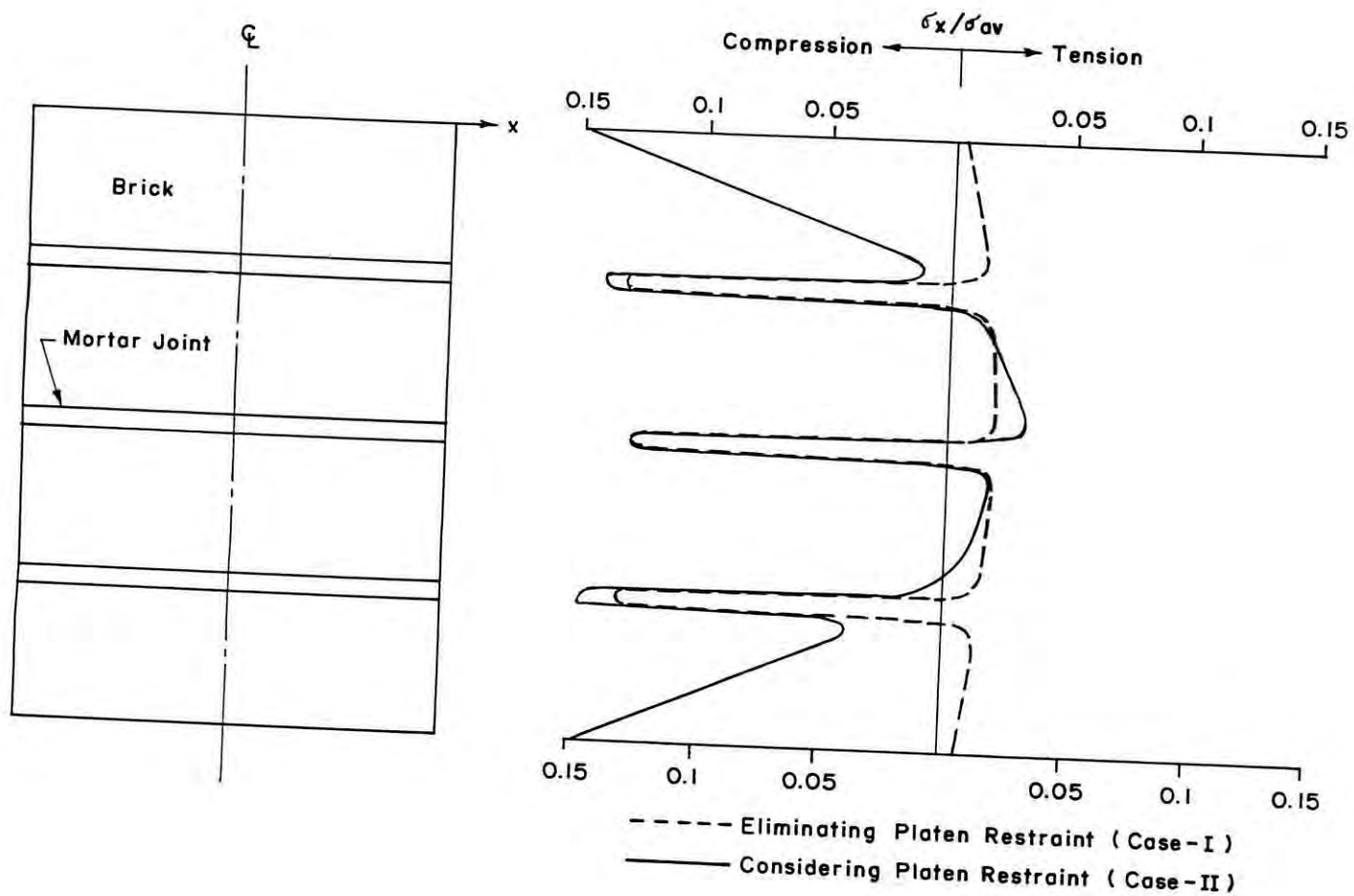


Fig. 6.9 Transverse Stress ( $\sigma_x$ ) Distributions Down Centre Line for 4SPC Prism.

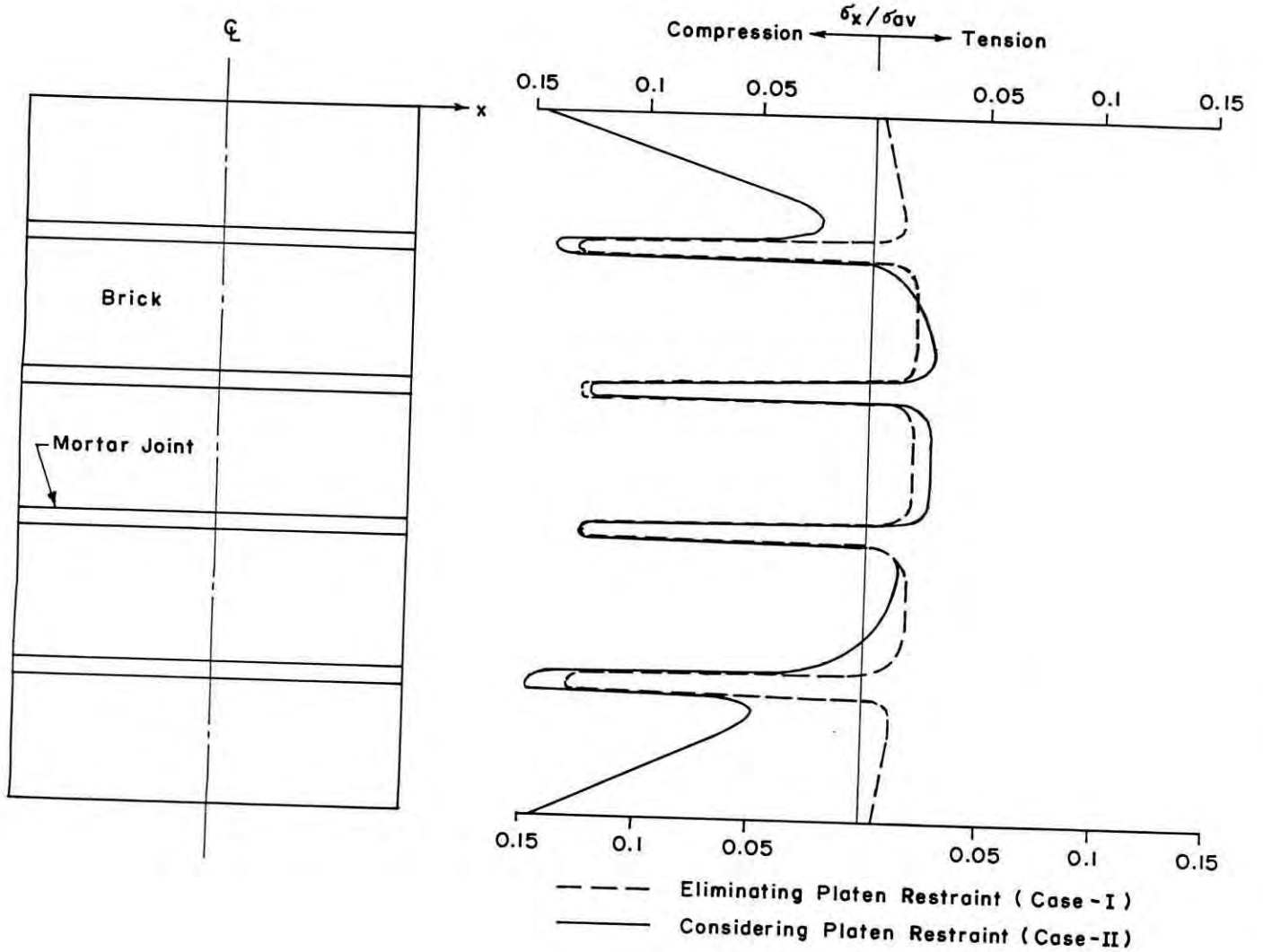


Fig. 6.10 Transverse Stress ( $\sigma_x$ ) Distributions Down Centre Line for 5SPC Prism.

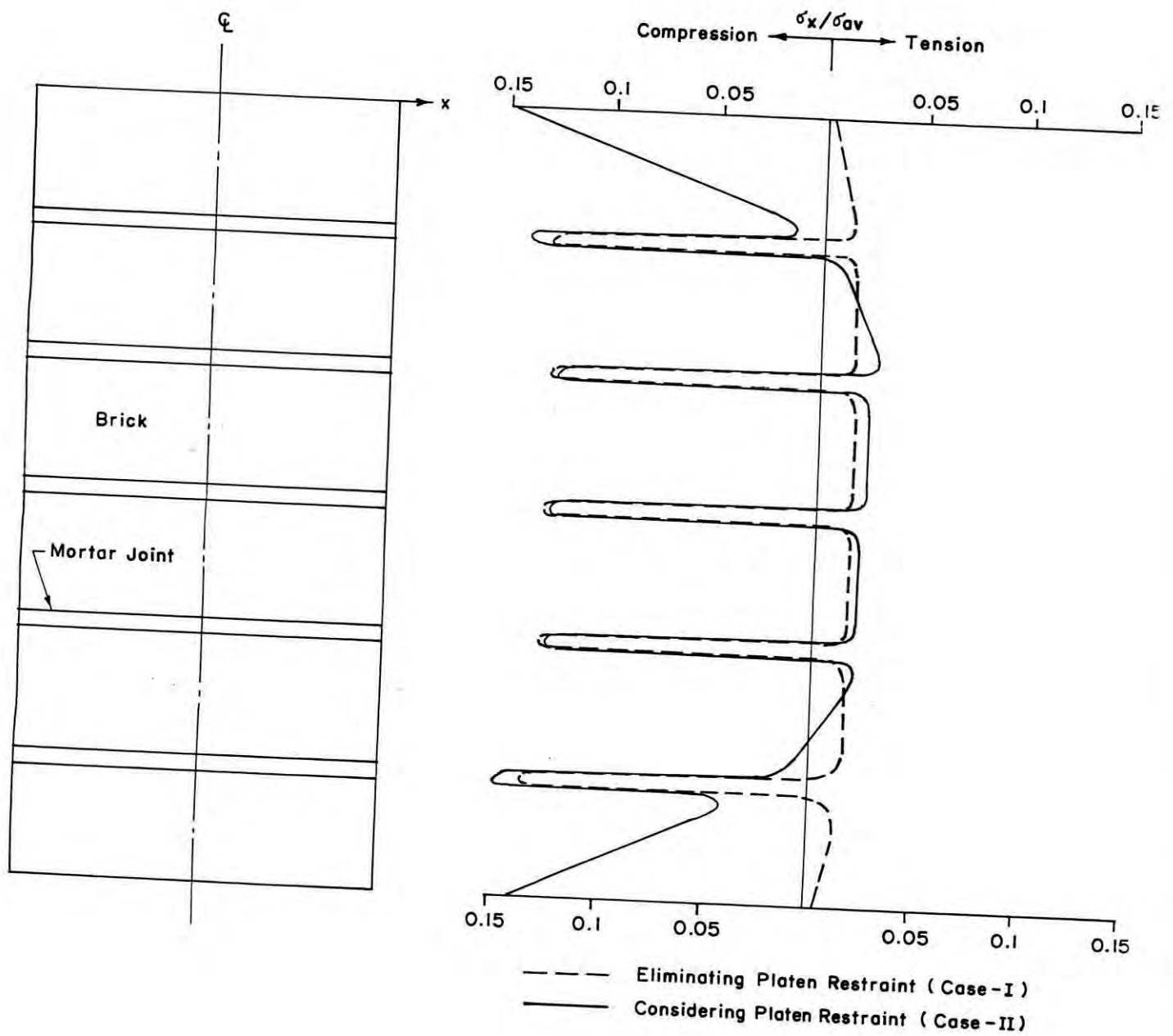


Fig. 6.11 Transverse Stress ( $\sigma_x$ ) Distributions Down Centre Line for 6SPC Prism.

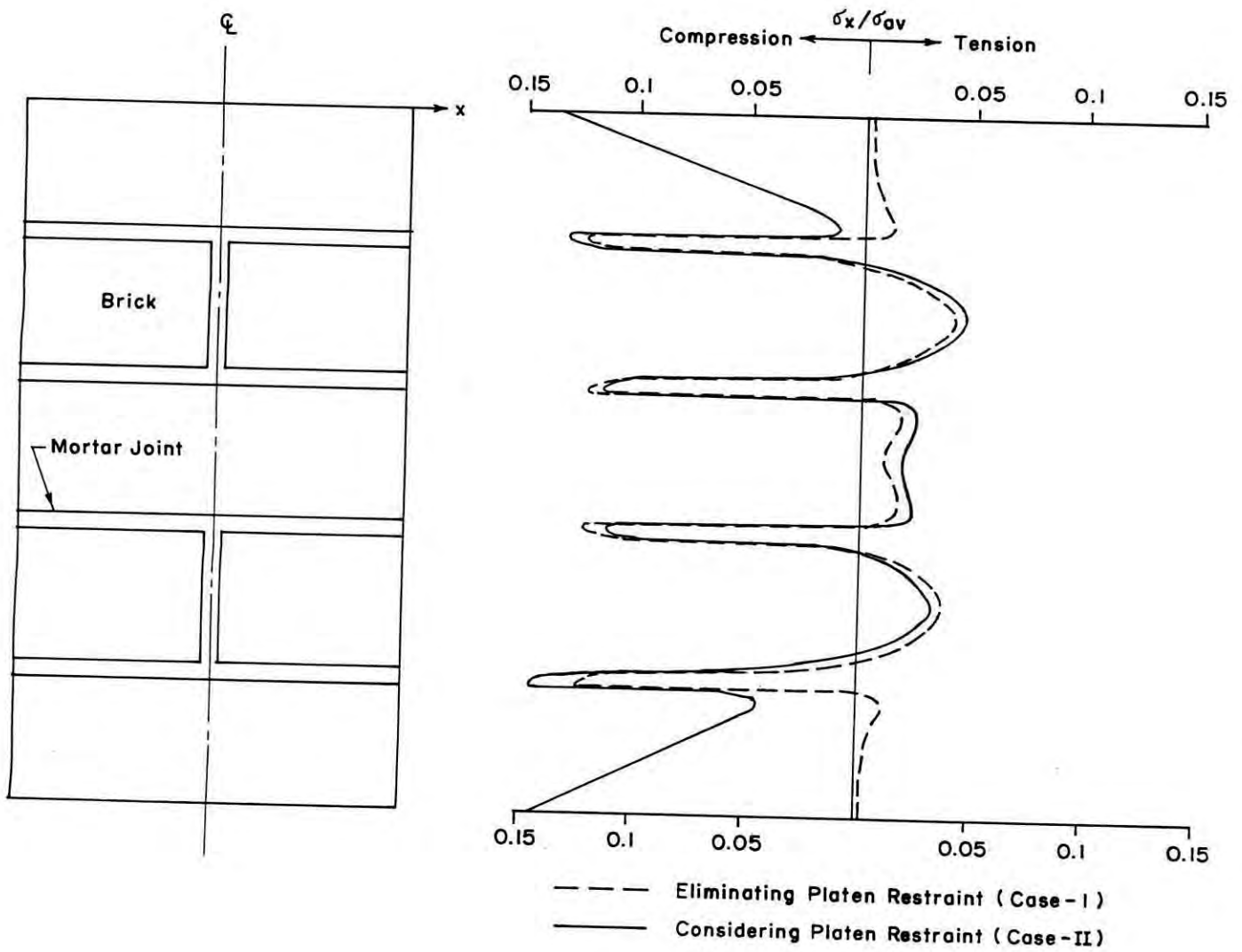


Fig. 6.12 Transverse Stress ( $\sigma_x$ ) Distributions Down Centre Line for 5VPC-A Prism.

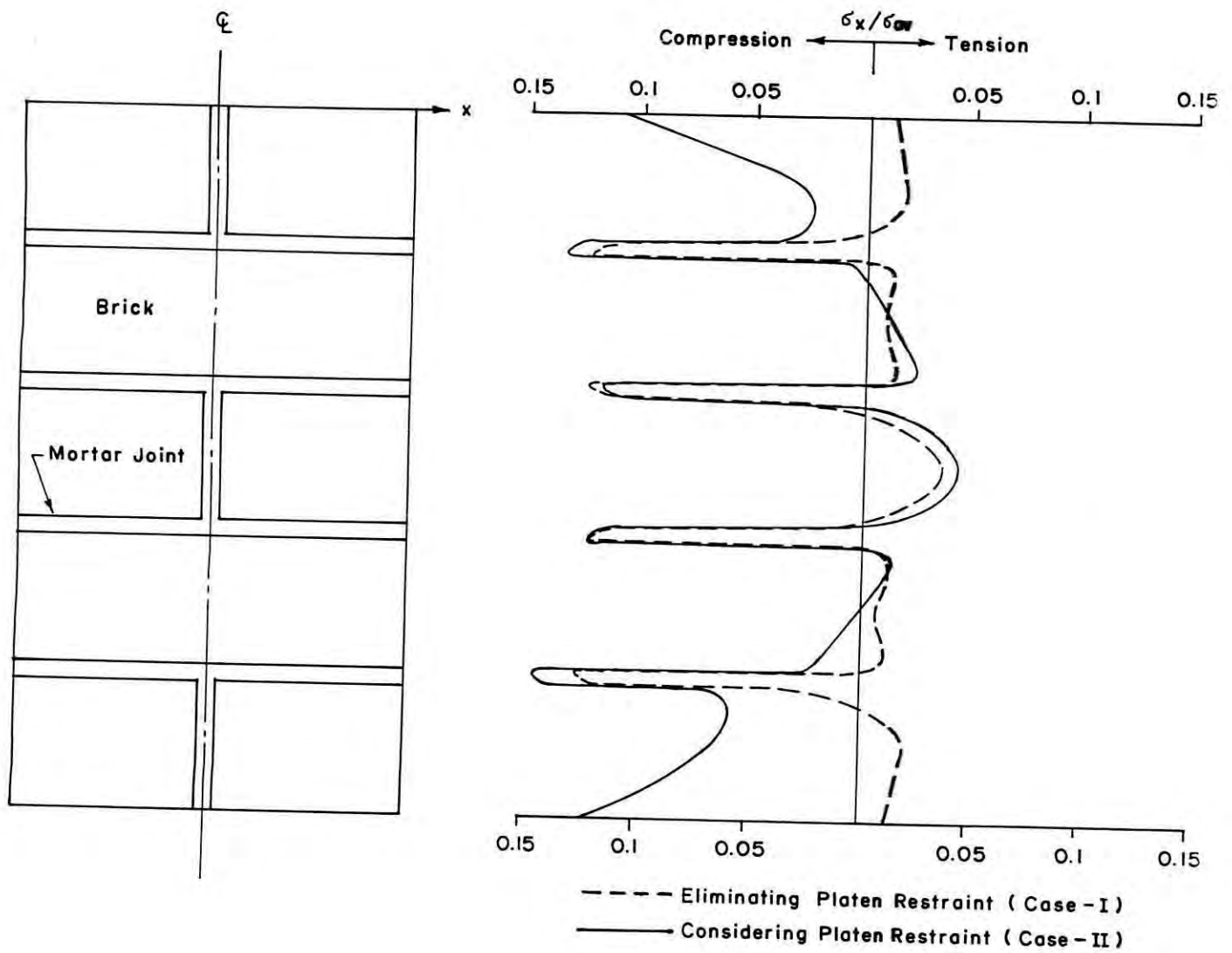


Fig. 6.13 Transverse Stress ( $\sigma_x$ ) Distributions Down Centre Line for 5VPC-B Prism.

study the friction between the platen and the specimen (platen effect) was not avoided.

From the figures it may be seen that due to the platen restraint transverse stresses are compressive near the loading point. Thus the restraining effect of the machine platen leads to a zone of triaxial compression which results in an artificial strengthening of the specimens. As the height of the specimen increases, the extent of area which is relatively free from restraining effect also increases. It indicates that the strengthening effect is greater for smaller prisms and decreases gradually as the height of the prism increases. This explains why the loss in compressive strength of stack bonded prisms takes place with an increase in prism height that emerges from Table 4.2 and Fig. 5.1. Again, Fig. 6.10 and Fig. 6.11 show that the middle brick of 5 brick high stack bonded (5SPC) prism and two middle bricks of 6 brick high stack bonded (6SPC) prism with platen effect not eliminated are free from restraining effect of machine platen and are subjected to tension. Therefore, the cracks are likely to initiate in these bricks. Since the magnitude and distribution of transverse stresses in the bricks of these two specimens (5SPC and 6SPC) are very similar, the failure load and the failure pattern of the specimens will be also similar. This supports the failure load and failure pattern observed for 5 brick high stack bonded (5SPC) prisms and 6 brick high stack bonded (6SPC) prism as can be seen from Fig. 5.1 and section 4.2.3(a) respectively.

The distribution of transverse stresses down the centre line of 5 brick high prism with vertical joints (5VPC-A and 5VPC-B) at different levels of the specimens is shown in Figs. 6.12 - 6.13. As mentioned earlier that the 5 brick high prism with vertical joints was selected to represent walls or wallettes. From the figures it is seen that in most of the cases the vertical joint is subjected to lateral tension. Since the tensile bond strength of mortar joint is very low, the fracture will start from these

vertical joints and will propagate through the bricks. This supports the failure mode observed for the prisms with vertical joints at different positions (see section 4.2.3(a)). However, this finite element analysis could not explain the reason of obtaining higher load for these specimens when compared with the failure load of wallettes. This is possibly due to the size of the specimen selected to represent the walls or wallettes. The prism contains only one plane of vertical joints (plane of weakness) whereas the walls or wallettes contain a large number of planes of weakness. Therefore the energy release after the fracture initiates for the wallettes per unit volume is higher than the energy release of prisms with only one plane of weakness resulting in lower load for the former case. This finite element analysis is also not able to explain the reason of obtaining higher failure load for 5 brick high prism with vertical joints than that of 5 brick high stack bonded prism. This is possibly due to the difference in fracture process in the specimens that has been described in section 4.2.3(a). The reason of obtaining higher strength has been explained in section 5.3.3 (a).

## CHAPTER 7

### CONCLUSIONS AND RECOMMENDATIONS FOR FUTURE STUDY

#### 7.1 CONCLUSIONS

An investigation has been made on the compressive behaviour of brick masonry. On the basis of the experimental and theoretical results of the investigation the following conclusions may be drawn:

1. Five brick high stack bonded prism has been found to be more suitable to determine the compressive behaviour of masonry. Experimental results show that a further increase in height does not appreciably change the behaviour of the prism. Finite element analysis on the other hand shows that significant portion of five brick high prism remains unaffected from the platen effect.
2. Deformation of masonry under vertical compression can be represented by a parabolic equation of best fit. Also, Saenz's equation with the proposed modification represents the vertical deformation characteristics of the masonry with good approximation.
3. The theoretical formula derived by the author on the basis of elastic analysis can be used to predict the initial tangent modulus of the masonry with good accuracy.



4. The incorporation of vertical joint in stack bonded prism provides similar failure mode as wallette but provides higher strength in comparison to stack bonded prism. The increase in strength of stack bonded prism with vertical joints is due to the distinct column action attained after the formation of well defined fracture plane at the centre line of the prism.
5. Prisms with vertical joint represent the failure mode of wall (wallette) more realistically than the stack bonded prism. But none of them resembles the compressive strength of the wall (wallette). To get the wall (wallette) strength a multiplying factor is required. The factor seems to be 0.75 for prisms with vertical joint and 0.87 for stack bonded prism.
6. The theoretical formula proposed in this study to determine the compressive strength is more representative than any other existing formula. The formula incorporates the actual confinement of the mortar joint within the bricks rather than from triaxial tests. From linear elastic finite element analysis it has been found that the confinement of mortar joints within the bricks is approximately half of the confinement used in Hilsdorf's formula.
7. Investigation into the role of randomly distributed jute fibres in mud mortar reveals that shrinkage limit of mud mortar increases with the increase of inclusion of fibre. Consequently, the volumetric shrinkage and thereby the formation of crack in the dried mortar bed is minimized. Inclusion of jute fibre increases the compressive strength and reduces the deformation of mud mortar bed in the lateral direction. The strength increases with the increase of percentage inclusion upto a certain limit. The limiting maximum inclusion is 1.9% which results in a maximum increase

of 35.3% of unconfined compressive strength. The limiting inclusion for the resistance to lateral deformation lies in between 1.5 to 2.0%. Above these limiting values the increase of both strength and resistance to lateral deformation are inhibited.

8. Neither randomly distributed Jute fibres nor jute mat in mud mortar bed improves the load carrying capacity of masonry with mud mortar. However, randomly distributed fibre can only be used to resist volumetric shrinkage and formation of channel when the mortar bed dries out. This will reduce the chance of structural movement and penetration of water in the wall which may eventually lead to the process of functional deterioration.

## 7.2 RECOMMENDATIONS FOR FUTURE STUDY

The above conclusions have been drawn on the basis of the the results of the experimental and the theoretical investigations carried out in this study. But it is evident that further investigations are required since the present study considers a particular brick-mortar combination.

The following recommendations are made in this regard:

1. Saenz's formula with minor modification represents the the deformation characteristics of masonry with good approximation. But it may not be representative for all brick-mortar combination. Therefore, it is suggested to carry out further investigation using various brick-mortar combination.

2. The test on five brick high stack bonded prism and full size wall should be performed for various brick-mortar combinations to get a reliable mean.
- 3) The artificial strength attained due to the frictional resistance developed at the interface of machine platen could be minimized by adopting flexible brush platen.
- 4) The modified Hilsdorf's formula proposed by the author appears to be promising in predicting the compressive strength of stack bonded prism. Before its general acceptability further investigation is recommended to determine the actual confinement of mortar joint in the bricks for different brick-mortar combinations.
- 5) Further investigation is recommended using cement or chemical stabilizer which will minimize the formation of cracks in mud mortar and at the same time will improve deformation characteristics, compressive strength and bond strength significantly.

## REFERENCES

1. Rahman, A. H., "Some Aspects of Plain and Reinforced Masonry", M.sc. Thesis, BUET., Aug., 1980.
2. West, H.W.H., Hodgkinson, H.R., Beech, D.G. and Davenport, S.T.E., "The Performance of Walls Built of Wirecut Bricks with and without Perforations; Part-2-Strength Tests", Proc. Br. Ceramic Soc., No.17, Load Bearing Brickwork(3), Feb., 1970. pp.14-39.
3. Beech, D.G. and West, H.W.H., "The Performance of Modular Bricks in Story-Height Walls", Proc. Br. Ceramic Soc., No.21, Load-Bearing Brickwork (4), April, 1973, pp. 25-37.
4. Hendry, A.W., "Structural Brick-Work", Macmillan and Co. Ltd., London.
5. Atkinson, R.H., Noland, J.L. and Abrams, B.P., "A Deformation Failure Theory for Stack-Bonded Brick Masonry Prisms in Compression", Proc. 7th Int. Brick Mas. Conf., Melbourne, Vol.1, Feb., 1985, pp. 577-592.
6. Page, A.W., "The Influence of Brick and Brickwork Prism Aspect Ratio on the Evaluation of Compressive Strength", Proc. 7th Int. Brick Mas. Conf., Melbourne, Vol.1, Feb., 1985, pp. 653-664.
7. Render, S. and Phipps, M.E., "The Effect of Unit Aspect Ratio on the Axial Compressive strength of Masonry", Masonry International, No. 8, 1986, pp.28.

8. Page, A.W., "Load Bearing Masonry - A Review", Proc. 7th Int. Brick Mas. Conf., Melbourne, Vol.1, Feb., 1985, pp. 81-99.
9. Annual Book of ASTM Standards, Vol. 0.4.05, Chemical-Resistant Material; Vitriified Clay, Concrete, Fibre-Cement Products; Mortars; Masonry, 1984.
10. AS 2733-1984, "Concrete Masonry Units", Standard Association of Australia.
11. Grim, C.T., "Strength and Related Properties of Brick Masonry", J. Struct. Div. Am. Soc. Civ. Engrs., Vol.101, No. ST1, Jan., 1975, pp. 217-232.
12. Shrive, N.G., "The Prism Test as a Measure of Masonry Strength", Proc. 8th Int. Load Bearing Brickwork Symp., B.C.R.A., London, 1983.
13. Shrive, N.G., "Compressive Strength and Strength Testing of Masonry", Proc. 7th Int. Brick Mas. Conf., Melbourne, Vol.1, Feb., 1985, pp. 699-709.
14. Kupfer H., Hilsdorf, K.H. and Rusch, H., " Behavior of Concrete Under Biaxial Stresses", Proc. Am. Conc. Inst., Vol.66, July, 1969, pp. 656-666.
15. Tasuji, M.E., Slate, F. and Nilson, A.H., "Stress-Strain Response and Fracture of Concrete in Biaxial Loading", J. Am., Conc. Inst., Vol.75, July, 1978, pp. 306-312.
16. Rosenhaupt, S., Van Riel, A.C. and Wyler, L., "A New Indirect Tensile Test for Concrete Theoretical Analysis and Preliminary Experiments". Bull. Res. Conc., of Israel 6C, (1)13, 1957.

17. Thomas & O'Leary, "Tensile Test on Two Types of Brick", SIBMAC Proc. 1, Stoke-on-Trent, England, 1970, pp. 69-74.
18. Hilsdorf, H.K., "An Investigation into the Failure Mechanism of Brick Masonry Loaded in Axial Compression", Designing, Engineering and Constructing with Masonry Products, Gulf Publishing Co., Texas, 1969, pp. 34-41.
19. Khoo, C.L. and Hendry, A.W., "A Failure Criterion for Brickwork in Axial Compression", Proc. 3rd Int. Brick Mas. Conf., Essen, 1973, pp. 141-145.
20. Shrive, N.G., "The Failure Mechanism of Face-Shell Bedded (UngROUTED and Grouted) Masonry", Int. J. of Mas. Constn., Vol.2, No.3, 1982, pp. 115-128.
21. Hamid, A.A., and Drysdale, R.G., "Suggested Failure Criteria for Grouted Concrete Masonry Under Axial Compression", J. Am. Conc. Inst., Vol.76, No.10, Oct. 1979, pp. 1047-1061.
22. Francis, A.J., Horman, C.B. and Jerrems, L.E., "The Effect of Joint Thickness and Other Factors on the Compressive Strength of Brickwork", Proc. 2nd Int. Brick Mas. Conf., Stoke-on-Trent, England, 1971, pp. 31-37.
23. Ali, S. and Page, A.W. "Linear Fracture Analysis of Solid Masonry Subjected to Concentrated Loads", Masonry International, No.8, 1986, pp. 28-38.
24. Anderson, G.W., "Small Specimens of Brickwork as Design and Construction Criteria", Civil Engg., Transactions, Instn. of Engrs., Australia, 1969, pp. 150-156.

25. McNary, W.S. and Abrams, M.D.P., "Mechanics of Masonry in Compression", J. of Struct. Engg., Vol. 111, No.4, April, 1985.
26. "Portland Cement-Lime Mortars for Brick Masonry", Technical Notes. 8, SCPI, Sept., 1972.
27. AS 1640-1974, "S.A.A Brick Code", Standard Association of Australia.
28. Hendry, A.W., Sinha, B.P. and Davies, S.R., "An Introduction to Load Bearing Brickwork Design", Ellis Harwood Ltd., 1981.
29. Pedreschi, R.F. and Sinha, B.P., "The Stress-strain Relationships of Brickwork", Proc. 6th Int. Brick Mas Conf., Rome, 1982, pp. 321-334.
30. Sinha, B.P. and Pedreschi, R., "Compressive Strength and Some Elastic Properties of Brickwork", Int. J. of Mas. Contn., Vol.3, No.1, 1983, pp. 19-25.
31. Francis, A.J., "The S.A.A. Brickwork Code: the Research Background", Civil Engg. Trans., Instn. of Engrs., Australia, Vol. CE II, No.2, 1969, pp. 165-176.
32. James, J., McNeilly, T. and Oren, P., "Predicting the Compressive Strength of Brickwork", Proc. 5th Int. Brick Mas. Conf., Washington D.C., Oct., 1979, pp. 334-339.
33. Anderson, G.W., "Site Control of Structural Brickwork in Australia", Documentation 3.1 MC, Bundesverband de Deutschen Ziegelindustrie, Bonn, 1975, pp. 187-191.

34. Johnston, V.R. and McNeilly, T.H., "Specification, Testing and Site Control for Structural Brickwork", Ibid, pp. 202-207.
35. James, J.A., "Investigation of the Effect of Workmanship and Curing Conditions on the Strength of Brickwork", Ibid, pp. 192-201.
36. Drysdale, R.G. and Hamid A.A., "Behavior of Concrete Block Masonry under Axial Compression", J. Am. Conc. Inst., Vol.76, No. 6, June, 1979, pp. 707-721.
37. Brick Institute of America, "Building Code Requirements for Engineered Brick Masonry", Aug., 1969.
38. BSI, "British Standard Code of Practice for Structural Use of Masonry: Part I, Unreinforced Masonry", BS5628, 1978.
39. "Building Code Requirement for the Contemporary Bearing Wall", Technical Notes on Brick & Tile Construction, No. 24A, SCPI, May 1970.
40. Haller, P., "The Physics of the Fired Brick: Part one Strength Properties", Libr. Commun. Bldg. Res. Stn. 929, 1960 (Trans. G.L. Cairus).
41. BaBa, A., "A Suggested Concept for Predicting Strength of UngROUTED Masonry", Proc. 7th Int. Brick Mas. Conf., Melbourne, Vol. 1, Feb. 1985, pp. 593-604.
42. Kirtsching K., "On the Failure Mechanism of Masonry Subjected to Compression", Proc. 7th Int. Brick Mas. Conf., Melbourne, Vol.1, Feb., 1985.



43. "Materials for Soil Stabilization", American Road Builders Association, Education and Information Guide, Washington, D.C, 1971.
44. Mitchel, J.K., "Soil Improvement-State of the Art Report", Proc. 10th Int. Conf. on Soil Mechanics and Foundation Engineering, Stockholm, 1981, pp. 509-565.
45. Swami Saran, MP Jain and PK Jain, "Strength and stability of Sun Dried Mud Bricks", J. Inst. Engrs. (INDIA), Civil Engg. Div., Vol. 64, Pt.CI6, May, 1984, pp. 386-389.
46. Babu T. Jose, Francis Alloysius and T.S. Ramanathan, "Improvement of Bearing Capacity of Soil by Reinforcing with Locally Available Material", Proc. Int. Conf. on Low Cost Housing for Developing Countries, Nov., 1984.
47. Rahman, K.S., Bhuiyan, M.A.S. and Rashid, M.A., "The Effect of Additive on Strength of Madhupur Soil, J. Int. Engrs., Bangladesh, Vol. 14, No. 2, April, 1986, pp. 45-46.
48. "Draft Indian Standard Guide for Preparation and Use of Mud Mortar in Masonry", Bureau of Indian Standards, July, 1989.
49. Ali, S., "Concentrated Loads on Solid Masonry", Ph.D. Thesis University of Newcastle, Feb., 1987.
50. ASTM (1979 b): Annual Book of ASTM Standards, Part 19, Stones, Soil and Rock.
51. BSI, British Standard 1377:1975, British Standard Methods for test for soils for Civil Engineering purpose.
52. Lenczner, D., "Elements of Load Bearing Brickwork", Pergamon, Oxford, 1972.
53. Annual Book of ASTM Standards, Vol. 04.01, Cement, Lime, Gypsum, 1984

## APPENDIX - A

## A.1 Francis et al.'s [22] Formula

Compressive strength of brick prism is given by,

$$f'_m = \frac{\sigma'_{1t}}{1 + \frac{\phi(\beta\nu_m - \nu_b)}{[(1 - \nu_b) + \alpha\beta(1 - \nu_m)]}} \quad (\text{A.1})$$

- Where.
- $f'_m$  = Compressive strength of brick prism
  - $\sigma'_{1t}$  = Compressive strength of brick
  - $\phi = \sigma'_{1t} / \sigma'_t$
  - $\sigma'_t$  = Tensile strength of brick
  - $\alpha = t_b / t_m$
  - $t_b$  = Thickness of brick
  - $t_m$  = thickness of mortar joint
  - $\beta = E_b / E_m$ , modular ratio
  - $E_b$  = Modulus of elasticity of brick
  - $E_m$  = Modulus of elasticity of mortar
  - $\nu_b$  = Poisson's ratio of brick
  - $\nu_m$  = Poisson's ratio of mortar

### A.2 Hilsdorf's<sup>[18]</sup> Formula

$$\text{Compressive Strength of Masonry} = \frac{f_b'}{U} \times \frac{f_{bt}' + a.f_j'}{f_{bt}' + a.f_b'} \quad (\text{A.2})$$

Where,  $f_b'$  = Uniaxial compressive strength of brick  
 $f_{bt}'$  = Strength of brick under biaxial tension  
 $f_j'$  = Uniaxial compressive strength of mortar

$$a = \frac{j}{4.1b}$$

$j$  = Thickness of mortar joint

$b$  = Height of brick

$U$  = Non-uniformity coefficient. This varies according to the brickwork strength, but for cement mortar it has been shown to have a value of around 1.3 in the medium strength range.

### A.3 Khoo & Hendry's<sup>[19]</sup> Formula

The formula is given by,

$$\begin{aligned} & [0.9968t_m + 0.1620\alpha\sigma_m] - [2.0264t_m(1/c_m) + 0.1126\alpha]x \\ & + [1.2781t_m(1/c_m)^2 - 0.0529\alpha(1/\sigma_m)]x^2 \\ & - [0.2487t_m(1/c_m)^3 - 0.0018\alpha(1/\sigma_m)^2]x^3 \end{aligned} \quad (\text{A.3})$$

Where,

$x$  = Compressive strength of brick masonry prism

$c_m$  = Uniaxial compressive strength of brick

$t_m$  = Tensile strength of mortar

$\sigma_m$  = Uniaxial compressive strength of mortar

$\alpha$  =  $t_m/t_b$

$t_m$  = Thickness of mortar joint

$t_b$  = Thickness of brick

#### A.4 Grim's<sup>(11)</sup> Formula

The compressive strength of brick masonry prism, concentrically loaded, relatively short and built with conventional material is given by,

$$f_m' = 1.42 \xi \eta f_b' 10^{-\epsilon} (f_c' + 9.45 \times 10^4) (1 + \epsilon)^{-1} \quad (\text{A.4})$$

Where,

$f_m'$  = Compressive strength of brick masonry prism, psi

$\epsilon$  = Workmanship factor,

= 0, for inspected work,

=  $8 \times 10^{-4} (12,000 - f_b')$  for uninspected work, in which  $f_b'$  is the crushing strength of brick,

$f_b' \leq 12,000$  psi (assume  $f_b' = 12,000$  psi for  $f_b' > 12,000$  psi)

$\xi$  = Prism slenderness factor,

=  $0.0178 [ 57.3 - \{(h_s/t_s) - 6\}^2 ]$ , where  $h_s/t_s$  is the prism slenderness ratio, height to least lateral dimension, and  $6 > h_s/t_s > 2$

$\eta$  = Material size factor,

=  $0.0048 [ 273 - \{(h_u/t_j) - 14\}^2 ]$ , where  $h_u/t_j$  is the ratio of brick height to mortar joint thickness and  $10 > h_u/t_j > 2.5$ .

$f_c'$  = mortar cube compressive strength.

A.5 Compressive Strength of Brick, Cement Mortar and 5 Brick  
High Stack Bonded Prism Eliminating Aspect Ratio Effect.

**Brick:**

Confined compressive strength = 3120 psi  
Aspect ratio = 0.61  
Aspect ratio correction factor = 0.57  
Unconfined compressive strength =  $3120 \times 0.57$   
= 1778.4 psi

**Cement Mortar:**

Confined Compressive strength = 1240 psi  
Aspect ratio = 1  
Aspect ratio correction factor = 0.7  
Unconfined compressive strength =  $1240 \times 0.7$   
= 868 psi

**Prism:**

Confined Compressive strength = 1168 psi  
Aspect ratio = 3.39  
Aspect ratio correction factor = 0.879  
Unconfined compressive strength =  $1168 \times 0.879$   
= 1026 psi

## A.6 Calculation of Compressive Strength using Different Formulae

A.6.1 Francis et al. (eqn. A.1)

$$\phi = 1778.4/126 = 14.11$$

$$\beta = 2.2 \times 10^{-6} / 1.0 \times 10^{-6}$$

$$\alpha = 2.75 / 0.375$$

Using eqn. A.1, compressive strength = 1392 psi

A.6.2 Hilsdorf (eqn. A.2)

$$a = 0.375 / (4.1 \times 2.75) = 0.033$$

Using eqn. A.2, compressive strength = 1145 psi

A.6.3 Khoo & Hendry (eqn. A.3)

The equation can be written as,

$$A - BX + CX^2 - DX = 0$$

where,  $A = 144.7205$ ,  $B = 0.158884$ ,  $C = 0.000042$  &  $D = 0.0000000052$

By trial and error,  $X = 1282$  psi.

## A.6.4 Grim (eqn. A.4)

$$h_s/t_s = 15.25/4.5 = 3.56$$

$$t_u/t_d = 2.75/0.375 = 7.33$$

$$\xi = 0.9139$$

$$\eta = 1.0968$$

$$\epsilon = 0, \text{ inspected work}$$

Using eqn. A.4, compressive strength = 258 psi

## A.6.5 Hilsdorf(modified)

The K value of triaxial strength of mortar from finite element analysis is calculated as follows:

From Hilsdorf's assumption the minimum lateral confinement of the mortar joint is

$$\sigma_{xj} = 1/K(\sigma_y - f_j') \quad (\text{A.5})$$

Where,  $\sigma_{xj}$  is the lateral compressive stress in the mortar joint  
 $\sigma_y$  is the local stress in the y direction  
 $f_j'$  is the uniaxial compressive strength of mortar

Now if we analyse the prism by finite element method applying the failure load on the prism we will get the local stress  $\sigma_y$  and the lateral stress  $\sigma_{xj}$  (lateral confinement). In this study  $\sigma_y$  and  $\sigma_{xj}$  are taken from the Fig. 6.10 (case-I) of chapter 6. The unconfined uniaxial compressive strengths (see Appendix A.5) of brick, mortar and prism are considered in this case.

From Fig.6.10,  $\sigma_y = 1168$  psi and  $\sigma_{xj} = 149.5$  psi  
 Using eqn. A.5,  $K = 2.032$

Using this value of K,  $a = j/Kb = 0.067$

Now substituting the value of "a" in the formula proposed by Hilsdorf (eqn. A.2),

compressive strength = 1027 psi



## APPENDIX - B

B.1 Water Absorption Characteristics of Bricks

Specimen no.	Water content(%)			
	Air dry	Immersed for 30 min.	Immersed for 1 hr.	Immersed for 24 hrs.
1	0.55	14.06	14.53	14.73
2	0.43	17.50	18.32	18.58
3	0.36	14.72	15.21	15.57
4	0.42	13.96	15.41	15.60
5	0.61	12.30	13.26	13.50
6	0.57	15.37	16.10	16.25
7	0.38	13.80	14.32	14.60
8	0.45	14.73	14.87	15.11
9	0.52	16.22	17.95	18.20
10	0.54	15.92	17.67	17.80
11	0.67	14.30	14.63	14.88
12	0.39	16.83	16.98	17.20
$\bar{X}$	0.49	14.97	15.77	15.99
S	0.09	1.39	1.55	1.53
C. of V. (%)	18.89	9.32	9.84	9.56

Note:  $\bar{X}$  = Mean

S = Standard deviation

C. of V. = Coefficient of variation

## B.2 Compressive Strength of Brick

Specimen no.	Compressive strength (psi)
1	3430
2	2810
3	3730
4	2540
5	2200
6	2600
7	3040
8	3190
9	3840
10	4280
11	2990
12	2810
$\bar{X}$	3120
S	577.70
C. of V. (%)	18.50

Note:  $\bar{X}$  = Mean

S = Standard deviation

C. of V. = Coefficient of variation

1 psi = 6.896 KPa

## B.3 Tensile Strength(Indirect) of Brick

Specimen no.	Tensile strength (psi)
1	128
2	120
3	125
4	110
5	130
6	120
7	135
8	140
9	138
10	98
11	146
12	125
$\bar{X}$	126
S	12.7
C. of V.(%)	10

Note:  $\bar{X}$  = Mean

S = Standard deviation,

C. of V. = Coefficient of variation.

1 psi = 6.896 KPa

B.4 Normal Stress-Strain Readings on 50mm Gauge Length on the Middle Brick of 5SPC Prism ( $\times 10^{-6}$ )

Stress (psi)	Prism no.						$\bar{X}$
	1	2	3	4	5	6	
94	20	40	20	60	40	36	36
190	40	60	60	140	100	80	80
285	40	80	100	200	160	140	120
380	80	120	160	240	200	160	160
477	120	160	240	240	240	200	200
568	180	220	260	260	280	240	240
663	240	260	300	320	400	280	300
758	280	320	320	360	440	440	360
853	300	380	400	440	480	520	420
947	400	440	540	560	580	600	520
1042	520	560	560	-	640	720	600
$E_b$ (psi)						$2.2 \times 10^{-6}$	

Note:  $\bar{X}$  = Mean

$E_b$  = Initial modulus of elasticity of brick  
 1 psi = 6.896 kPa

B.5 Mean Normal Stress-Strain Readings for Mortar joint from  
Compression Test on 5SPC Prism

Stress (psi)	Middle brick Mean $\epsilon_b$ ( $\times 10^{-6}$ )	Prism Mean $\epsilon_t$ ( $\times 10^{-6}$ )	Mean mortar $\epsilon_m = 9.045\epsilon_t - 8.045\epsilon_b$ ( $\times 10^{-6}$ )
94	36	40	72
190	80	90	170
285	120	140	301
380	160	190	431
477	200	240	560
568	240	290	692
663	300	370	933
758	360	450	1174
853	420	510	1234
947	520	620	1424
1042	600	700	1504
$E_m$ (psi)			$1.0 \times 10^6$

Note:  $E_m$  = Initial modulus of elasticity of mortar

1 psi = 6.896 kPa

B.6 Normal Stress-Strain Readings on 200mm Gauge Length on 5SPC Prism ( $\times 10^{-6}$ )

Stress (psi)	Prism no.						$\bar{X}$
	1	2	3	4	5	6	
94	30	30	40	60	20	60	40
190	80	90	90	110	70	100	90
285	140	140	130	160	120	150	140
380	200	180	170	230	150	210	190
477	250	230	220	260	210	270	240
568	300	290	270	320	260	300	290
663	360	380	360	400	340	380	370
758	450	470	430	480	420	450	450
853	510	540	490	530	470	520	510
947	610	650	590	660	580	630	620
1042	680	720	680	750	670	-	700
1136	770	810	-	830	-	-	-
1231	882	932	-	950	-	-	-
1326	915	-	-	1103	-	-	-
$f'_m$ (psi)	1330	1250	1070	1376	1042	1010	1180
$E_{bm}$ (psi)							$1.92 \times 10^6$
$E_{bms}$ (psi)							$1.3 \times 10^6$
$\epsilon_{bmu}$							$920 \times 10^{-6}$

Note:  $\bar{X}$  = Mean

$f'_m$  = Ultimate compressive strength

$E_{bm}$  = Initial modulus of elasticity of brick masonry

$E_{bms}$  = Secant modulus of elasticity of brick masonry at  $\epsilon_{bmu}$

$\epsilon_{bmu}$  = Strain in masonry at  $f'_m$

1 psi = 6.896 KPa

B.7 Mean Normal Stress-Strain Readings for Concrete Brick,  
Mortar Joint and Brick Masonry obtained by Ali<sup>[49]</sup>

Stress (MPa)	Brick strain( $\epsilon_m$ ) ( $10^{-6}$ )	Mortar strain( $\epsilon_b$ ) ( $10^{-6}$ )	Brick masonry strain ( $\epsilon_t = 1/9\epsilon_m + 8/9\epsilon_b$ ) ( $10^{-6}$ )
0.79	50	110	57
1.58	90	220	105
2.37	140	390	167
3.16	190	580	233
3.95	240	810	303
4.74	290	1150	385
5.53	350	1530	481
6.32	420	2050	601
7.11	490	2760	742
7.90	580	3830	941
8.69	690	4650	1130
9.09	750	4710	1190
$E_b$ (MPa)	17000	-	-
$E_m$ (MPa)	-	7400	-
$E_{bm}$ (MPa)	-	-	15000

Note:  $E_b$  = Initial modulus of elasticity of brick  
 $E_m$  = Initial modulus of elasticity of mortar  
 $E_{bm}$  = Initial modulus of elasticity of brick masonry  
 1 psi = 6.896 kPa

## B.8 Compressive Strength of 2SPC Prism

Specimen no.	$f_{ve}$ (psi)	$f'_m$ (psi)	$f_{ve}/f'_m$ (%)
1	*	2270	-
2	*	2726	-
3	*	2810	-
4	*	2471	-
5	*	2946	-
6	*	2389	-
$\bar{X}$	-	2620	-
S	-	-	-
C. of V. (%)	-	-	-

Note: \*Failed to predict

$f_{ve}$  = Strength at first visible crack

$f'_m$  = Ultimate strength

$\bar{X}$  = Mean

S = Standard deviation

C. of V. = Coefficient of variation

1 psi = 6.896 KPa



## B.9 Compressive Strength of 3SPC Prism

Specimen no.	$f_{ve}$ (psi)	$f'_m$ (psi)	$f_{ve}/f'_m$ (%)
1	1751	1926	90.9
2	1735	1956	89.7
3	1686	2005	84.0
4	1490	1711	87.0
5	1488	1686	88.2
6	1471	1711	85.9
$\bar{X}$	1603	1832	87.5
S	-	-	-
C. of V. (%)	-	-	-

Note:  $f_{ve}$  = Strength at first visible crack

$f'_m$  = Ultimate strength

$\bar{X}$  = Mean

S = Standard deviation

C. of V. = Coefficient of variation

1 psi = 6.896 KPa

## B.10 Compressive Strength of 4SPC Prism

Specimen No.	$f_{ve}$ (psi)	$f'_m$ (psi)	$f_{ve}/f'_m$ (%)
1	1249	1540	81.1
2	998	1143	87.3
3	1196	1417	84.4
4	1000	1245	80.3
5	1263	1466	86.1
6	853	1074	79.4
$\bar{X}$	1093	1314	83.1
S	-	-	-
C. of V. (%)	-	-	-

Note:  $f_{ve}$  = Strength at first visible crack

$f'_m$  = Ultimate strength

$\bar{X}$  = Mean

S = Standard deviation

C. of V. = Coefficient of variation

1 psi = 6.896 KPa

## B.11 Compressive Strength of 5SPC Prism

Specimen no.	$f_{ve}$ (psi)	$f'_m$ (psi)	$f_{ve}/f'_m$ (%)
1	1024	1280	80.0
2	*	1275	-
3	1024	1210	84.6
4	796	1090	73.0
5	810	990	81.8
6	795	950	83.6
7	1210	1480	81.7
8	1240	1475	84.0
9	920	1230	74.8
10	775	1040	74.5
11	850	985	86.2
12	830	1010	82.1
$\bar{X}$	935	1168	80.5
S	160	178	4.28
C.of V.(%)	17.1	15.2	5.31

Note: \*Failed to predict.

$f_{ve}$  = Strength at first visible crack

$f'_m$  = Ultimate strength

$\bar{X}$  = Mean

S = Standard deviation

C. of V. = Coefficient of variation.

1 psi = 6.896 KPa

## B.12 Compressive Strength of 6SPC Prism

Specimen no.	$f_{ve}$ (psi)	$f'_m$ (psi)	$f_{ve}/f'_m$ (%)
1	998	1293	77.1
2	861	1007	85.5
3	846	1156	73.1
4	884	1075	82.2
5	982	1303	75.3
6	738	958	77.0
$\bar{X}$	885	1132	78.3
S	-	-	-
C.of V.(%)	-	-	-

Note: \*Failed to predict

$f_{ve}$  = Strength at first visible crack

$f'_m$  = Ultimate strength

$\bar{X}$  = Mean

S = Standard deviation

C. of V. = Coefficient of variation

1 psi = 6.896 KPa

## B.13 Compressive Strength of 5VPC-A Prism

Specimen no.	$f_{ve}$ (psi)	$f'_m$ (psi)	$f_{ve}/f'_m$ (%)
1	*	1677	-
2	1095	1330	82.2
3	910	1260	72.2
4	880	1197	73.5
5	924	1128	81.9
6	728	1097	66.3
7	1010	1593	63.4
8	1087	1457	74.6
9	904	1418	63.7
10	896	1256	71.3
11	968	1254	77.1
12	910	1192	76.3
$\bar{X}$	937	1321	73.0
S	97.7	173	6.18
C. of V. (%)	10.42	13	8.46

Note: \*Failed to predict

$f_{ve}$  = Strength at first visible crack

$f'_m$  = Ultimate strength

$\bar{X}$  = Mean

S = Standard deviation

C. of V. = Coefficient of variation

1 psi = 6.896 KPa

## B.14 Compressive Strength of 5VPC-B Prism

Specimen no.	$f_{vc}$ (psi)	$f'_m$ (psi)	$f_{vc}/f'_m$ (%)
1	992	1490	61.8
2	804	1330	60.4
3	902	1455	61.9
4	992	1507	65.8
5	835	1360	61.3
6	756	1051	71.9
7	751	1331	56.4
8	725	1386	52.3
9	836	1426	56.8
10	682	1098	62.1
11	1006	1433	70.2
12	787	1519	51.8
$\bar{X}$	834	1365	61.2
S	99.1	90.5	5.9
C.of V.(%)	11.9	10.5	9.6

Note: \*Failed to predict

$f_{vc}$  = Strength at first visible crack

$f'_m$  = Ultimate strength

$\bar{X}$  = Mean

S = Standard deviation

C. of V. = Coefficient of variation

1 psi = 6.896 KPa

## B.15 Compressive Strength of Walleette

Specimen no.	$f_{vc}$ (psi)	$f'_m$ (psi)	$f_{vc}/f'_m$ (%)
1	401	955	41.8
2	538	992	54.2
3	557	1051	53.0
4	592	1018	58.1
5	447	1037	43.1
6	587	1082	54.2
$\bar{X}$	520	1023	50.7
S	-	-	-
C.of V.(%)	-	-	-

Note:  $f_{vc}$  = Strength at first visible crack

$f'_m$  = Ultimate strength

$\bar{X}$  = Mean

S = Standard deviation

C. of V. = Coefficient of variation

1 psi = 6.896 KPa

### B.16 Unconfined Compression Test on Mud Mortar

#### B.16.1 Specimen without Fibre

Strain ( $\times 10^{-4}$ )	Stress (psi)				$\bar{X}$
	Specimen no.				
	1	2	3		
17.85	95.3	93.1	98.8	95.7	
35.70	141.1	145.4	155.6	147.3	
53.55	187.5	177.6	184.1	183.3	
71.40	210.5	194.1	206.3	203.6	
U.C.S	218.4	198.5	213.2	210.0	
W.C	2.3	2.4	2.3	2.33	

#### B.16.2 Specimen with 0.5% Fibre

Strain ( $\times 10^{-4}$ )	Stress (psi)				$\bar{X}$
	Specimen no.				
	1	2	3		
17.85	114.2	113.1	101.7	109.6	
35.70	170.0	163.5	148.5	160.6	
53.55	215.7	197.5	185.5	199.5	
71.40	229.5	225.0	249.5	234.6	
U.C.S	232.0	236.6	254.2	241.0	
W.C	2.2	2.2	2.3	2.23	

Note:  $\bar{X}$  = Mean, U.C.S = Unconfind comp. strength &  
W.C = Water content during test

1 psi = 6.896 KPa



## B.16.3 Specimen with 1.0% Fibre

Strain ( $\times 10^{-4}$ )	Stress (psi)				$\bar{X}$
	Specimen no.				
	1	2	3		
17.85	122.3	130.2	113.6	122.0	
35.70	168.5	172.0	163.5	168.0	
53.55	213.7	216.1	201.3	210.3	
71.40	239.2	246.7	227.3	237.7	
89.25	-	262.1	243.5	252.8	
U.C.S	248.2	269.2	252.4	256.6	
W.C	2.1	2.3	2.1	2.16	

## B.16.4 Specimen with 1.5% Fibre

Strain ( $\times 10^{-4}$ )	Stress (psi)				$\bar{X}$
	Specimen no.				
	1	2	3		
17.85	118.2	136.4	127.1	127.2	
35.70	165.1	179.3	171.6	172.0	
53.55	211.4	225.1	217.2	218.0	
71.40	248.0	239.4	241.6	243.0	
89.25	263.2	248.7	262.8	258.2	
107.10	277.0	254.3	272.1	267.8	
U.C.S	281.3	260.1	275.0	272.1	
W.C	2.0	2.1	2.3	2.13	

Note:  $\bar{X}$  = Mean, U.C.S = Unconfined comp. strength &

W.C = Water content during test

1 psi = 6.896 KPa

## B.16.5 Specimen with 2.0% Fibre

Strain ( $\times 10^{-4}$ )	Stress (psi)			
	Specimen no.			$\bar{X}$
	1	2	3	
17.85	109.2	119.1	117.3	115.2
35.70	156.3	172.1	167.4	165.2
53.55	196.5	211.6	203.5	203.8
71.40	218.5	236.1	226.3	226.9
89.25	235.4	249.2	256.1	246.9
107.10	259.7	261.6	271.1	264.1
124.95	267.3	270.1	280.2	272.5
U.C.S	273.2	277.3	286.3	278.9
W.C	2.4	2.1	2.2	2.23

## B.16.6 Specimen with 2.5% Fibre

Strain ( $\times 10^{-4}$ )	Stress (psi)			
	Specimen no.			$\bar{X}$
	1	2	3	
17.85	99.4	114.6	110.3	108.1
35.70	138.2	158.3	151.4	149.3
53.55	162.1	188.4	176.3	175.6
71.40	187.8	206.3	200.5	198.2
89.25	204.2	227.8	218.4	216.8
107.10	222.6	248.5	235.7	235.6
124.95	239.4	258.1	253.1	250.2
142.80	248.1	262.6	257.6	256.1
U.C.S	253.5	262.3	268.2	261.3
W.C	2.4	2.3	2.4	2.36

Note:  $\bar{X}$  = Mean, U.C.S = Unconfind comp. strength &  
W.C = Water content during test  
1 psi = 6.896 KPa

Brick

**B.17 Compressive Strength of 5/High Stack Bonded Prism with Mud Mortar**

B.17.1 Prism without Fibre in the Mud Mortar bed

Specimen no.	$f_{vc}$ (psi)	$f'_m$ (psi)	$f_{vc}/f'_m$ (%)	W.C (%)
1	237	881	26.9	2.81
2	353	1023	34.5	2.65
3	218	971	22.4	2.53
4	284	945	30.0	2.58
5	222	971	22.8	2.63
6	273	853	32.0	2.71
7	261	715	36.5	2.86
8	*	801	-	2.62
9	225	664	33.9	2.75
10	*	982	-	2.67
11	346	1160	29.8	2.84
12	300	942	31.8	2.67
$\bar{X}$	272	909	30.0	2.69
S	49.5	130.5	4.51	0.10
C. of V. (%)	18.16	14.36	15.0	3.68

Note: \*Failed to predict.

$f_{vc}$  = Strength at first visible crack

$f'_m$  = Ultimate strength

W.C = Water content during test

$\bar{X}$  = Mean

S = Standard deviation

C. of V. = Coefficient of variation.

1 psi = 6.896 KPa

## B.17.2 Prism with 0.5% Fibre in the Mud Mortar bed

Specimen no.	$f_{vc}$ (psi)	$f'_m$ (psi)	$f_{vc}/f'_m$ (%)	W.C (%)
1	190	959	19.8	2.80
2	237	711	33.3	3.10
3	284	1058	26.8	2.48
4	212	634	33.4	2.61
5	284	876	32.4	2.82
6	221	785	28.1	2.56
$\bar{X}$	238	837	28.5	2.73
S	-	-	-	-
C.of V.(%)	-	-	-	-

## B.17.3 Prism with 1.0% Fibre in the Mud Mortar bed

Specimen no.	$f_{vc}$ (psi)	$f'_m$ (psi)	$f_{vc}/f'_m$ (%)	W.C (%)
1	221	865	25.5	2.62
2	215	782	27.5	2.44
3	236	654	36.0	2.53
4	261	965	27.0	2.48
5	237	1089	21.7	2.73
6	237	1018	23.2	2.76
$\bar{X}$	235	893	26.2	2.59
S	-	-	-	-
C.of V.(%)	-	-	-	-

Note:  $f_{vc}$  = Strength at first visible crack,  $f'_m$  = Ultimate strength, W.C = Water content during test,  $\bar{X}$  = Mean  
 S = Standard deviation & C. of V. = Coefficient of variation.

1 psi = 6.896 KPa

## B.17.4 Prism with 2.0% Fibre in the Mud Mortar bed

Specimen no.	$f_{ve}$ (psi)	$f'_m$ (psi)	$f_{ve}/f'_m$ (%)	W.C (%)
1	237	630	37.6	2.89
2	222	647	34.3	2.61
3	237	994	23.8	2.73
4	212	758	27.9	2.68
5	218	780	27.9	2.64
6	226	683	33.0	2.72
$\bar{X}$	225	748	30.0	2.71
S	-	-	-	-
C.of V.(%)	-	-	-	-

## B.17.5 Prism with Jute Mat in the Mud Mortar bed

Specimen no.	$f_{ve}$ (psi)	$f'_m$ (psi)	$f_{ve}/f'_m$ (%)	W.C (%)
1	222	758	29.2	2.58
2	237	805	29.4	2.63
3	237	966	24.5	2.69
4	292	916	31.8	2.47
5	208	874	23.8	3.13
6	332	685	48.4	2.41
$\bar{X}$	255	834	30.6	2.65
S	-	-	-	-
C.of V.(%)	-	-	-	-

Note:  $f_{ve}$  = Strength at first visible crack,  $f'_m$  = Ultimate strength, W.C = Water content during test,  $\bar{X}$  = Mean, S = Standard deviation & C. of V. = Coefficient of variation.

1 psi = 6.896 KPa

